NASA TECHNICAL MEMORANDUM

NASA TM X-62,281

NASA TM X- 62,281

(NASA-TM-X-62281) AERODYNAMIC CHARACTERISTICS OF A LARGE-SCALE MODEL WITH A SWEPT WING AND A JET FLAP HAVING AN EXPANDABLE DUCT (NASA) 96 p HC $7.00 CSCL 01C G3/02

N74-11826

Unclas 22576

# AERODYNAMIC CHARACTERISTICS OF A LARGE-SCALE MODEL WITH A SWEPT WING AND A JET FLAP HAVING AN EXPANDABLE DUCT

Thomas N. Aiken, Kiyoshi Aoyagi, and Michael D. Falarski

Ames Research Center
and
U.S. Army Air Mobility R&D Laboratory
Moffett Field, Calif. 94035

September 1973

## NOTATION

| | |
|---|---|
| AR | wing aspect ratio, $\frac{b^2}{S}$ |
| b | wing span, m (ft) |
| BLC | boundary layer control |
| c | chord (streamwise), m (ft) |
| $\bar{c}$ | mean aerodynamic chord, m (ft) |
| $C_D$,CD | drag coefficient, $\frac{\text{drag}}{qS}$ (see data reduction section) |
| $C_{D_R}$ | momentum drag coefficient due to engine inlet flow |
| $C_{J_I}$ | total isentropic thrust coefficient, $C_{J_{JF}} + C_{\mu_{BLC_1}} + C_{\mu_{BLC_2}} + C_{\mu_a}$ |
| $C_{J_{JF}}$ | isentropic jet thrust coefficient of main blowing slot, $\frac{\text{isentropic thrust}}{qS}$ |
| $C_l$,CR | rolling moment coefficient, $\frac{\text{rolling moment}}{qSb}$ |
| $C_L$,CL | lift coefficient, $\frac{\text{lift}}{qS}$ |
| $C_m$,CM | pitching moment coefficient, $\frac{\text{pitching moment}}{qS\bar{c}}$ |
| $C_n$,CN | yawing moment coefficient, $\frac{\text{yawing moment}}{qSb}$ |
| $C_P$ | local pressure coefficient, $\frac{P-P_\infty}{q}$ |
| $C_T$ | tailpipe thrust coefficient, $\frac{\text{tailpipe thrust}}{qS}$ |
| $C_Y$,CY | side force coefficient, $\frac{\text{side force}}{qS}$ |
| $C_{\mu_a}$ | isentropic jet thrust coefficient of aileron, $\frac{\text{isentropic thrust}}{qS}$ |
| $C_{\mu_{BLC_1}}$ | isentropic jet thrust coefficient of flap BLC blowing slot, $\frac{\text{isentropic thrust}}{qS}$ |

$C_{\mu_{BLC_2}}$ isentropic jet thrust coefficient of aft BLC blowing slot, $\frac{\text{isentropic thrust}}{qS}$

h blowing nozzle slot height, cm (in)

$i_t$ horizontal tail incidence, positive with trailing edge down, deg

m mass rate of flow, Kg/sec (lbm/sec)

P local pressure, N/sq m (lb/sq ft)

q freestream dynamic pressure, N/sq m (lb/sq ft)

S wing planform area, sq m (sq ft)

t airfoil thickness, m (ft)

x chordwise station, m (ft)

y spanwise station, m (ft)

z vertical distance from wing chord plane, m (ft)

α,AL model angle of attack, deg

β,BETA angle of sideslip of plane of symmetry, deg

$\delta_a$ aileron deflection ($\delta_a$ = 30/0 denotes left aileron at 30°, right aileron at 0°) positive with trailing edge down, deg

$\delta_c$ control flap deflection ($\delta_c$ = 0/20 denotes left control flap at 0°, right control flap at 20°; control flaps are not deflected on ailerons) positive with trailing edge down, deg; see figure 2(d)

$\delta_f$ flap deflection ($\delta_f$ = 60/30 denotes inboard flap at 60° and outboard flap (no aileron) at 30°; $\delta_f$ = 60 denotes inboard flap at 60° and no outboard flap) positive with trailing edge down, deg

$\delta_s$ slat deflection, positive with leading edge down, deg

| | |
|---|---|
| $\eta$ | spanwise position, $\frac{2y}{b}$ |

Subscripts

| | |
|---|---|
| a | aileron |
| $BLC_1$ | aft BLC blowing slot |
| $BLC_2$ | flap BLC blowing slot |
| e | elevator |
| f | flap |
| JF | main blowing slot |
| s | slat |
| t | horizontal tail |
| T | total conditions |
| u | uncorrected |
| vt | vertical tail |
| 1 | original slat geometry (T-415) |
| 2 | modified slat geometry (T-418) |
| $\infty$ | freestream conditions |

# AERODYNAMIC CHARACTERISTICS OF A LARGE-SCALE MODEL WITH A SWEPT WING AND A JET FLAP HAVING AN EXPANDABLE DUCT

Thomas N. Aiken, Kiyoshi Aoyagi, and
Michael D. Falarski

Ames Research Center
and
U.S. Army Air Mobility R&D Laboratory
Moffett Field, Calif., 94035

## SUMMARY

This report presents the data from an investigation of the aerodynamic characteristics of the expandable duct-jet flap concept. The investigation was made using a large-scale model in the Ames 40- by 80-foot Wind Tunnel.

The expandable duct-jet flap concept uses a lower surface, split flap and an upper surface, Fowler flap to form an internal, variable area cavity for the blowing air. Small amounts of blowing are used on the knee of the upper surface flap and the knee of a short-chord, trailing edge control flap. The bulk of the blowing is at the trailing edge. The flap could extend the full span of the model wing or over the inboard part only, with blown ailerons outboard.

Primary configurations tested were two flap angles, typical of takeoff and landing; symmetric control flap deflections, primarily for improved landing performance; and asymmetric aileron and control flap deflections, for lateral control. The tests were made with and without the horizontal tail at wind tunnel dynamic pressures from 1144 Newtons per square meter (23.9 pounds per square foot) to 158 Newtons per square meter (3.3 pounds per square foot). These correspond to Reynolds numbers from 5.35 million to 1.99 million, based on the wing mean aerodynamic chord. The range of jet thrust coefficients was 0 to 2.31.

## INTRODUCTION

The expandable duct-jet flap concept is being studied as a means of attaining STOL performance in a turbofan powered aircraft. The concept is a derivative of a basic jet flap and has the principal jet located at the flap trailing edge.

The basic jet flap concept has been extensively considered as a propulsive high lift device on many types of aircraft. Integration of this concept into high wing-loading aircraft has been difficult because of the problem of providing sufficient duct area needed for high thrust from the wing jet. Additionally, it is difficult to achieve the proper values of lift to drag ratios needed for STOL descent without high flap deflections and subsequent flow separation and buffet problems.

The expandable duct-jet flap is an attempt to provide solutions to these problems while maintaining the inherent characteristics of the basic jet flap. It has a cavity formed by a lower surface of the expanding flap, the rear wing spar, and the upper surface of the flap system. The resulting cavity increases with flap deflection and is used for the ducting of compressor air to the blowing system. The blowing system primarily consists of the main jet near the flap trailing edge and a BLC slot at the knee of the flap. In addition, a short-chord, control flap is available at the trailing edge to provide additional deflection of the main jet. The control flap's purpose is to control the lift to drag ratio without adverse separation and buffet problems.

A large-scale model was built and tested in the Ames 40- by 80-foot Wind Tunnel to determine the aerodynamic characteristics of the expandable duct-jet flap concept. The wing planform of the model was geometrically similar to that of the augmentor wing model discussed in reference 1, 2 and 3. The flap system extended either the full span or 70 percent of the span with the remainder used as a blown aileron. The compressed air for the blowing nozzles was provided by the cold air from two turbofan engines mounted in the fuselage. Tests at forward speed, out of ground effect, were made for flap angles of 30° and 60° and various deflections of the control flap. The investigation also included the effects of a high-position horizontal tail, sideslip, and differential aileron and control flap deflection.

The tests were performed in cooperation with the Lockheed-Georgia Company and the Flight Dynamics Laboratory of the Department of the Air Force.

## MODEL AND APPARATUS

Figures 1(a) through 1(e) show the model installed in the Ames 40- by 80-foot Wind Tunnel. The wing chord plane is in the approximate center of the test section.

### Basic Model

Tables I and II give geometric data for the model. Sketches of the model are shown in figure 2. A three-view of the model and a typical wing section are shown in figures 2(a) and 2(b) respectively.

The wing was equipped with a full-span, leading edge slat. The slat position was modified midway through the investigation (see figure 2(c)). The flap system could be configured either as a full span flap or with the outboard 30 percent as a blown aileron.

The horizontal tail was equipped with a fixed, leading edge slat (see figure 2(d)). The elevator and rudder deflection were 0° throughout the test. When the horizontal tail was not installed, a rake having five directional probes was used in its place. A nose fairing was installed during

part of the test (see figure 2(a)). The model was equipped with sound suppressors on the engine inlet and the tailpipe exit.

## Blowing System

Supply – The model was equipped with a separate blowing system for each wing. The blowing system is shown schematically in Figure 2(e). The compressed air was the cold or bypass air of two JT15D-1 turbofan engines.

The hot gas from the engine core exhausted out tailpipes in the rear of the fuselage. Tailpipe cooling air was brought into the fuselage through the inlet on the underside of the fuselage (see figure 2(a)) and ejected through an annular ejector at the tailpipe exit. The cold air was ducted to the wing blowing slots through the wing box spar.

Main jet – The blowing slot dimensions for the main jet and the BLC jets are shown in figure 3 while typical spanwise total pressure distributions for $C_{J_I}$'s less than and greater than 0.4 are given in figure 4. The main jet slot dimensions are controlled by the movable segment on the trailing edge of the lower surface of the flap system (see figure 2(f)). The dimensions did not change with changes in control flap deflection. The overall dimensions did differ for 30° and 60° flap deflection (see figure 3). Where the outboard 30 percent of the flap system was used as a blown aileron, the main jet slot was blocked.

BLC jets – The flap BLC slot was located on the knee of the upper surface of the flap as shown in figure 2(f). The overall dimension differed for 30° and 60° flap deflections (see figure 3). The flap BLC slot was used for the blowing slot on the blown aileron. The aft BLC slot was located on the upper knee of the control flap as shown in figure 2(f). The dimensions were fixed as shown in figure 3. The aft BLC slot was blocked on the blown aileron.

## Instrumentation

The instrumentation used to measure the flow conditions in the blowing system is shown schematically in figure 5. Surface static pressure orifices were located at three spanwise stations on the right wing ($\eta$ = .195, .467, .816).

## TESTS

Table III is an index to the investigation. The investigation was done in two phases (T-415 and T-418). The only change in configuration between the two phases was a change in the wing slat from position 1 to position 2. The tests were primarily done by increasing angle of attack at constant airspeed and duct pressure. The angle of attack range was -8° to 24°. Sideslip was varied from -18° to 4° at constant angle of attack. The wind tunnel dynamic

pressure range was from 1144 N/sq m (23.9 lb/sq ft) to 158 N/sq m (3.3 lb/sq ft) giving a Reynolds number range from 5.35 million to 1.99 million.

Two basic flap deflections were used; 30° representing a takeoff configuration; and 60° representing a landing configuration. The model was tested with both a full-span flap and with the outboard 30 percent span configured as a blown aileron and set at 30° or 10°. Several values of symmetric control flap deflection were tested for each flap configuration Asymmetric control flap and aileron deflections were tested for lateral control. The range of the jet thrust coefficient, $C_{J_I}$, was from 0 to 2.31. The division of $C_{J_I}$ into its components; $C_{J_{JF}}$, $C_{\mu_{BLC}}$, $C_{\mu_{BLC_2}}$, $C_{\mu_a}$ is shown in figure 6 for the various configurations.

The horizontal tail was installed during part of the investigation and tested at several values of incidence. For two power-off runs, the nose fairing was installed and the model tested at two flap deflections; 0° and 60°.

## DATA ACQUISITION AND REDUCTION

### Data Acquisition

Six-component force data were obtained from the wind tunnel balance system. The moment center was located at the .35 $\bar{c}$ point and .20 $\bar{c}$ below the wing chord plane.

Total temperature and pressure within the duct were recorded for the locations shown in figure 5. The tailpipe mass flow and thrust were measured with a total pressure and temperature rake installed during a wind-off test prior to model assembly. These measurements were used to evaluate the tailpipe thrust and mass flow as functions of tailpipe total pressure and temperature which were recorded during the wind tunnel tests.

Other data obtained during the test included surface static pressures at three spanwise stations on the right wing ($\eta$ = .195, .467, .816), directional probe measurements of the downwash at the horizontal tail location, and photographs of wing surface tufts.

### Data Reduction

Blowing parameters – The thrusts for the three blowing slots on each wing were computed from the measured duct total pressures and temperatures and the measured areas for each slot. No correction was made for nozzle discharge or velocity efficiencies. Results of several wind-off tests indicated that the nozzle thrust coefficient (actual thrust/isentropic thrust) is approximately 0.85.

Force and moment data – The forces and moments due to the inlet momentum drag and the tailpipe thrust have been subtracted from all force and moment data presented. The inlet momentum drag was computed using the calibrations of the tailpipe for the core mass flow and the computed, isentropic mass flow from the blowing slots for the fan flow. The forces are resolved with respect to the wind axes while the moments are resolved with respect to the stability axes. The corrections for inlet momentum drag and tailpipe thrust are as follows:

$$C_L = C_{L_u} - C_T \sin \alpha$$

$$C_{D_c} = C_{D_u} + C_T \cos \alpha - C_{D_R}$$

$$C_{m_c} = C_{m_u} - .134\, C_T + C_{D_R} (.347 \cos \alpha - 2.816 \sin \alpha)$$

$$C_y = C_{y_u}$$

$$C_n = C_{n_u}$$

$$C_l = C_{l_u}$$

where $C_{L_u}$, $C_{D_u}$, $C_{m_u}$, $C_{y_u}$, $C_{n_u}$, $C_{l_u}$ are based on measured forces and moments and $\alpha$ is the corrected angle of attack.

Wind tunnel wall corrections – All of the data presented have been corrected for wind tunnel wall constraints. Conventional corrections are used, but the lift coefficient is replaced by the effective circulation lift coefficient, $C_{L_{aero}}$, defined as:

$$C_{L_{aero}} = C_L - \left(C_{J_{JF}} + C_{\mu_{BLC_1}} + C_{\mu_{BLC_2}}\right) \sin (\Delta f + \alpha)$$

(full-span flap)

$$C_{L_{aero}} = C_L - \left(C_{J_{JF}} + C_{\mu_{BLC_1}} + C_{\mu_{BLC_2}} + C_{\mu_a}\right) \sin (\Delta f + \alpha)$$

(part-span flap plus aileron)

where $\Delta f$ is a jet angle determined from wind-off tests.

The wind tunnel wall corrections are, therefore:

$$\alpha = \alpha_u + .453\, C_{L_{aero}}$$

$$C_D = C_{D_C} + .00793\, C_{L_{aero}}^2$$

and with the horizontal tail on,

$$C_m = C_{m_c} + .0326\, C_{L_{aero}} \quad .$$

## DATA PRESENTATION

The data are presented in figures 7 to 24. Table IV is an index to the data figures. The jet coefficients and dynamic pressures listed are nominal values.

## REFERENCES


1. Falarski, M. D.; Koenig, D. G.: Aerodynamic Characteristics of a Large-Scale Model with a Swept Wing and Augmented Jet Flap. NASA TM X-62,029, July, 1971.

2. Falarski, M. D.; Koenig, D. G.: Longitudinal and Lateral Stability and Control Characteristics of a Large-Scale Model with a Swept Wing and Augmented Jet Flap. NASA TM X-62,145, April, 1972.

3. Falarski, M. D.; Koenig, D. G.: Longitudinal Aerodynamic Characteristics of a Large-Scale Model with a Swept Wing and Augmented Jet-Flap in Ground Effect. NASA TM X-62,174, October, 1972.

TABLE I. — MODEL REFERENCE DIMENSIONS

| | | |
|---|---|---|
| **Wing** | | |
| Area, sq m (sq ft) | | 21.37 (230.0) |
| Aspect ratio | | 8.00 |
| Taper ratio | | 0.30 |
| Span, m (ft) | | 13.080 (42.895) |
| Root chord, m (ft) | | 2.510 (8.250) |
| Tip chord, m (ft) | | .750 (2.475) |
| Mean aerodynamic chord, m (ft) | | 1.790 (5.881) |
| Sweep at 1/4 chord, deg | | 27.5 |
| Airfoil section (see Table II) | NACA | 65A - 4 XX |
| | root t/c = | .125 |
| | tip t/c = | .105 |
| Incidence, twist | | 0 |
| **Vertical Tail** | | |
| Area, sq m (sq ft) | | 6.32 (68.0) |
| Aspect ratio | | 1.20 |
| Taper ratio | | .74 |
| Span, m (ft) | | 2.760 (9.04) |
| Root chord, m (ft) | | 2.630 (8.65) |
| Tip chord, m (ft) | | 1.950 (6.40) |
| Mean aerodynamic chord, m (ft) | | 2.310 (7.58) |
| Sweep at 1/4 chord, deg | | 38.5 |
| Airfoil section | NACA | 0012 |
| Volume coefficient | | .114 |
| **Horizontal Tail** | | |
| Area, sq m (sq ft) | | 6.72 (72.3) |
| Aspect ratio | | 4.00 |
| Taper ratio | | .49 |
| Span, m (ft) | | 2.590 (8.50) |
| Root chord, m (ft) | | 1.740 (5.71) |
| Tip chord, m (ft) | | .850 (2.80) |
| Mean aerodynamic chord, m (ft) | | 1.350 (4.42) |
| Sweep at 1/4 chord, deg | | 25 |
| Airfoil section (inverted) | NACA | 64-012 |
| Volume coefficient | | 1.038 |

TABLE II. — WING AIRFOIL COORDINATES, $\eta$ = .1945

| Basic Airfoil x/c (100) | Z upper/c | Z lower/c |
|---|---|---|
| 0 | 0 | 0 |
| .0625 | .0054 | -.0023 |
| .125 | .0071 | -.0033 |
| .25 | .0093 | -.0048 |
| .375 | .0109 | -.0059 |
| .50 | .0123 | -.0069 |
| .625 | .0134 | -.0077 |
| .75 | .0146 | -.0085 |
| 1.0 | .0166 | -.0099 |
| 1.25 | .0184 | -.0110 |
| 1.50 | .0200 | -.0120 |
| 1.75 | .0215 | -.0129 |
| 2.00 | .0228 | -.0137 |
| 2.50 | .0253 | -.0150 |
| 5.00 | .0350 | -.0192 |
| 7.50 | .0432 | -.0224 |
| 10.00 | .0501 | -.0252 |
| 15.00 | .0613 | -.0293 |
| 20.00 | .0700 | -.0322 |
| 25.00 | .0767 | -.0343 |
| 30.00 | .0817 | -.0356 |
| 35.00 | .0853 | -.0362 |
| 36.25 | .0859 | -.0363 |
| 40.00 | .0873 | -.0361 |
| 45.00 | .0878 | -.0353 |
| 50.00 | .0866 | -.0334 |
| 55.00 | .0836 | -.0305 |
| 57.50 | .0815 | -.0288 |
| 60.00 | .0791 | -.0269 |
| 65.00 | .0732 | -.0227 |
| 69.50 | .0667 | -.0188 |
| 69.831 | .0662 | -.0185 |
| 70.00 | .0660 | -.0183 |
| 75.00 | .0576 | -.0139 |
| 80.00 | .0478 | -.0099 |
| 85.00 | .0365 | -.0070 |
| 90.00 | .0246 | -.0046 |
| 92.50 | .0185 | -.0035 |
| 95.00 | .0125 | -.0024 |
| 97.00 | .0076 | -.0016 |
| 98.00 | .0052 | -.0012 |
| 99.00 | .0027 | -.0007 |
| 100.00 | .0003 | -.0003 |

TABLE II. – CONCLUDED

Slat Inner Surface

| x/c (100) | Z upper/c | Z lower/c |
|---|---|---|
| 2.50 | -.0030 | -.0030 |
| 2.625 | .0028 | .0088 |
| 2.75 | .0052 | .0110 |
| 3.00 | .0086 | .0137 |
| 3.25 | .0112 | .0154 |
| 3.50 | .0134 | .0165 |
| 3.75 | .0154 | .0173 |
| 4.00 | .0172 | .0178 |
| 4.25 | .0189 | .0182 |
| 4.50 | .0204 | .0185 |
| 4.75 | .0219 | |
| 5.00 | .0233 | |
| 5.50 | .0260 | |
| 6.00 | .0285 | |
| 6.50 | .0308 | |
| 7.00 | .0330 | |
| 7.50 | .0352 | |
| 8.00 | .0373 | |
| 9.00 | .0412 | |
| 10.00 | .0450 | |
| 11.00 | .0487 | |
| 12.00 | .0522 | |
| 13.00 | .0556 | |
| 14.00 | .0590 | |

Flap Upper Contour

| x/c (100) | Z upper/c |
|---|---|
| 58.347 | -.0201 |
| 58.50 | -.0148 |
| 58.75 | -.0083 |
| 59.00 | -.0028 |
| 60.00 | .0139 |
| 61.00 | .0262 |
| 62.00 | .0358 |
| 63.00 | .0435 |
| 64.00 | .0497 |
| 65.00 | .0546 |
| 66.00 | .0585 |
| 67.00 | .0613 |
| 68.00 | .0633 |
| 69.00 | .0644 |
| 70.00 | .0647 |
| 71.00 | .0641 |
| 71.50 | .0635 |
| 72.00 | .0627 |

TABLE III. - INDEX TO RUNS

T-2.5

| | TUNNEL | | | BLOWING | WING | | | | TAIL | | | | REMARKS | FIGURE |
|---|---|---|---|---|---|---|---|---|---|---|---|---|---|---|
| RUN | $q$ psf | $\alpha$ deg | $\beta$ deg | $C_J$ | $\delta_f$ deg | $\delta_s$ deg | $\delta_a$ deg | $\delta_e$ deg | $i_t$ deg | $\delta_{se}$ deg | $\delta_e$ deg | $\delta_r$ deg | | |
| 1 | 0 | 0 | 0 | — | 60/60 | 45 | — | 0 | OFF | —— | | 0 | STATIC CALIBRATION | — |
| 2 | 0 | | | — | | | | | | | | | POLARS | — |
| 3 | 0 | | | — | | | | | | | | | | — |
| 4 | 11.5 | ~ | | 0 | | | | | | | | | | 73 |
| 5 | 23.9 | | | .32 | | | | | | | | | | 70 |
| 6 | 5.8 | | | .31 | | | | | | | | | | 79 |
| 7 | 5.8 | | | .88 | | | | | | | | | | 79 |
| 8 | 11.7 | | | .66 | | | | | | | | | | 71 |
| 9 | 17.5 | | | .45 | | | | | | | | | | 71 |
| 10 | 17.5 | | | .25 | | | | | | | | | | 71 |
| 11 | 5.8 | | | .72 | | | | | | | | | | — |
| 12 | 5.8 | | | 1.31 | | 45/60/80 | | | | | | | | — |
| 13 | 5.8 | | | 1.31 | | | | 0/-16 | | | | | | — |
| 14 | 0 | 0 | | — | 60/30 | | | 0 | | | | | STATIC CALIBRATION | — |
| 15 | 5.8 | ~ | | 1.49 | | | | | | | | | POLARS | 75 |
| 16 | 8.7 | | | 1.00 | | | | | | | | | | 76 |
| 17 | 11.7 | | | .74 | | | | | | | | | | 76 |
| 18 | 17.5 | | | .50 | | | | | | | | | | 76 |
| 19 | 17.5 | | | .25 | | | | | | | | | | 76 |
| 20 | 99! | | | 0 | | | | | | | | | | 73 |

TABLE III.- CONTINUED

T-415

| | TUNNEL | | | FLOWING | WING | | | | TAIL | | | | REMARKS | FIGURE |
|---|---|---|---|---|---|---|---|---|---|---|---|---|---|---|
| RUN | q psf | α deg | β deg | $C_J$ | $\delta_f$ deg | $\delta_s$ deg | $\delta_a$ deg | $\delta_c$ deg | $i_t$ deg | $\delta_{sp}$ deg | $\delta_e$ deg | $\delta_r$ deg | | |
| 21 | 9.9 | ~ | 0 | 0 | 60/30 | 45 | — | 0 | OFF | —— | | 0 | POLARS | 7c, 8a |
| 22 | 5.8 | | | 1.48 | | 60 | | | | | | | | 7c |
| 23 | 8.8 | | | .99 | | | | | | | | | | 7c |
| 24 | 11.7 | | | .74 | | | | | | | | | | 7c |
| 25 | 17.3 | | | .51 | | | | | | | | | | 7c |
| 26 | 17.3 | | | .23 | | | | | | | | | | 7c |
| 27 | 0 | 0 | | — | 60 | | 30 | | | | | | STATIC CALIBRATION | — |
| 28 | 4.5 | ~ | | 1.73 | | | | | | | | | POLARS | 8a |
| 29 | 2.7 | | | 1.15 | | | | | | | | | | 8a |
| 30 | 0 | | | .85 | | | | | | | | | | 8a |
| 31 | 13.4 | | | .38 | | | | | | | | | | 8a |
| 32 | 12.6 | | | .30 | | | | | | | | | | 8a |
| 33 | 0 | 0 | | — | | | | 30 | | | | | STATIC CALIBRATION | — |
| 34 | 4.4 | ~ | | 1.75 | | | | | | | | | POLARS | 8a |
| 35 | 6.6 | | | 1.16 | | | | | | | | | | 8a |
| 36 | 13.4 | | | .58 | | | | | | | | | | 8a |
| 37 | 9.9 | | | 0 | | | | | | | | | | 8a |
| 38 | 0 | 0 | | — | | | | 30 | | | | | STATIC CALIBRATION | — |
| 39 | 4.4 | ~ | | 1.77 | | | | | | | | | POLARS | 8a |
| 40 | 6.6 | | | 1.17 | | | | | | | | | | 8a |

TABLE III. - CONTINUED

T-45

| | TUNNEL | | | BLOWING | WING | | | | TAIL | | | | REMARKS | FIGURE |
|---|---|---|---|---|---|---|---|---|---|---|---|---|---|---|
| RUN | $q$ psf | $\alpha$ deg | $\beta$ deg | $C_\mu$ | $\delta_f$ deg | $\delta_s$ deg | $\delta_a$ deg | $\delta_{sc}$ deg | $i_t$ deg | $\delta_{st}$ deg | $\delta_e$ deg | $\delta_r$ deg | | |
| 41 | 13.4 | ~ | 0 | .58 | 60 | 30 | 30 | 50 | OFF | —— | 0 | | POLARS | 3a |
| 42 | 9.9 | | | 0 | | | | | | | | | | 3a |
| 43 | 4.5 | | | 1.73 | | | | 0 | | | | | | -- |
| 44 | 0 | 0 | | — | 30 | | | | | | | | STATIC CALIBRATION | — |
| 45 | 4.9 | ~ | | 1.50 | | | | | | | | | POLARS | 5a |
| 46 | 7.5 | | | 1.00 | | | | | | | | | | 5a |
| 47 | 9.9 | | | .77 | | | | | | | | | | 5a |
| 48 | 14.7 | | | .51 | | | | | | | | | | 5a |
| 49 | 18.4 | | | .29 | | | | | | | | | | 5a |
| 50 | 9.7 | | | 0 | | | | | | | | | | 15a |
| 51 | 4.9 | | | 1.52 | | | | 30 | | | | | | 5c |
| 52 | 7.4 | | | 1.00 | | | | | | | | | | 5c |
| 53 | 14.6 | | | .51 | | | | | | | | | | 5c |
| 54 | 9.9 | | | 0 | | | | | | | | | | 5c |
| 55 | 0 | 0 | | — | | | | | | | | | STATIC CALIBRATION | — |
| 56 | 5.0 | ~ | | 1.95 | | | | 50 | | | | | POLARS | 15a |
| 57 | 7.5 | | | .97 | | | | | | | | | | 15a |
| 58 | 14.7 | | | .50 | | | | | | | | | | 15a |
| 59 | 10.0 | | | 0 | | | | | | | | | | 15a |
| 60 | 0 | 0 | | — | 30/30 | | — | 0 | | | | | STATIC CALIBRATION | — |

TABLE III – CONTINUED

| | TUNNEL | | | BLOWING | | WING | | | | TAIL | | | | REMARKS | FIGURE |
|---|---|---|---|---|---|---|---|---|---|---|---|---|---|---|---|
| RUN | $q$ psf | $\alpha$ deg | $\beta$ deg | $C_J$ | | $\delta_f$ deg | $\delta_s$ deg | $\delta_a$ deg | $\delta_c$ deg | $i_t$ deg | $\delta_{se}$ deg | $\delta_e$ deg | $\delta_r$ deg | | |
| 61 | 5.2 | ~ | 0 | 1.51 | | 30/30 | 60 | — | 0 | OFF | —— | | 0 | BLANK | 43 |
| 62 | 7.9 | | | .99 | | | | | | | | | | | 45 |
| 63 | 10.5 | | | .75 | | | | | | | | | | | 46 |
| 64 | 15.6 | | | .51 | | | | | | | | | | | 47 |
| 65 | 17.3 | | | .26 | | | | | | | | | | | 48 |
| 66 | 9.7 | | | 0 | | | | | | | | | | | 49 |
| 67 | 5.2 | | | 1.50 | | | | | 30 | | | | | | 50 |
| 68 | 7.9 | | | 1.00 | | | | | | | | | | | 51 |
| 69 | 5.7 | | | .51 | | | | | | | | | | | 52 |
| 70 | 9.7 | | | 0 | | | | | | | | | | | 53 |

TABLE III. – CONTINUED

T-418

| | TUNNEL | | | FLOWING | WING | | | | TAIL | | | | REMARKS | FIGURE |
|---|---|---|---|---|---|---|---|---|---|---|---|---|---|---|
| Run | q psf | α deg | β deg | $C_T$ | $\delta_f$ deg | $\delta_s$ deg | $\delta_a$ deg | $\delta_e$ deg | $i_t$ deg | $\delta_{sr}$ deg | $\delta_e$ deg | $\delta_r$ deg | | |
| 1 | 0 | 0 | 0 | – | 00/30 | 60 | — | 0 | OFF | —— | | 0 | STATIC CALIBRATION | – |
| 2 | 3.3 | ~ | | 2.31 | | | | | | | | | BASIC POLARS, LANDING $\delta_f$ | 7d |
| 3 | 4.9 | | | 1.57 | | | | | | | | | | 7d |
| 4 | 6.7 | | | 1.15 | | | | | | | | | | 7d |
| 5 | 10.0 | | | .77 | | | | | | | | | | 7d |
| 6 | 0 | 0 | | – | | | | | | | | | NOISE | – |
| 7 | 0 | | | – | 60 | | 30 | | | | | | STATIC CALIBRATION | – |
| 8 | 4.8 | ~ | | .55 | | | | | | | | | POLARS | 8a, 20a |
| 9 | 7.2 | | | .39 | | | | | | | | | | 8b, 20a |
| 10 | 14.5 | | | .21 | | | | | | | | | | 8c, 20a |
| 11 | 14.5 | | 18 | .51 | | | | | | | | | DISTORTION CHECK | – |
| 12 | 7.2 | | 0 | 1.02 | | | | 40 | | | | | POLARS, ASYM. $\delta_e$ | 8f |
| 13 | 14.7 | | | .51 | | | | | | | | | | 8f |
| 14 | 7.3 | | | 1.09 | | | | 10 | | | | | | 8c |
| 15 | 14.5 | | | .52 | | | | | | | | | | 8c |
| 16 | 7.3 | | | 1.05 | | | | 0/40 | | | | | POLARS, ASYM. $\delta_e$ | 12b, 20d |
| 17 | 14.6 | | | .53 | | | | | | | | | | 12b, 20d |
| 18 | 7.3 | | | 1.05 | | | | 0/-20 | | | | | | 12a, 20c |
| 19 | 14.5 | | | .53 | | | | | | | | | | 12a, 20c |
| 20 | 7.6 | | | 87 | | | | 0 | | | | | POLARS, TWICE CUBIC NORMAL | 7 |

TABLE III.- CONTINUED

T-413

| Run | INNER: V pps | INNER: α deg | INNER: β deg | ELEVATOR: $C_J$ | WING: $\delta_f$ deg | WING: $\delta_s$ deg | WING: $\delta_a$ deg | WING: $\delta_c$ deg | TAIL: $i_t$ deg | TAIL: $\delta_{s_t}$ deg | TAIL: $\delta_e$ deg | TAIL: $\delta_r$ deg | REMARKS | FIGURE |
|---|---|---|---|---|---|---|---|---|---|---|---|---|---|---|
| 21 | 14.5 | ~ | 0 | .59 | 60 | 60 | 30 | 0 | OFF | —— | | 0 | POLARS TWICE SYMM. NORMAL | 11 |
| 22 | 21.4 | | | .30 | | | | | | | | | | 11 |
| 23 | 4.8 | | | 1.62 | | | 30/10 | | | | | | POLARS DIFF. $\delta_a$ | 13, 21 |
| 24 | 7.2 | | | 1.08 | | | | | | | | | | 13, 21 |
| 25 | 14.5 | | | .59 | | | | | | | | | | 13, 21 |
| 26 | 4.8 | | | 1.59 | | | 30 | 20 | | | | | POLARS, SYM. $\delta_c$ | 8d, 20a |
| 27 | 7.3 | | | 1.05 | | | | | | | | | | 8d, 20b |
| 28 | 14.5 | | | .53 | | | | | | | | | | 8d, 20b |
| 29 | 9.6 | | | 0 | | | | | | | | | | 8d, 20 |
| 30 | 4.8 | | | 1.59 | | | 10 | 0 | | | | | POLARS $10^\circ$ $\delta_a$ | 10 |
| 31 | 7.2 | | | 1.07 | | | | | | | | | | 10 |
| 32 | 14.5 | | | .54 | | | | | | | | | | 10 |
| 33 | 9.6 | | | 0 | | | | | | | | | | 10 |
| 34 | 0 | 0 | | — | 30 | | 30 | | | | | | STATIC CALIBRATION | — |
| 35 | 5.0 | ~ | | 1.49 | | | | | | | | | BASIC POLARS, TAKEOFF $\delta_f$ | 15b, 23a |
| 36 | 7.4 | | | 1.01 | | | | | | | | | | 15b, 23a |
| 37 | 19.6 | | | .51 | | | | | | | | | | 15b, 23a |
| 38 | 4.8 | | | 1.53 | | | 0/-20 | | | | | | POLARS, ASYM. $\delta_a$ | 17a, 22b |
| 39 | 7.2 | | | 1.03 | | | | | | | | | | 17a, 22b |
| 40 | 14.5 | | | .52 | | | | | | | | | | 17a, 22b |

TABLE III. - CONTINUED

T-418

| | TUNNEL | | | FLOWING | WING | | | | TAIL | | | | REMARKS | FIGURE | |
|---|---|---|---|---|---|---|---|---|---|---|---|---|---|---|---|
| RUN | q psf | α deg | β deg | $C_J$ | $\delta_f$ deg | $\delta_s$ deg | $\delta_a$ deg | $\delta_c$ deg | $i_t$ deg | $\delta_{sf}$ deg | $\delta_e$ deg | $\delta_r$ deg | | | |
| 41 | 5.0 | ~ | 0 | 1.50 | 30 | 60 | 30 | 0/20 | OFF | —— | | 0 | POLARS, ASYM. $\delta_c$ | 17b, | 23c |
| 42 | 7.4 | | | 1.02 | | | | | | | | | | 17b, | 23c |
| 43 | 14.5 | | | .52 | | | | | | | | | | 17b, | 23c |
| 44 | 4.8 | | | 1.59 | | | | 0/40 | | | | | | 17c | 23d |
| 45 | 7.2 | | | 1.06 | | | | | | | | | | 17c, | 23d |
| 46 | 7.3 | | | 1.02 | | | | 0 | 0 | 40 | 0 | | BASIC POLARS, TAIL ON | 16b | |
| 47 | 7.3 | | | 1.03 | | | | | -5 | | | | | 16b | |
| 48 | 7.3 | | | 1.03 | | | | | -15 | | | | | 16b, | |
| 49 | 4.9 | | | 1.53 | | | | | | | | | | 16b | |
| 50 | 14.5 | | | .52 | | | | | | | | | | 16b | |
| 51 | 9.6 | | | 0 | | | | | | | | | | 16b | |
| 52 | 4.9 | 4 | ~ | 1.52 | | | | | | | | | BASIC YAWLERS | 24a | |
| 53 | 7.3 | | | 1.02 | | | | | | | | | | 24a | |
| 54 | 7.3 | 12 | | 1.02 | | | | | | | | | | 24b | |
| 55 | 14.6 | | | .51 | | | | | | | | | | 24b | |
| 56 | 14.6 | 4 | | .51 | | | | | | | | | | 24b | |
| 57 | 4.9 | 12 | | 1.52 | | | | | | | | | | 24b | |
| 58 | 9.6 | | | 0 | | | | | | | | | | 24b | |
| 59 | 9.6 | 4 | | 0 | | | | | | | | | | 24b | |
| 60 | 7.1 | ~ | 0 | 1.04 | 60 | | | | | | | | BASIC POLARS, TAIL ON | — | |

TABLE III. - CONTINUED

T-418

| | TUNNEL | | | BLOWING | WING | | | | TAIL | | | | REMARKS | FIGURE |
|---|---|---|---|---|---|---|---|---|---|---|---|---|---|---|
| RUN | $q$ psf | $\alpha$ deg | $\beta$ deg | $C_J$ | $\delta_f$ deg | $\delta_s$ deg | $\delta_a$ deg | $\delta_c$ deg | $i_t$ deg | $\delta_{st}$ deg | $\delta_e$ deg | $\delta_r$ deg | | |
| 61 | 7.1 | ~ | 0 | 1.06 | 60 | 60 | 30 | 20 | -20 | 40 | 0 | 0 | BASIC POLARS, TAIL ON | - |
| 62 | 7.1 | | | 1.06 | | | | | -15 | | | | | - |
| 63 | 7.1 | | | 1.06 | | | | | -10 | | | | | 9b |
| 64 | 7.1 | 0 | | 1.06 | | | | | ~ | | | | TAIL INCIDENCE SWEEP | - |
| 65 | 4.8 | ~ | | 1.59 | | | | | -10 | | | | BASIC POLARS, TAIL ON | 9b |
| 66 | 9.6 | | | .79 | | | | | | | | | | 9b |
| 67 | 19.6 | | | .52 | | | | | | | | | | 9b |
| 68 | 21.2 | | | .27 | | | | | | | | | | 9b |
| 69 | 14.5 | 4 | ~ | .52 | | | | | | | | | BASIC YAWLERS | 22b |
| 70 | 14.5 | 12 | | .52 | | | | | | | | | | 22c |
| 71 | 7.3 | | | 1.05 | | | | | | | | | | 22c |
| 72 | 7.2 | 4 | | 1.06 | | | | | | | | | | 22b |
| 73 | 4.8 | | | 1.58 | | | | | | | | | | 22b |
| 74 | 4.8 | 12 | | 1.59 | | | | | | | | | | 22c |
| 75 | 9.5 | | | 0 | | | | | | | | | | 22c |
| 76 | 9.5 | 4 | | 0 | | | | | | | | | | 22b |
| 77 | 9.5 | ~ | 0 | 0 | | | | | | | | | | — |
| 78 | 4.8 | | | 1.56 | | | | 0 | | | | | BASIC POLARS | 9a |
| 79 | 7.3 | | | 1.05 | | | | | | | | | | 9a |
| 80 | 9.7 | | | .78 | | | | | | | | | | 9a |

TABLE III.- CONCLUDED

T-418

| Run | Tunnel | | | Flowing | Wing | | | | Tail | | | | Remarks | Figure |
|---|---|---|---|---|---|---|---|---|---|---|---|---|---|---|
| | q psf | α deg | β deg | $C_J$ | $\delta_f$ deg | $\delta_s$ deg | $\delta_a$ deg | $\delta_c$ deg | $i_t$ deg | $\delta_{st}$ deg | $\delta_e$ deg | $\delta_r$ deg | | |
| 81 | 14.5 | ~ | 0 | .53 | 60 | 60 | 30 | 0 | -10 | 40 | 0 | 0 | Basic Pol | 9a |
| 82 | 21.4 | | | .27 | | | | | | | | | | 9a |
| 83 | 7.3 | 4 | ~ | 1.05 | | | | | | | | | Yawers | 22a |
| 84 | 7.3 | 12 | | 1.05 | | | | | | | | | | 22a |
| 85 | 9.6 | ~ | 0 | 0 | | | | | | | | | Polars | 9a |
| 86 | 4.9 | | | 1.54 | | | | 40 | | | | | | 9c |
| 87 | 7.3 | | | 1.03 | | | | | | | | | | 9c |
| 88 | 9.6 | | | .79 | | | | | | | | | | 9c |
| 89 | 14.5 | | | .52 | | | | | | | | | | 9c |
| 90 | 7.2 | 4 | ~ | .84 | | | | | | | | | Yawers | 22a |
| 91 | 7.2 | 12 | | 1.09 | | | | | | | | | | 22a |
| 92 | 21.3 | ~ | 0 | .27 | | | | | | | | | Polars | 9c |
| 93 | 4.9 | | | 1.28 | | | | | | | | | Polar; $C_{J_L} = 1.5\, C_{J_R}$ | — |
| 94 | 9.7 | | | 0 | | | | | | | | | Polar | 9c |
| 95 | ~ | 0,8 | | 0 | | | | 0 | | | | | Nose Fairing on, Noise | — |
| 96 | 9.6 | -8, ~ | | 0 | 0 | | 0 | | ~0 | | | | $i_t$ sweep, Polar | — |
| 97 | 9.6 | -8, 0 | | 0 | | | | | ~0 | OFF | | | | 18, 19 |
| 98 | ~ | 0,8 | | 0 | | | | | 0 | | | | Noise | — |
| 99 | ~ | — | — | — | — | — | — | — | — | — | — | — | Noise, Model Out | — |

REPRODUCIBILITY OF THE ORIGINAL PAGE IS POOR

## TABLE IV.- INDEX TO FIGURES

### LONGITUDINAL DATA

| FIGURE | | EFFECT OF | VARIABLES | $\delta_f$ | $\delta_a$ | $\delta_c$ | $\delta_s$ | HOR. $i_t$, TAIL |
|---|---|---|---|---|---|---|---|---|
| 7 | a | $C_{JI}$ | $\alpha, \delta_f, \delta_s$ | 60/60 | — | 0 | 1-45 | OFF |
| | b | | | 60/30 | | | | |
| | c | | | | | | 1-60 | |
| | d | | | | | | 2-60 | |
| 8 | a | $C_{JI}$ | $\alpha, \delta_c$ | 60 | 30 | 0 | 1-60 | |
| | b | | | | | | 2-60 | |
| | c | | | | | 10 | | |
| | d | | | | | 20 | | |
| | e | | | | | 30 | 1-60 | |
| | f | | | | | 40 | 2-60 | |
| | g | | | | | 50 | 1-60 | |
| 9 | a | $C_{JI}$ | $\alpha, \delta_c$ | 60 | 30 | 0 | 2-60 | -10 |
| | b | | | | | 20 | | |
| | c | | | | | 40 | | |
| 10 | | $C_{JI}$ | $\alpha$ | 60 | 10 | 0 | | OFF |
| 11 | | $C_{JI}$ | $\alpha, C_{HBLC}$ | 60 | 30 | 0 | | |
| 12 | a | $C_{JI}$ | $\alpha, \delta_c$ | 60 | 30 | 0/-20 | | |
| | b | | | | | 0/40 | | |
| 13 | | $C_{JI}$ | $\alpha$ | 60 | 30/10 | 0 | | |
| 14 | a | $C_{JI}$ | $\alpha, \delta_c$ | 30/30 | — | 0 | 1-60 | |
| | b | | | | | 30 | | |
| 5 | a | $C_{JI}$ | $\alpha, \delta_c$ | 30 | 30 | 0 | | |
| | b | | | | | | 2-60 | |
| | c | | | | | 20 | 1-60 | |
| | d | | | | | 50 | | |
| 16 | a | $C_{JI}$ | $\alpha$ | 30 | 30 | 0 | 2-60 | -15 |
| | b | | | | | | | ~ |
| 17 | a | $C_{JI}$ | $\alpha, \delta_c$ | 30 | 30 | 0/-20 | | OFF |
| | b | | | | | 0/20 | | |
| | c | | | | | 0/40 | | |
| 18 | | BASE RUN | $\alpha$ | 0 | 0 | 0 | 2-60 | 0 |
| 19 | | " | " | 0 | 0 | 0 | " | ~ |

## TABLE IV. - CONCLUDED

### LATERAL - DIRECTIONAL DATA

| FIGURE | EFFECT OF | VARIABLE | $\delta_f$ | $\delta_a$ | $\delta_c$ | $\delta_s$ | HOR. TAIL $i_t$ |
|---|---|---|---|---|---|---|---|
| 20 a | $C_{J_I}$ | $\alpha$, $\delta_c$ | 60 | 30 | 0 | 2-60 | OFF |
| b | | | | | 20 | | |
| c | | | | | 0/-20 | | |
| d | | | | | 0/40 | | |
| 21 | $C_{J_I}$ | $\alpha$ | 60 | 30/10 | 0 | | |
| 22 a | $\alpha$ | $\beta$, $\alpha$ | 60 | 30 | 0 | | -10 |
| b | $C_{J_I}$ | | | | 20 | | |
| c | | | | | | | |
| d | $\alpha$ | | | | 40 | | |
| 23 a | $C_{J_I}$ | $\alpha$, $\delta_c$ | 30 | 30 | 0 | | OFF |
| b | | | | | 0/-20 | | |
| c | | | | | 0/20 | | |
| d | | | | | 0/40 | | |
| 24 a | $C_{J_I}$ | $\beta$, $\alpha$ | 30 | 30 | 0 | | -15 |
| b | | | | | | | |

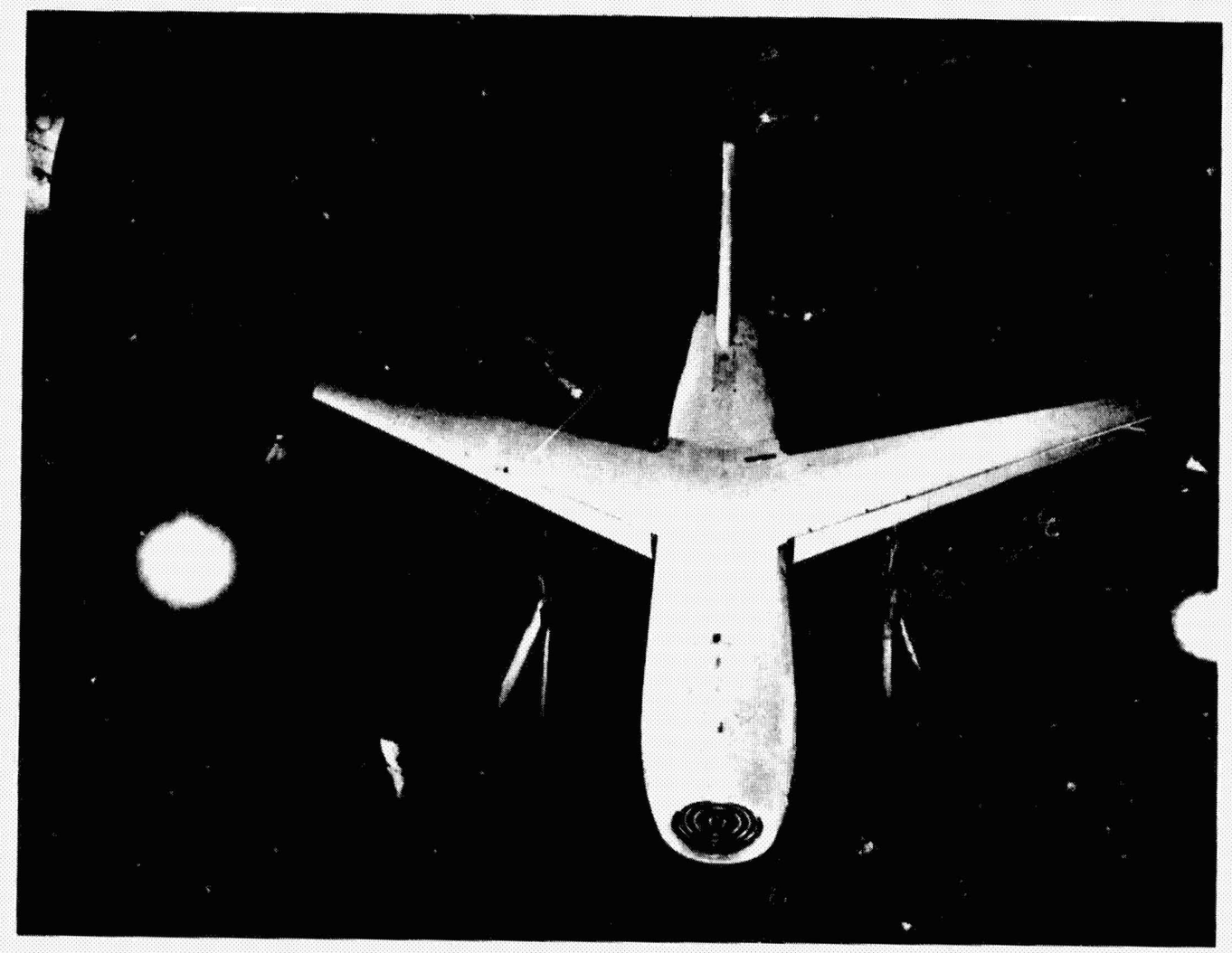

(a) Top view of model.

Figure 1. — Views of the model installed in the Ames 40- by 80-foot Wind Tunnel.

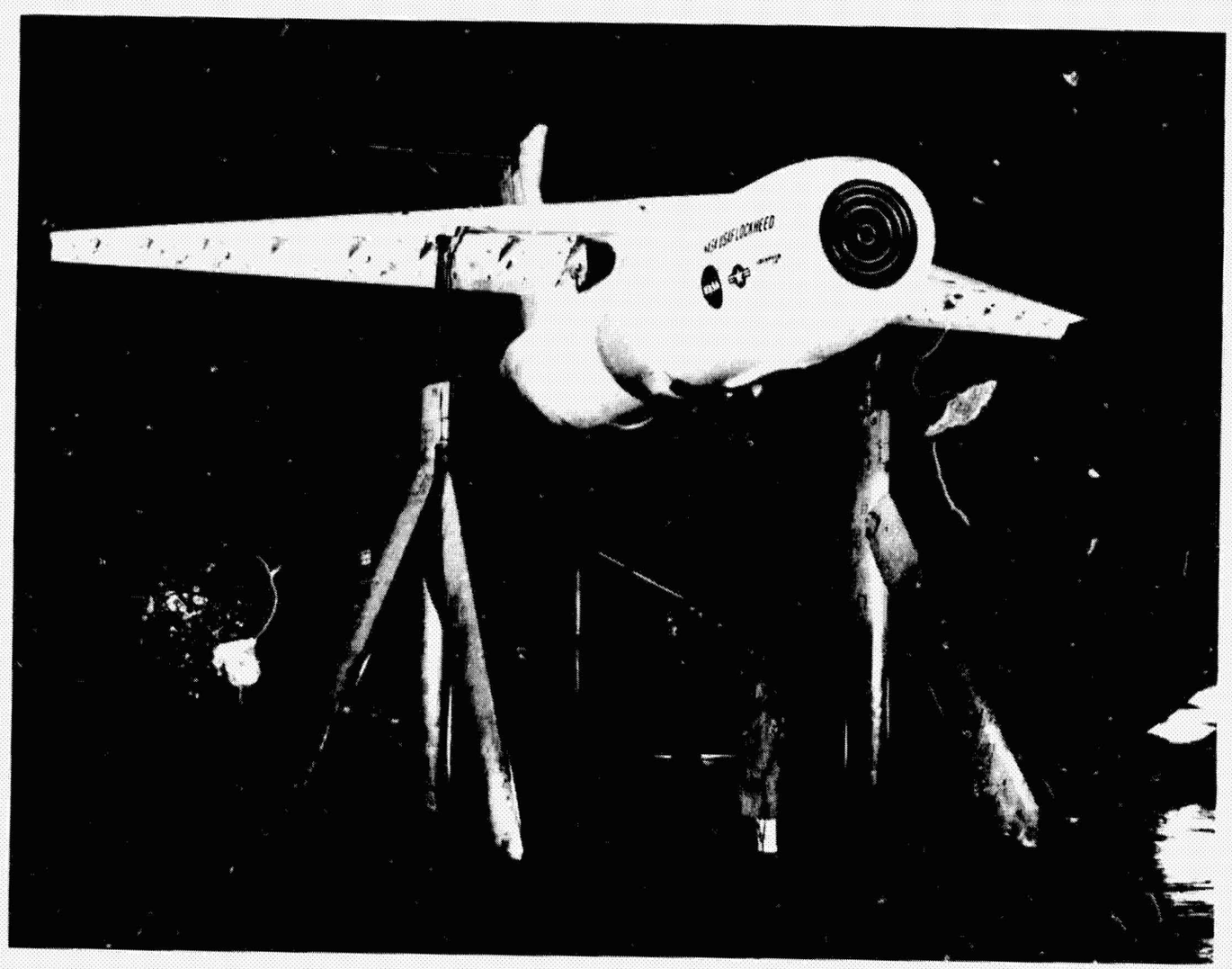


(b) Front view of model.

Figure 1. — Continued.

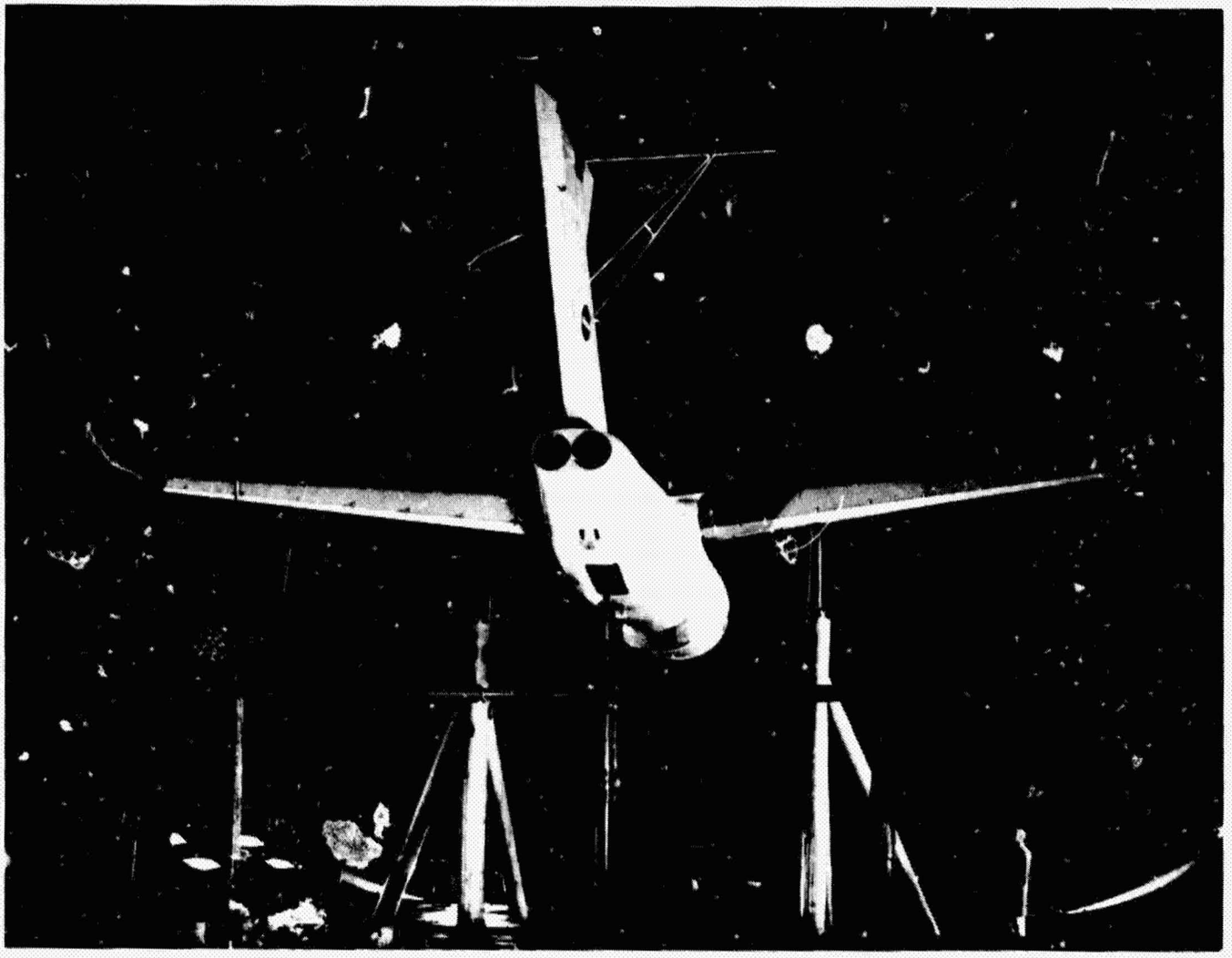

(c) Rear view of model.

Figure 1. — Continued.

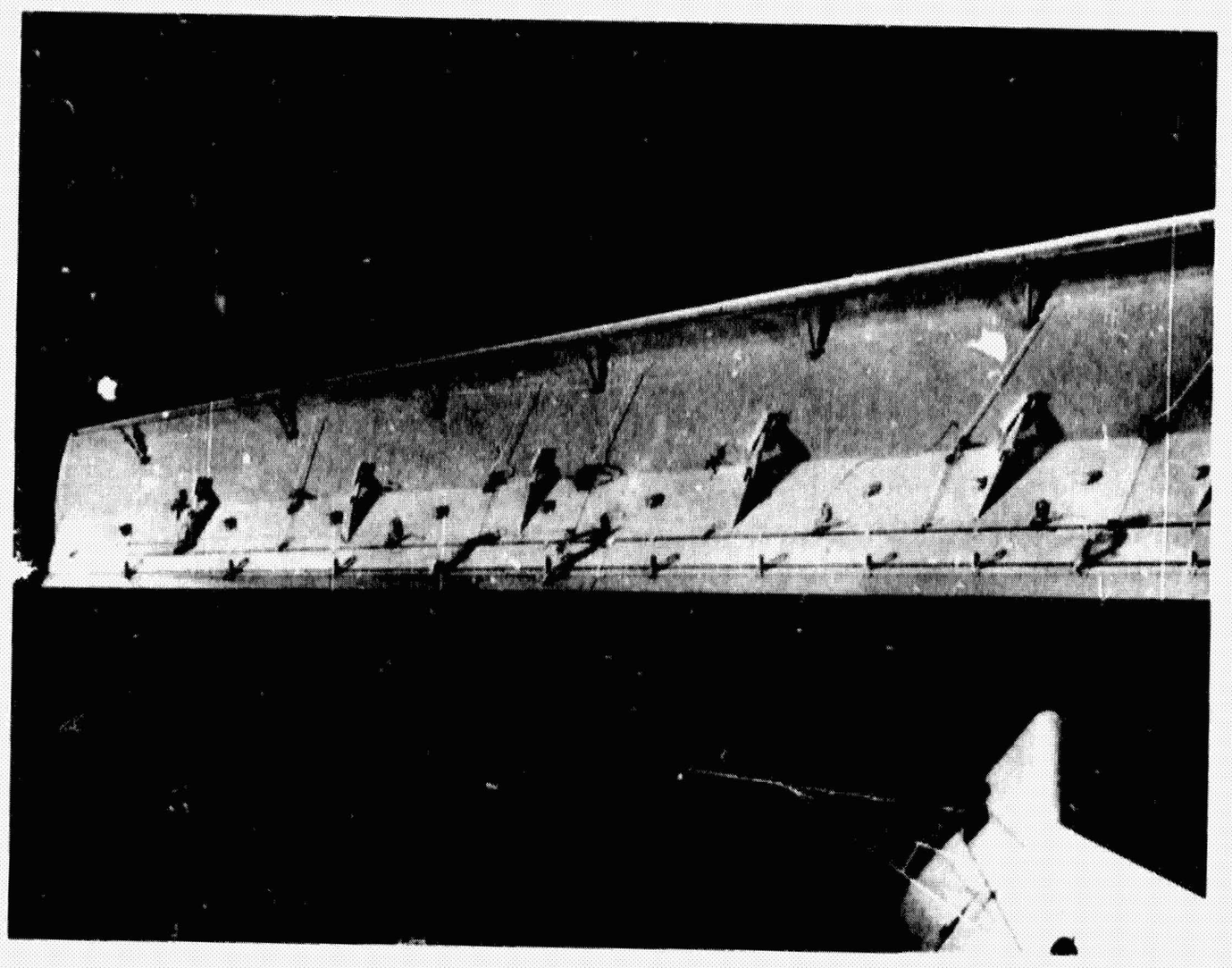

(d) View of the lower wing surface.

Figure 1. — Continued

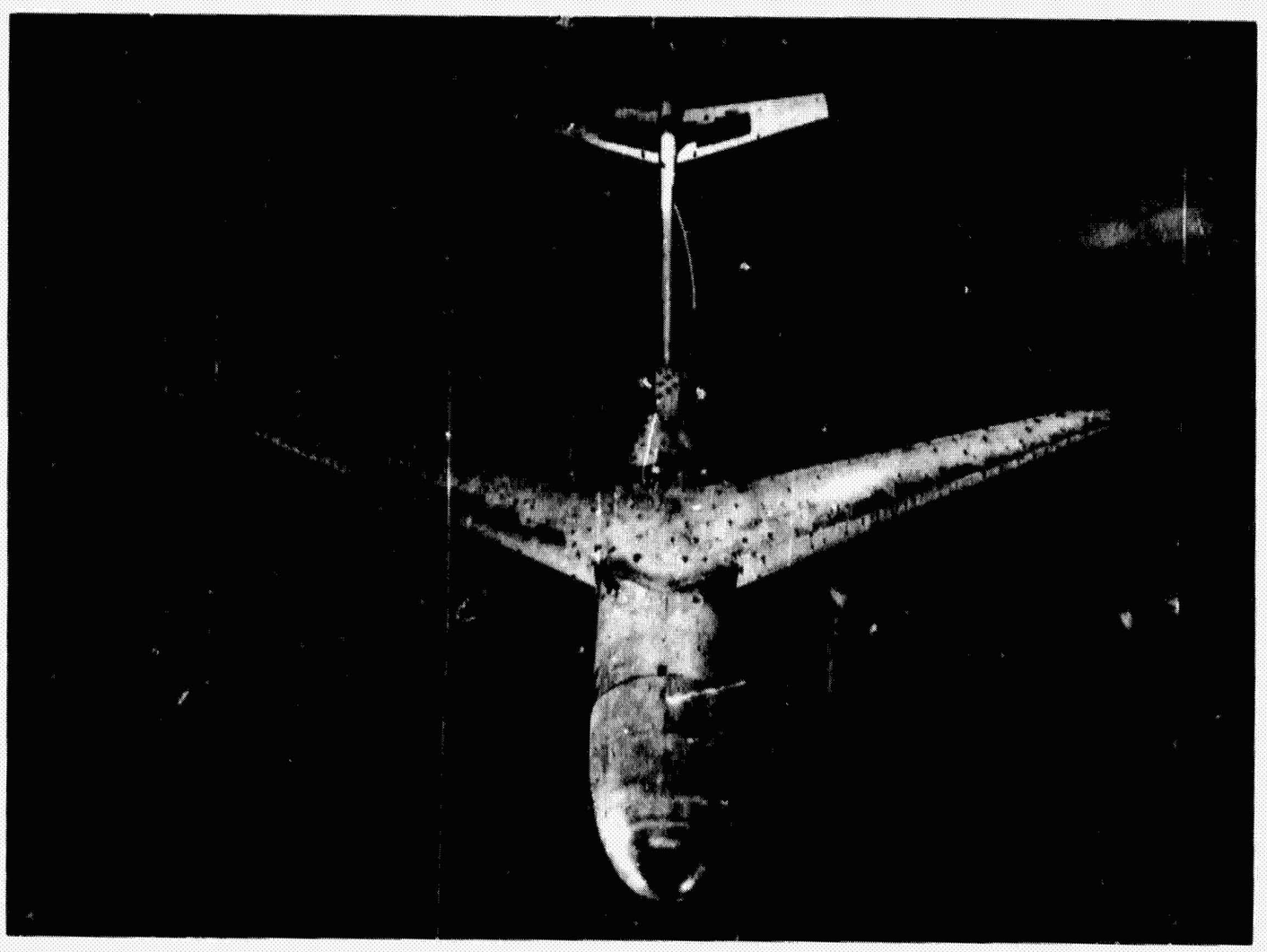

(e) Top view of model with horizontal tail and nose fairing installed.

Figure 1. – Concluded.

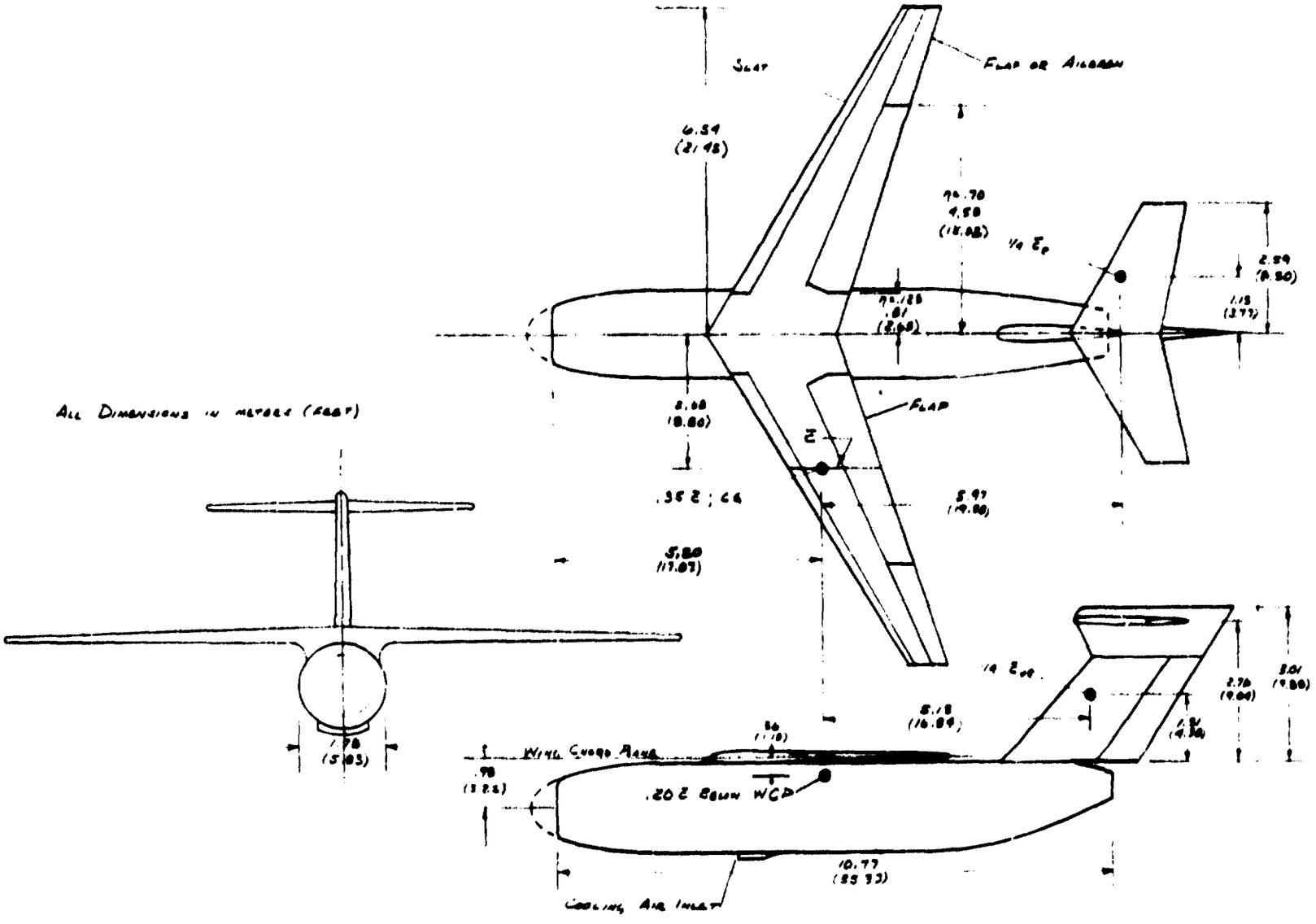


(a) Three-view sketch of the model.

Figure 2. — Geometric details of the model.

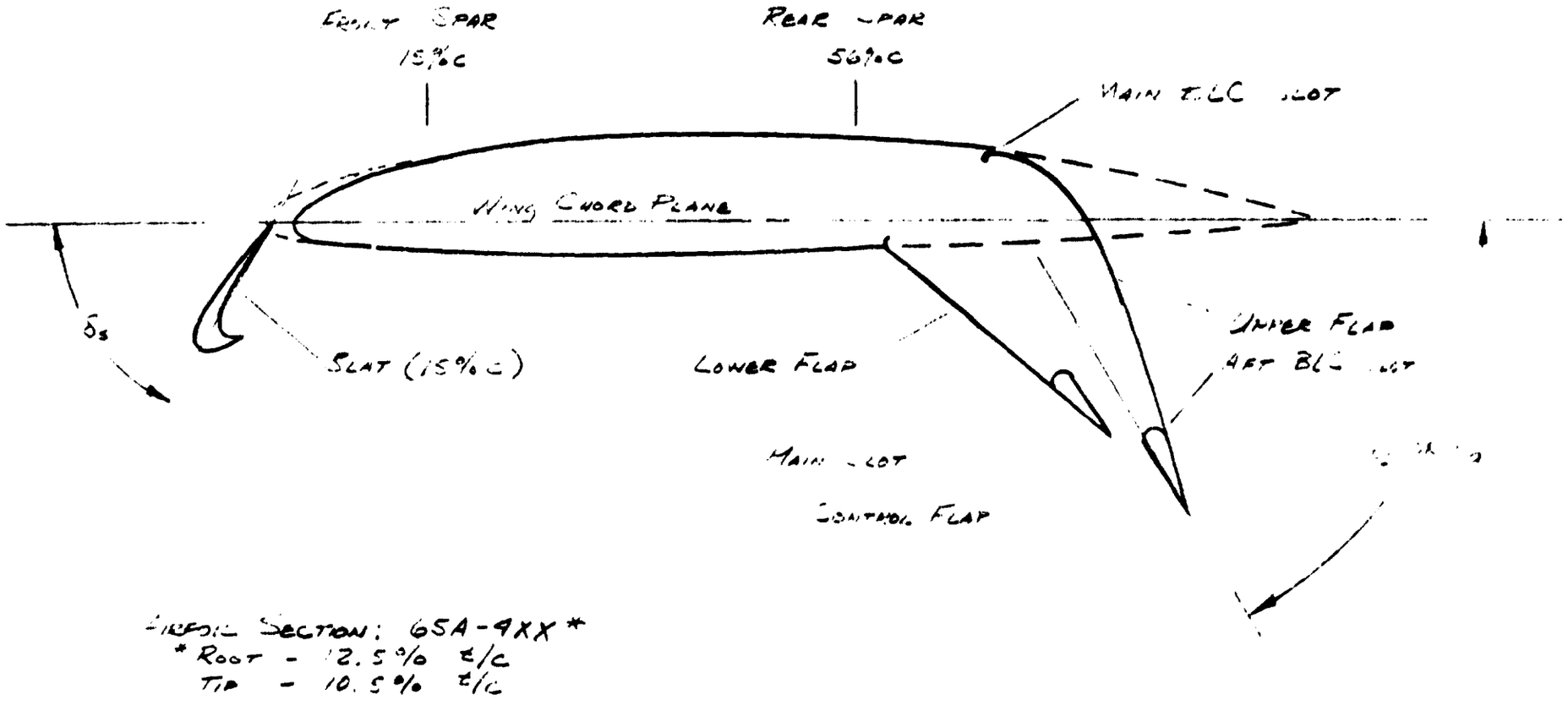


(b) Wing section geometry.

Figure 2. — Continued

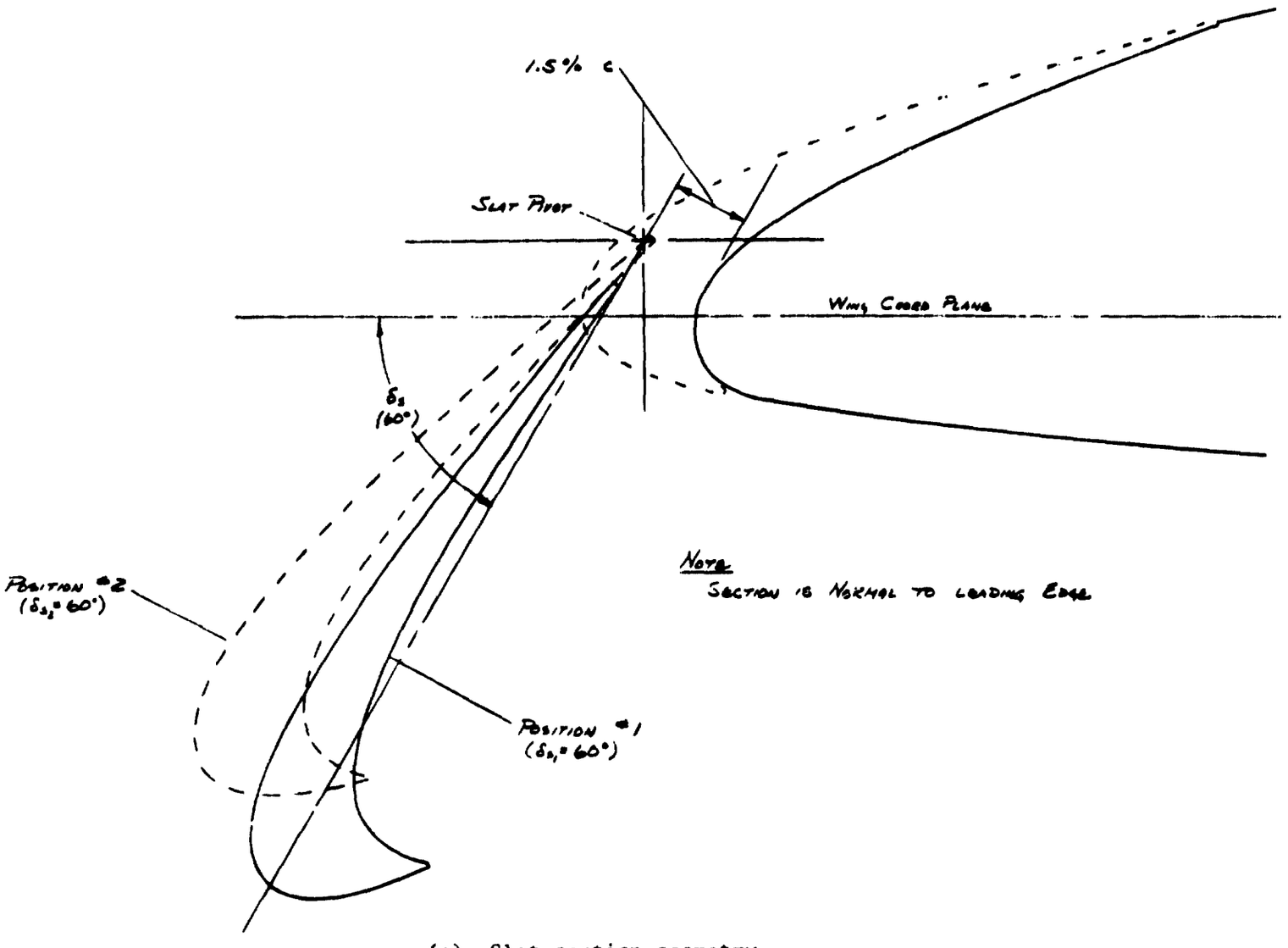


(c) Slat section geometry.

Figure 2. – Continued.

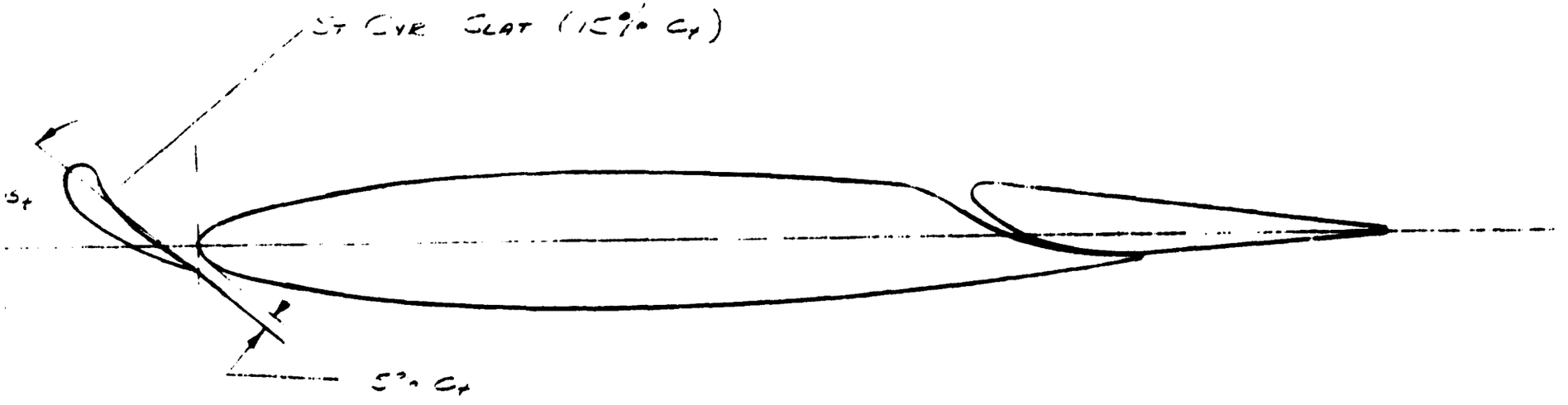


(d) Horizontal tail section geometry.

Figure 2. — Continued.

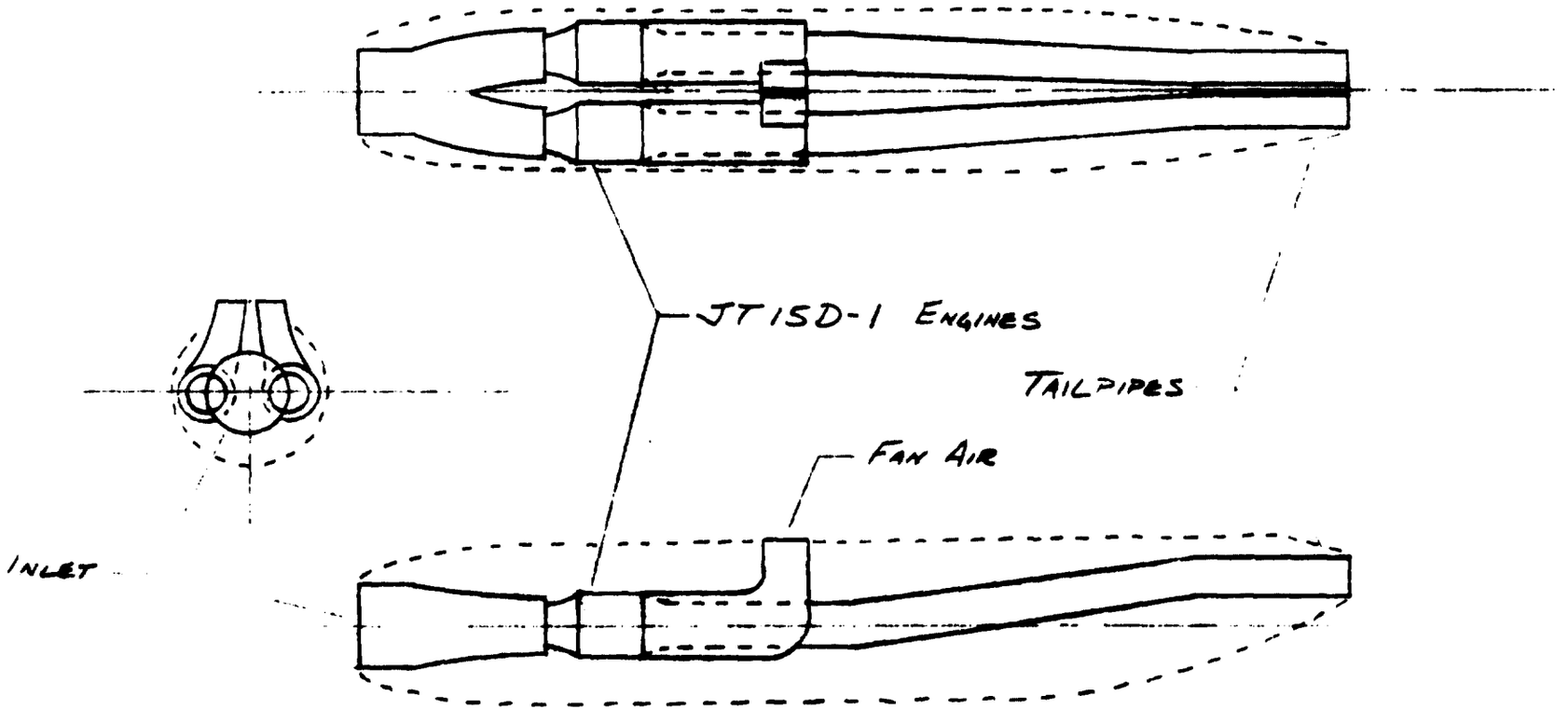


(e) Schematic of the air supply system.

Figure 2. – Continued.

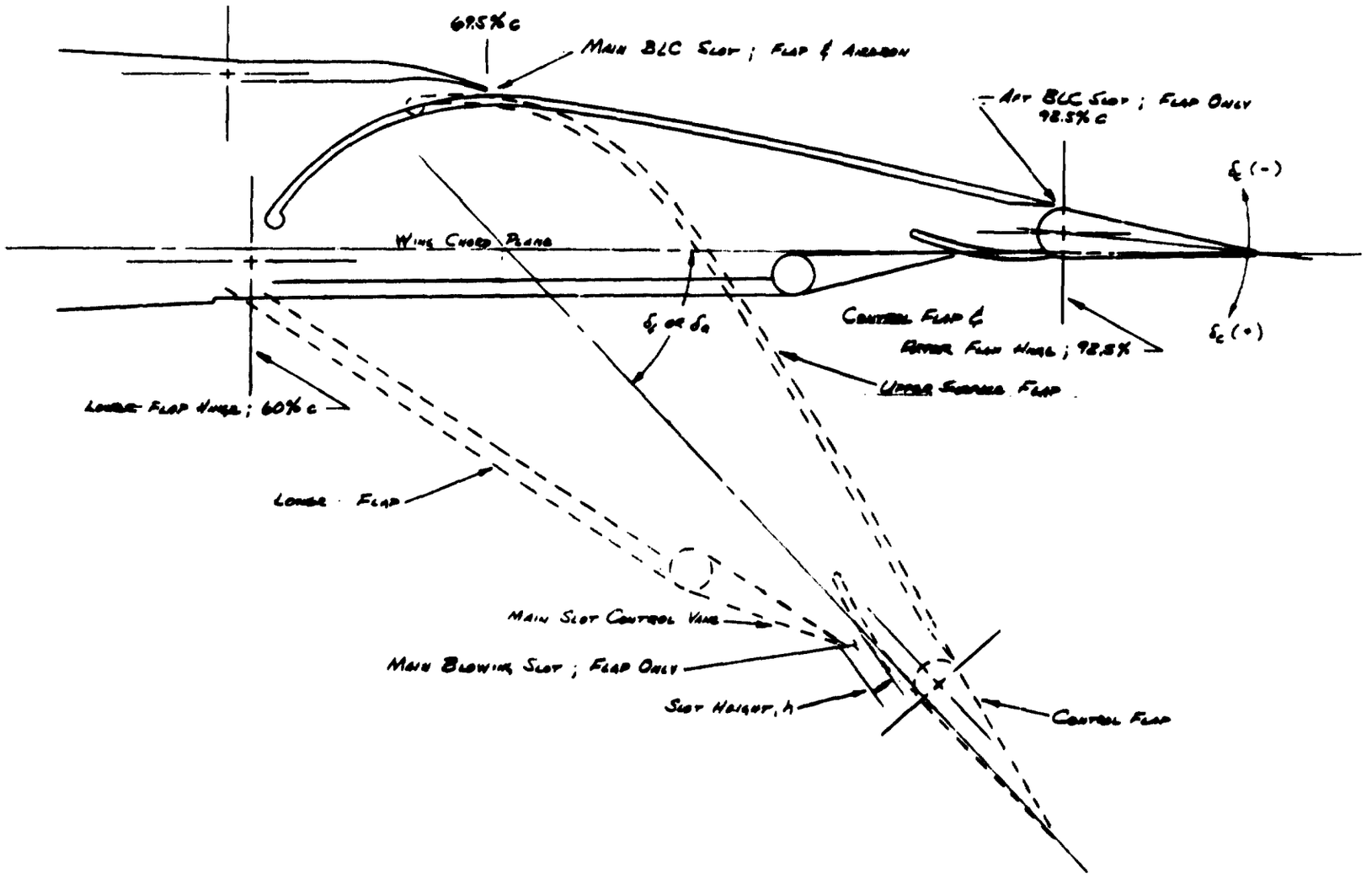


(f) Flap section geometry.

Figure 2. — Concluded.

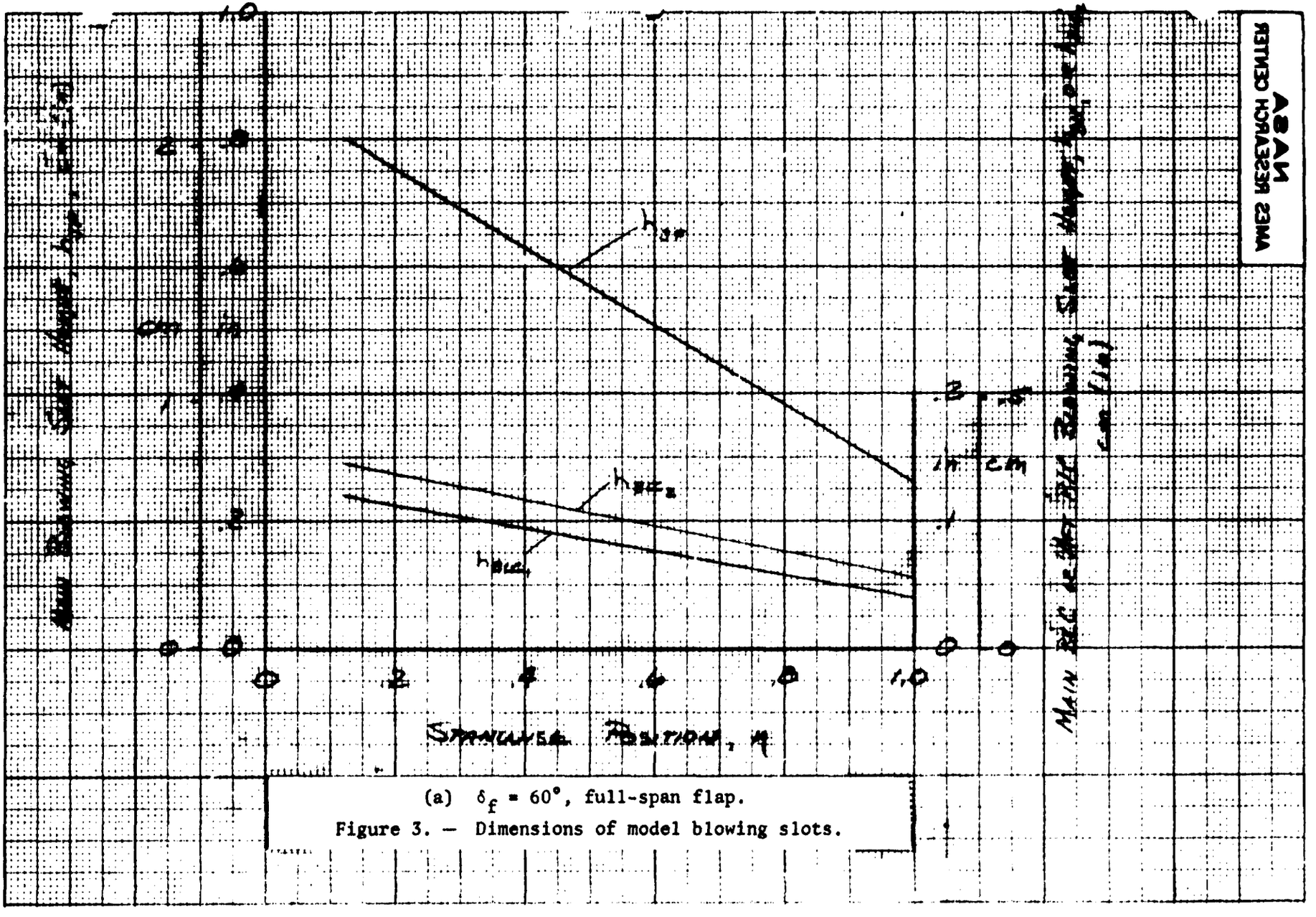

(a) $\delta_f = 60°$, full-span flap.

Figure 3. — Dimensions of model blowing slots.

(b) $\delta_f = 60°$, part-span flap.

Figure 3. — Continued.

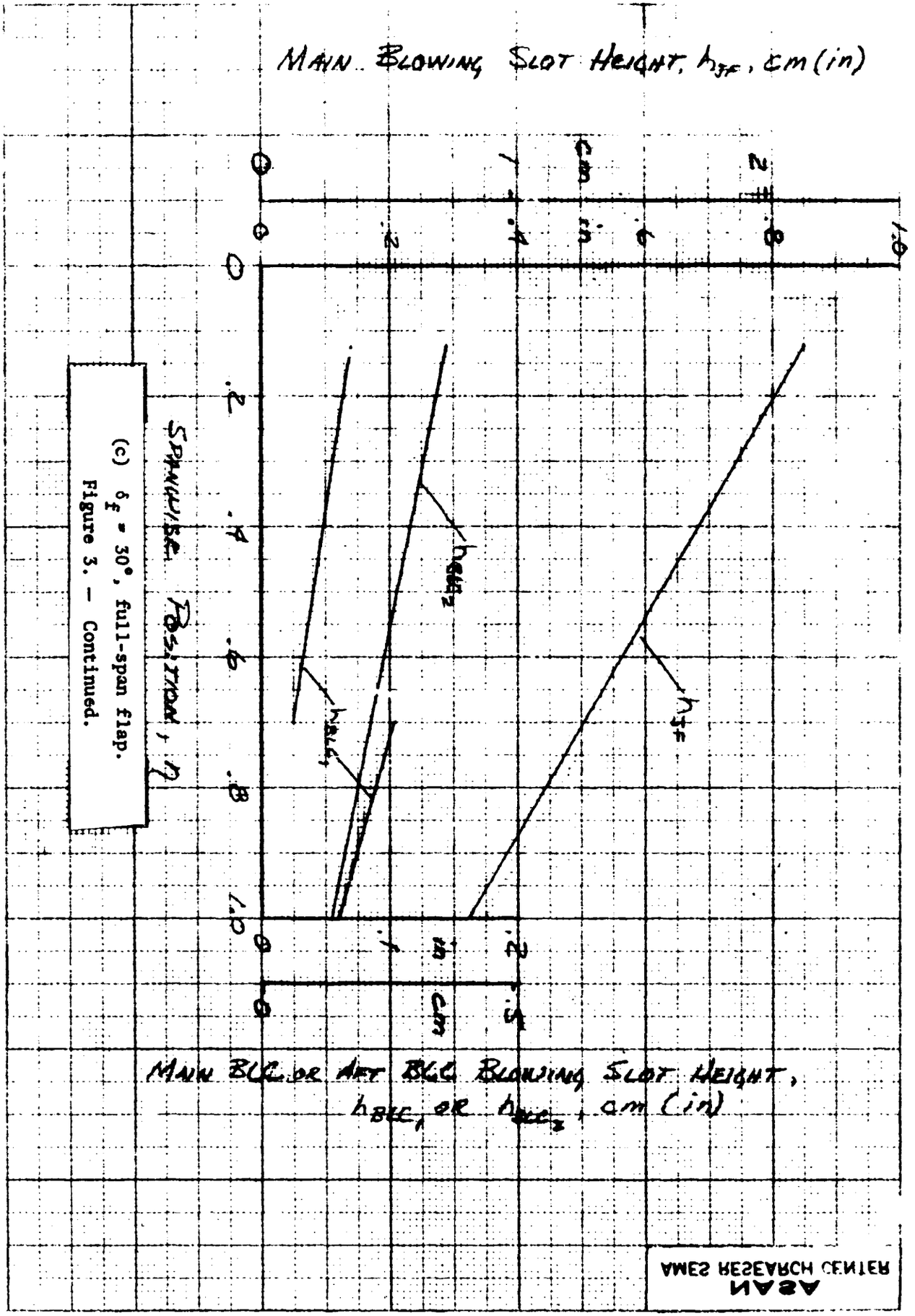


(c) $\delta_f = 30°$, full-span flap.

Figure 3. — Continued.

(d) $\delta_f = 30°$, part-span flap.

Figure 3. — Concluded.

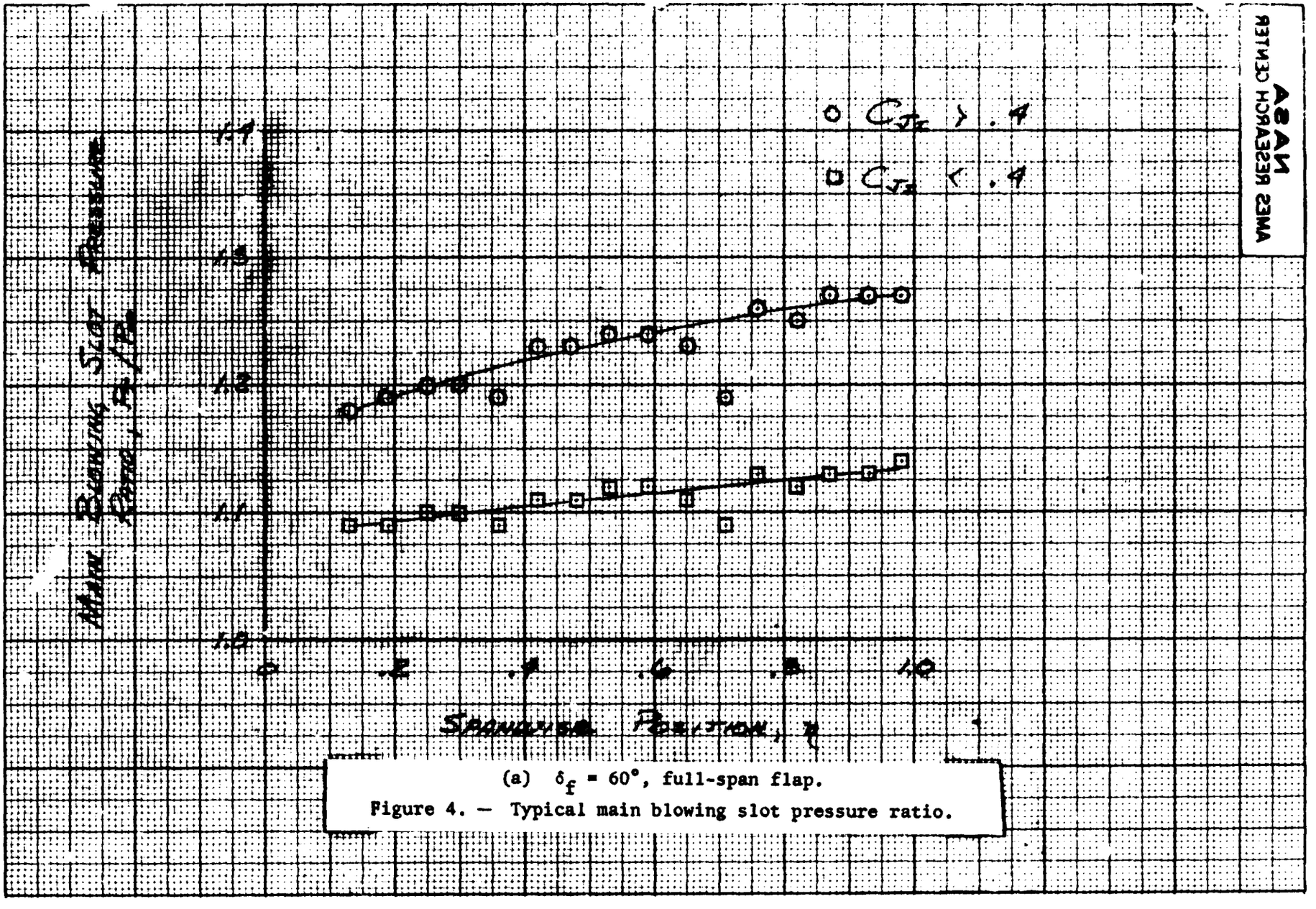


(a) $\delta_f = 60°$, full-span flap.

Figure 4. — Typical main blowing slot pressure ratio.

(b) $\delta_f = 60°$, part-span flap.

Figure 4. — Continued.

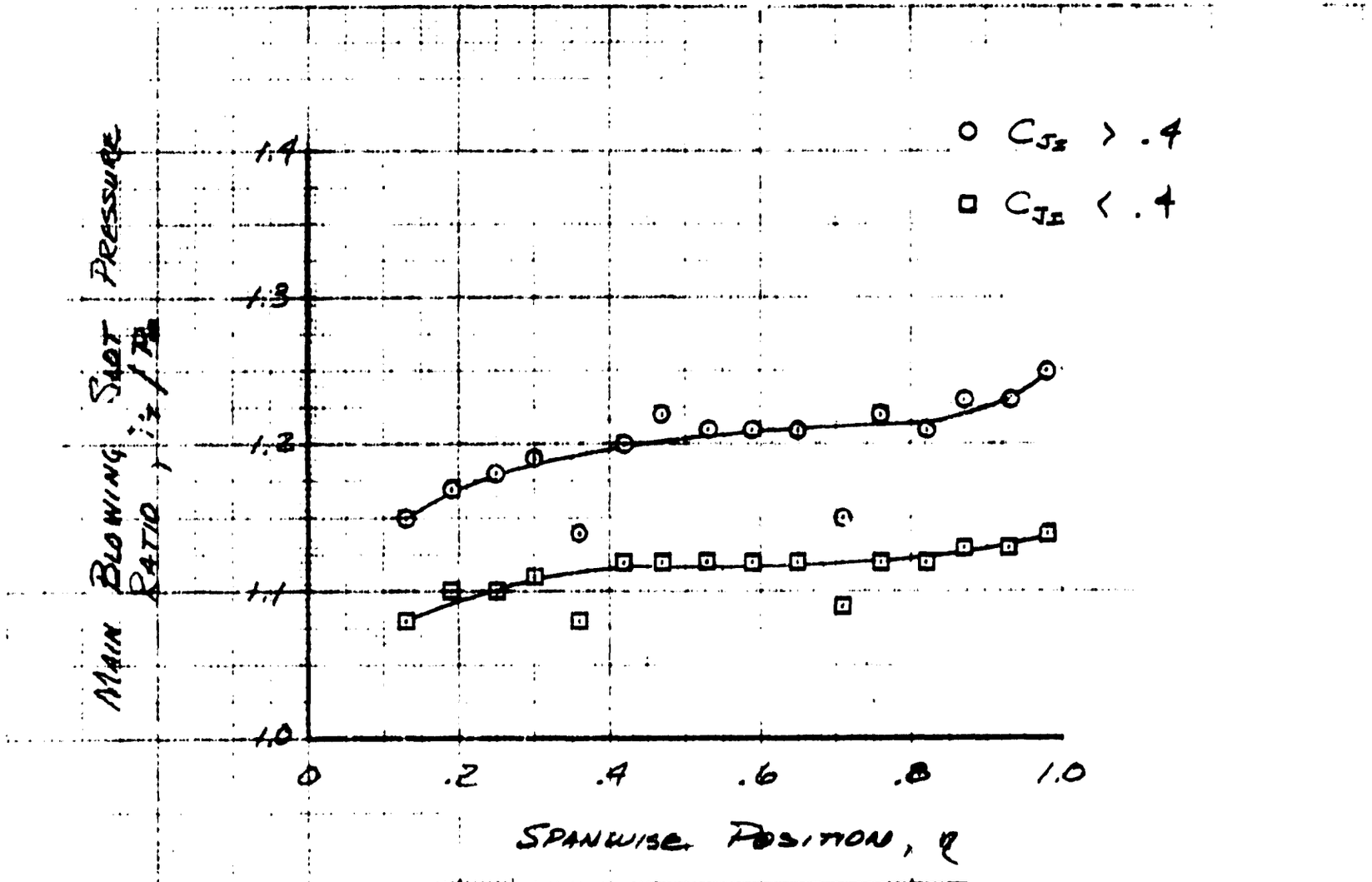


(c) $\delta_f = 30°$, full-span flap.

Figure 4. – Continued.

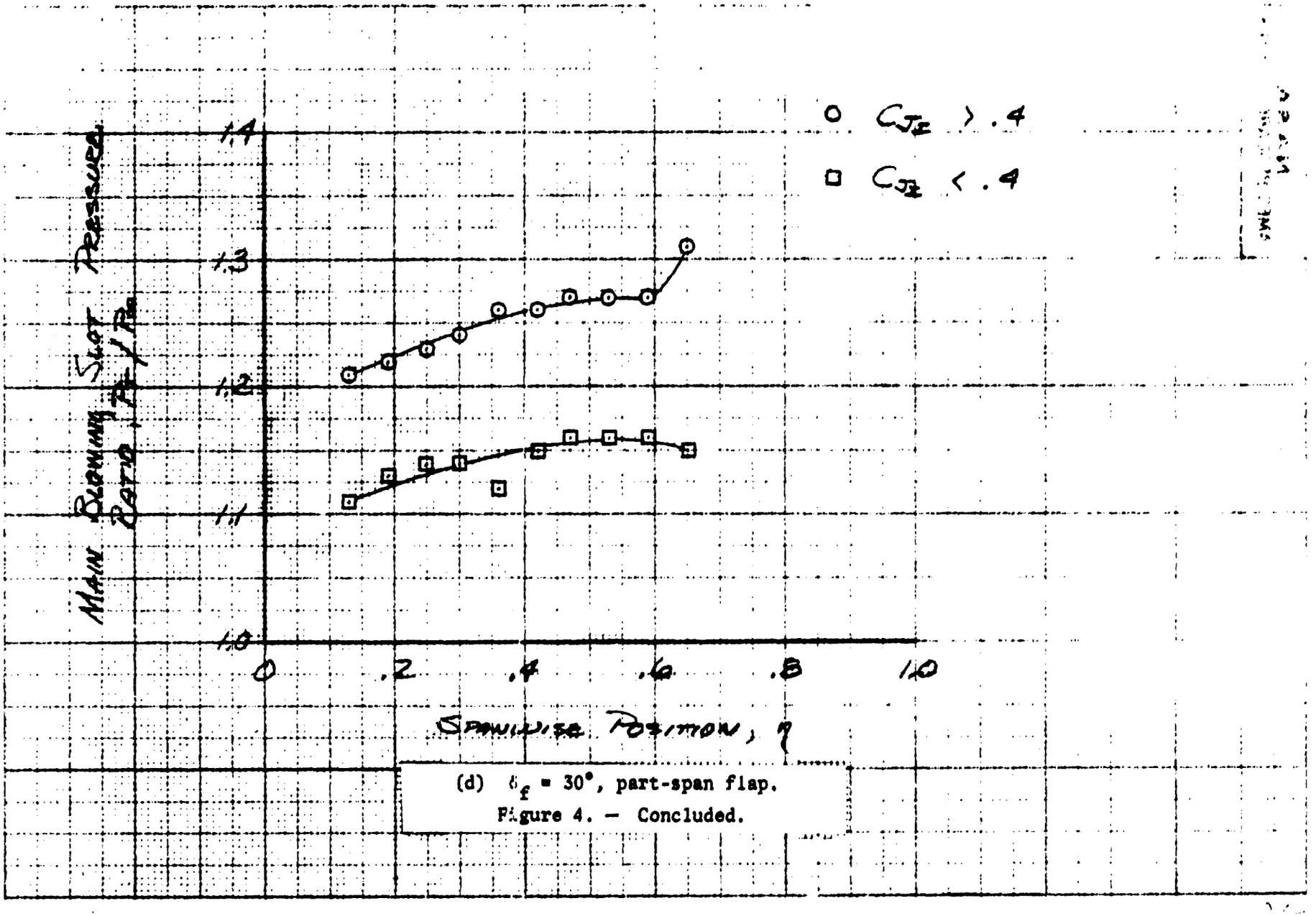


(d) $\delta_f = 30°$, part-span flap.

Figure 4. — Concluded.

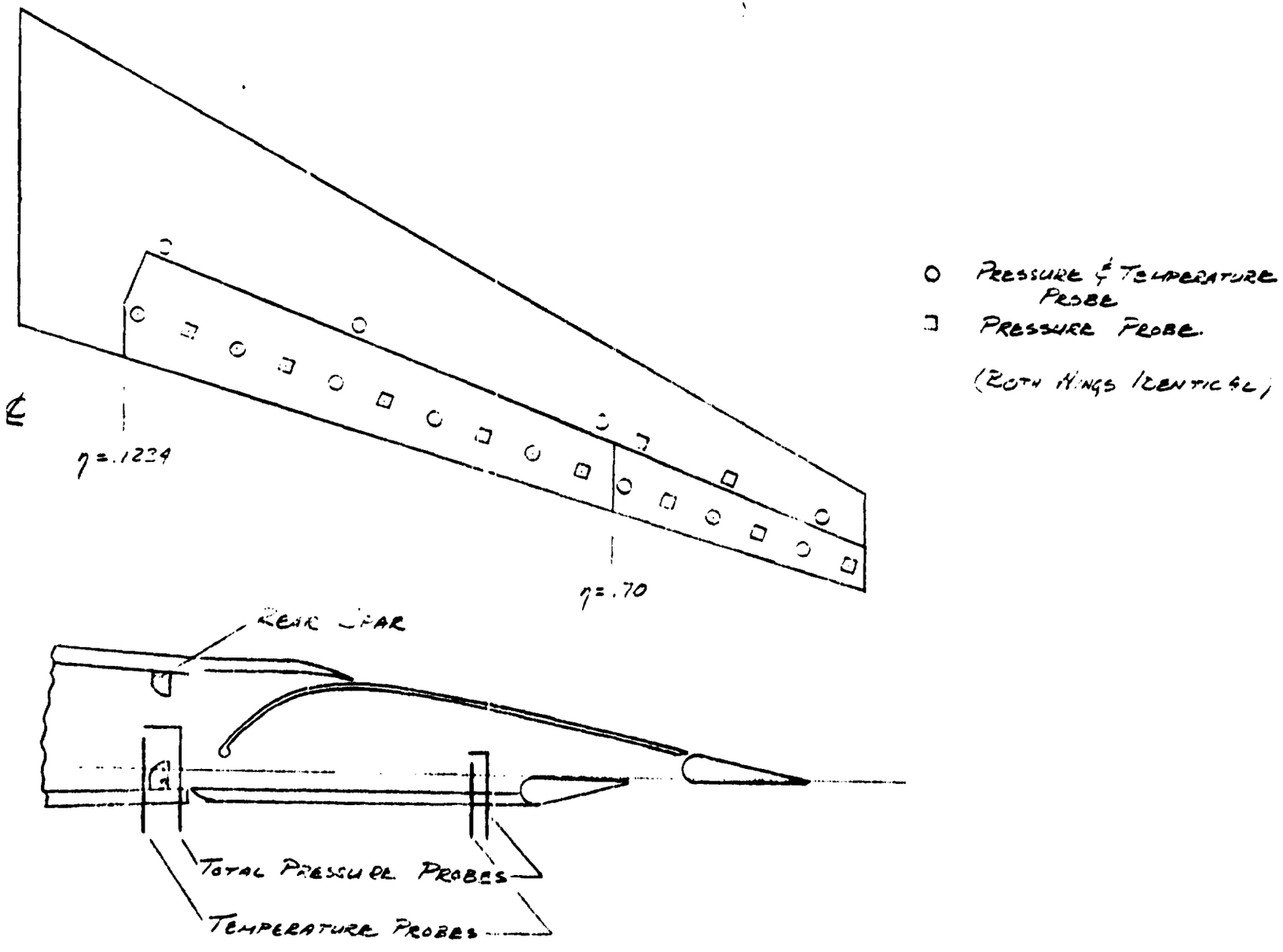


Figure 5. — Schematic of wing duct instrumentation layout.

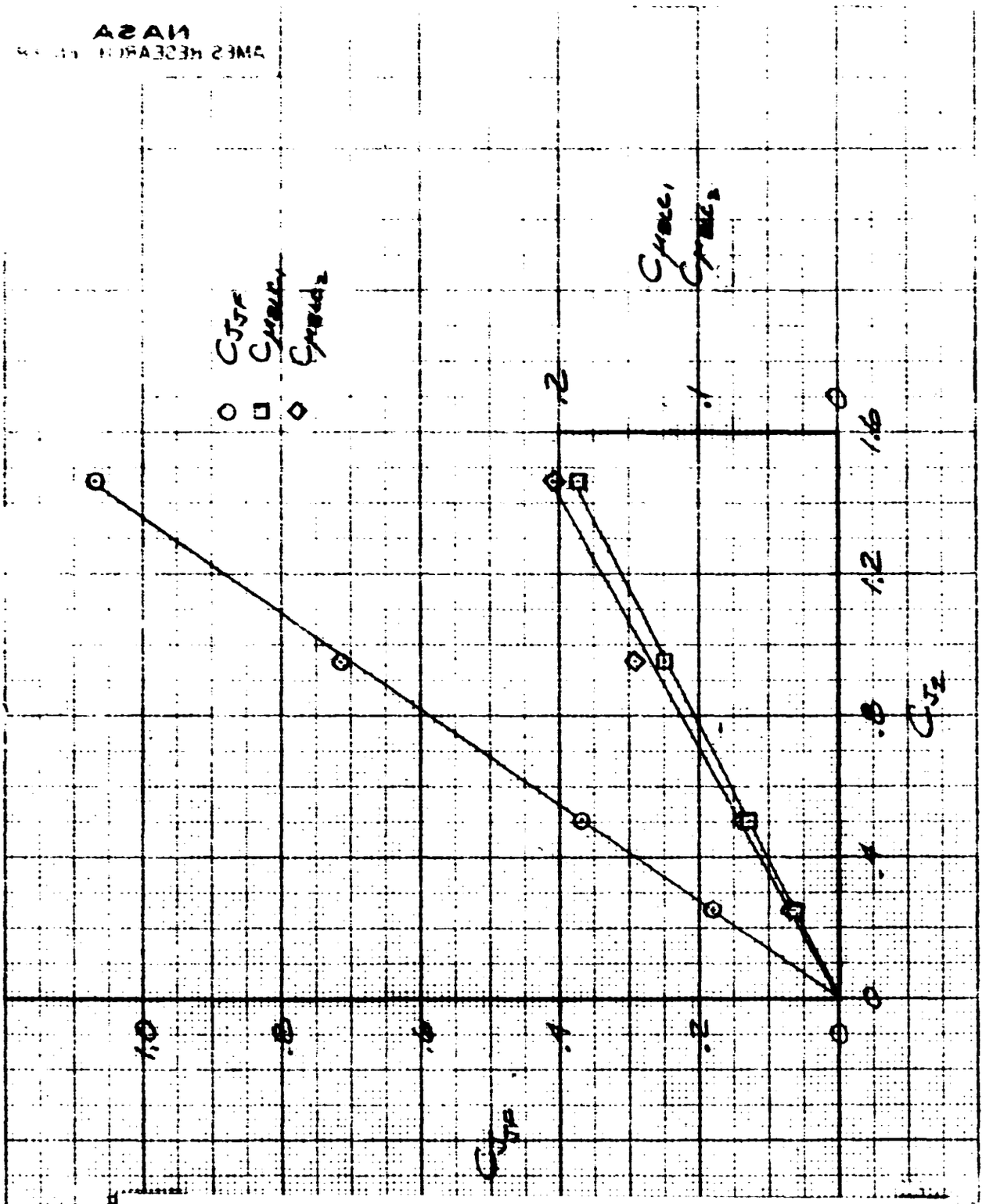

(a) $\delta_f = 60°$, full-span flap.

Figure 6. — The division of $C_{J_I}$ into its components, $C_{J_{JF}}$, $C_{\mu_{BLC_1}}$, $C_{\mu_{BLC_2}}$, $C_{\mu_a}$.

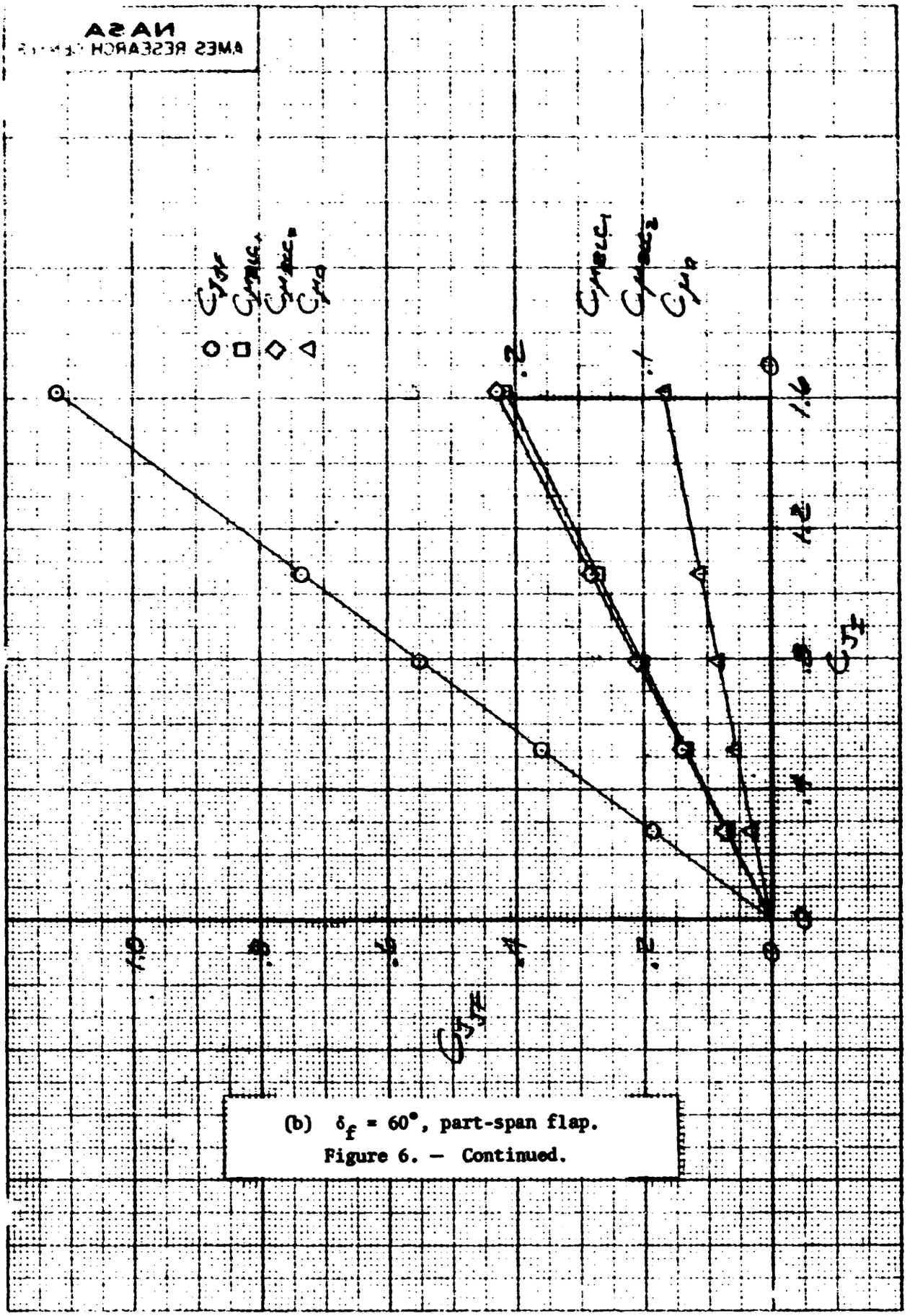

(b) $\delta_f = 60°$, part-span flap.

Figure 6. — Continued.

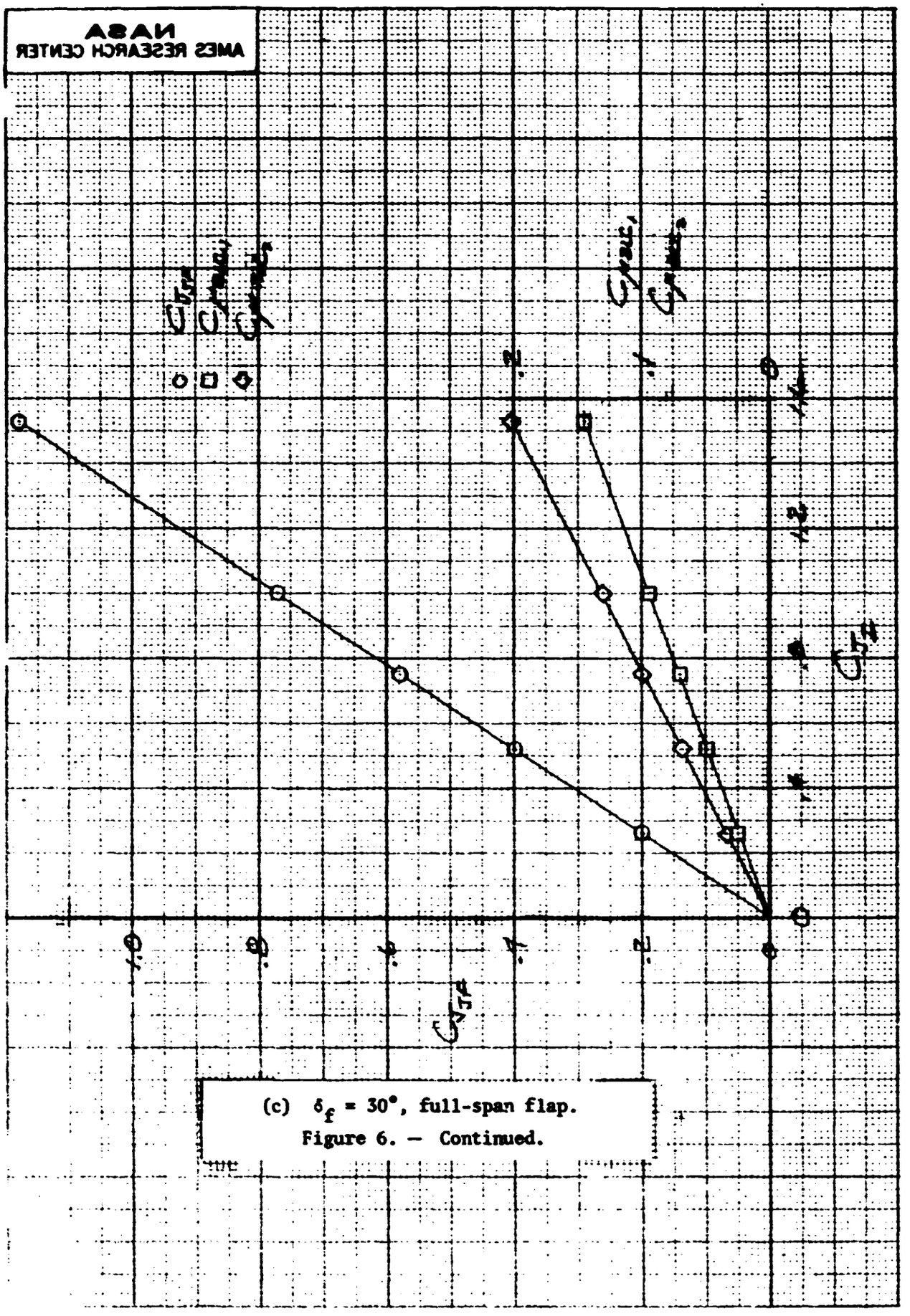

(c) $\delta_f = 30°$, full-span flap.

Figure 6. — Continued.

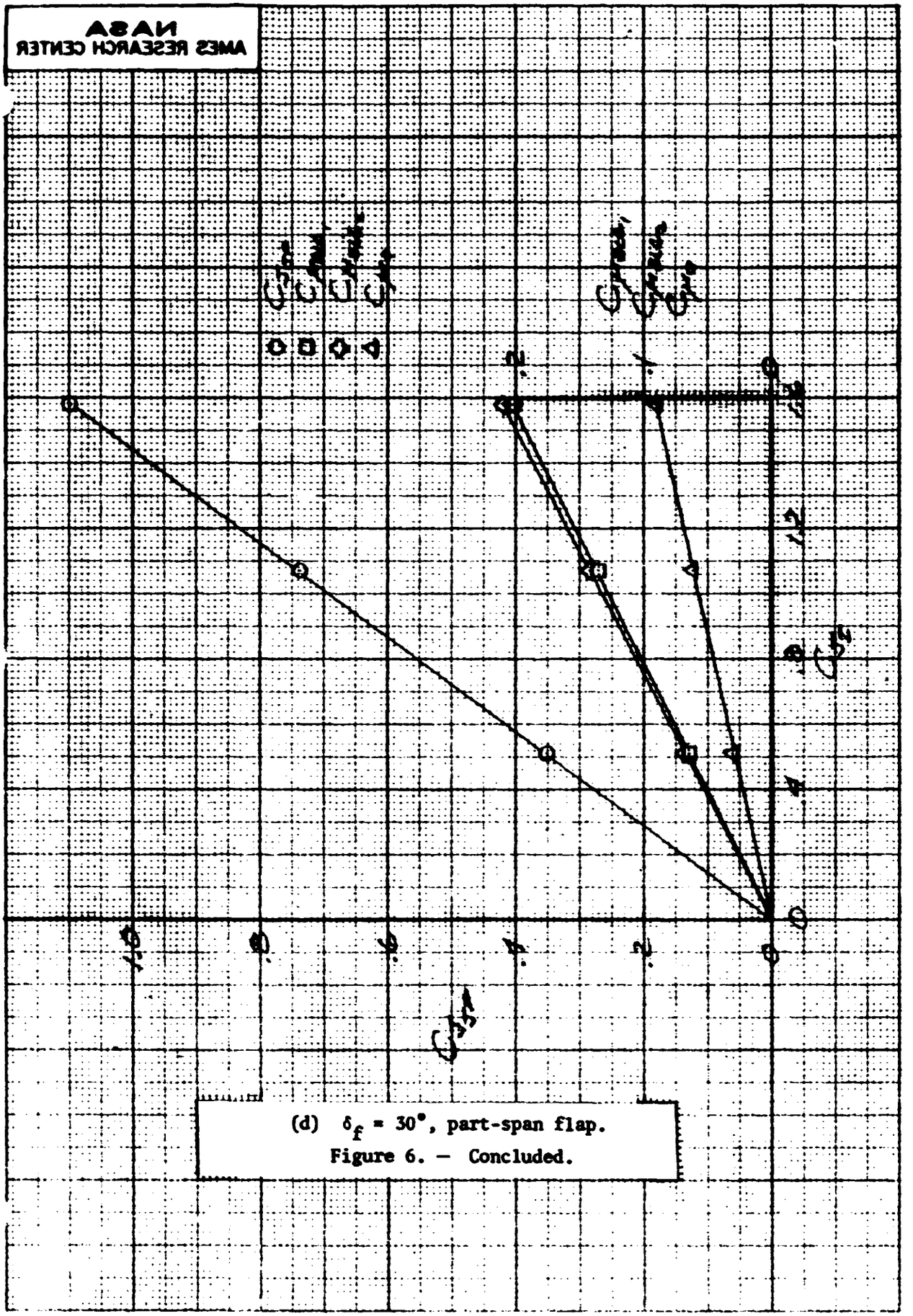

(d) $\delta_f = 30°$, part-span flap.

Figure 6. — Concluded.

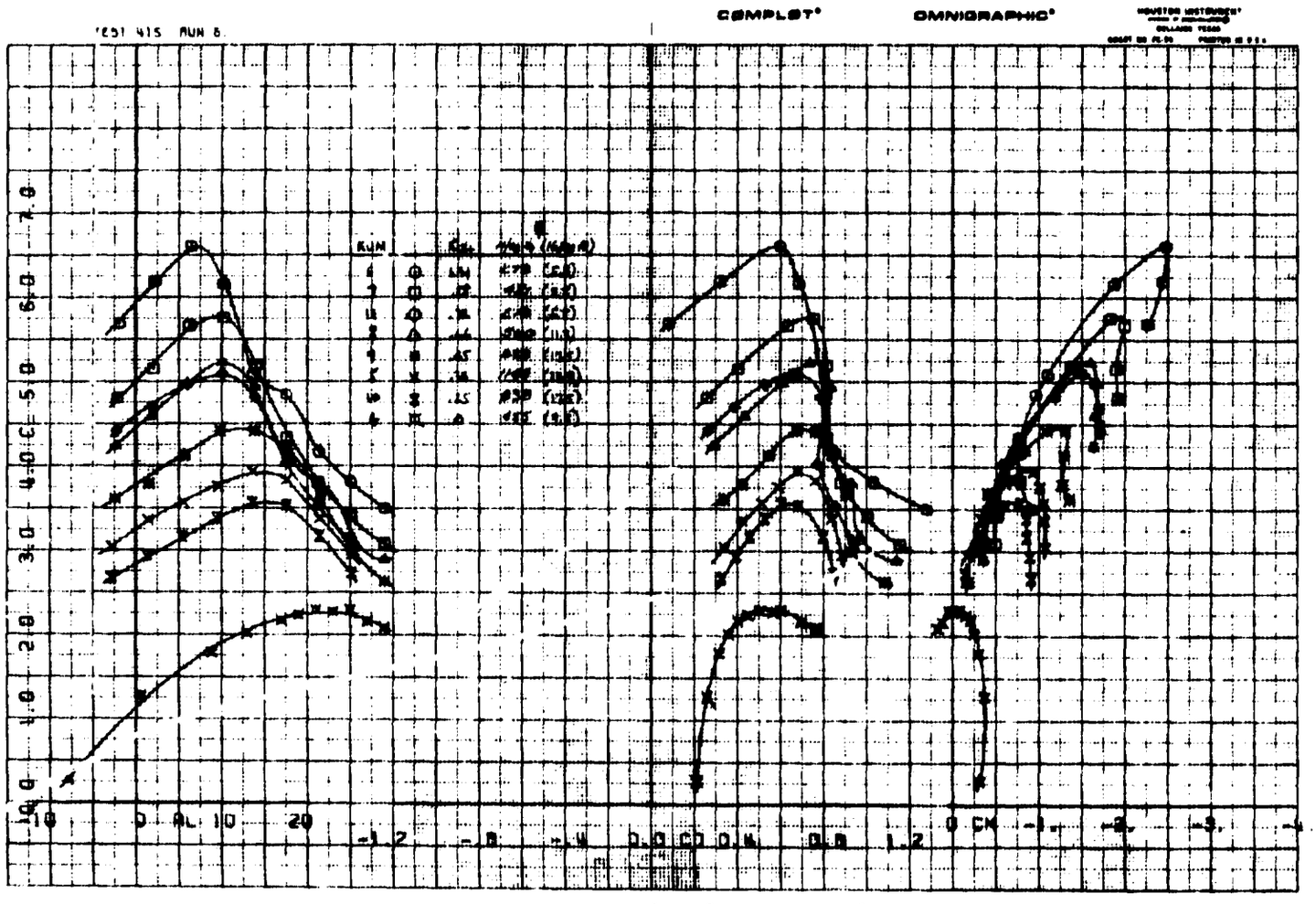


(a) $\delta_f = 60°/60°$, $\delta_{s_1} = 45°$.

Figure 7. — The affect of $C_{J_I}$ on the longitudinal characteristics of the model; full-span flap, $\delta_c = 0°$, horizontal tail off.

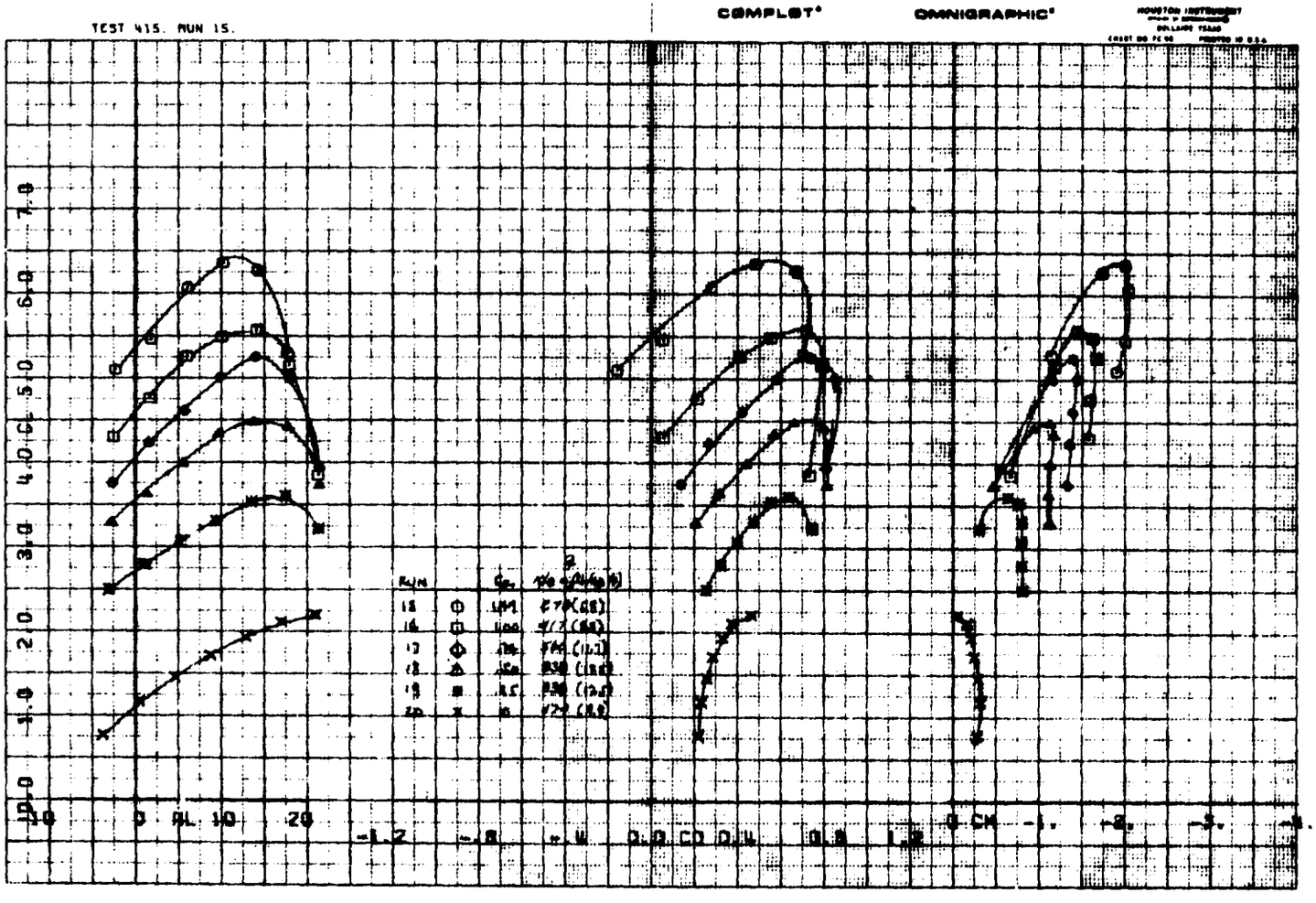


(b) $\delta_f = 60°/30°$, $\delta_{s_1} = 45°$.

Figure 7. – Continued.

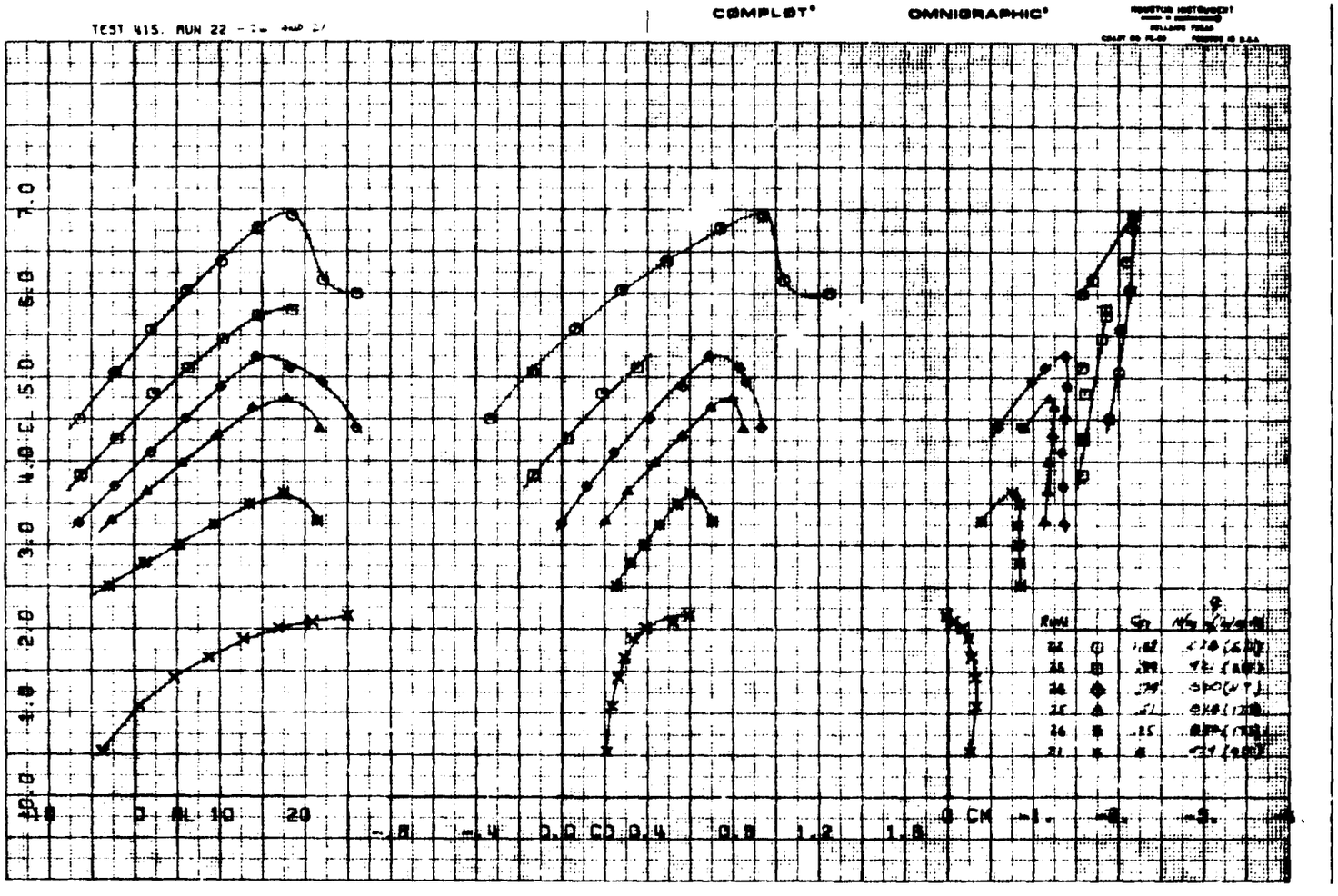


(c) $\delta_f = 60°/30°$, $\delta_{s_1} = 60°$.

Figure 7. – Continued.

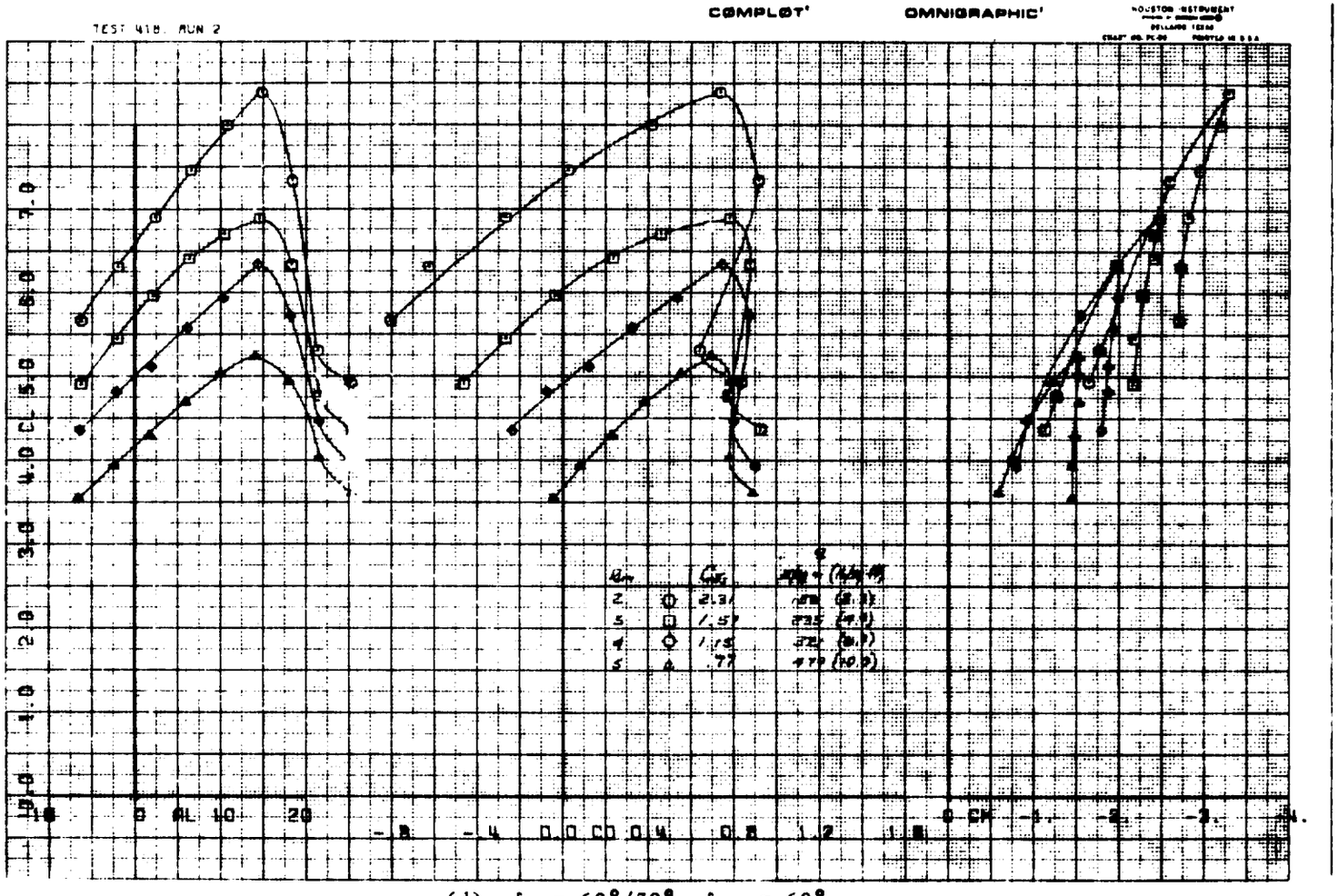


(d) $\delta_f = 60°/30°$, $\delta_{s_2} = 60°$.

Figure 7. — Concluded.

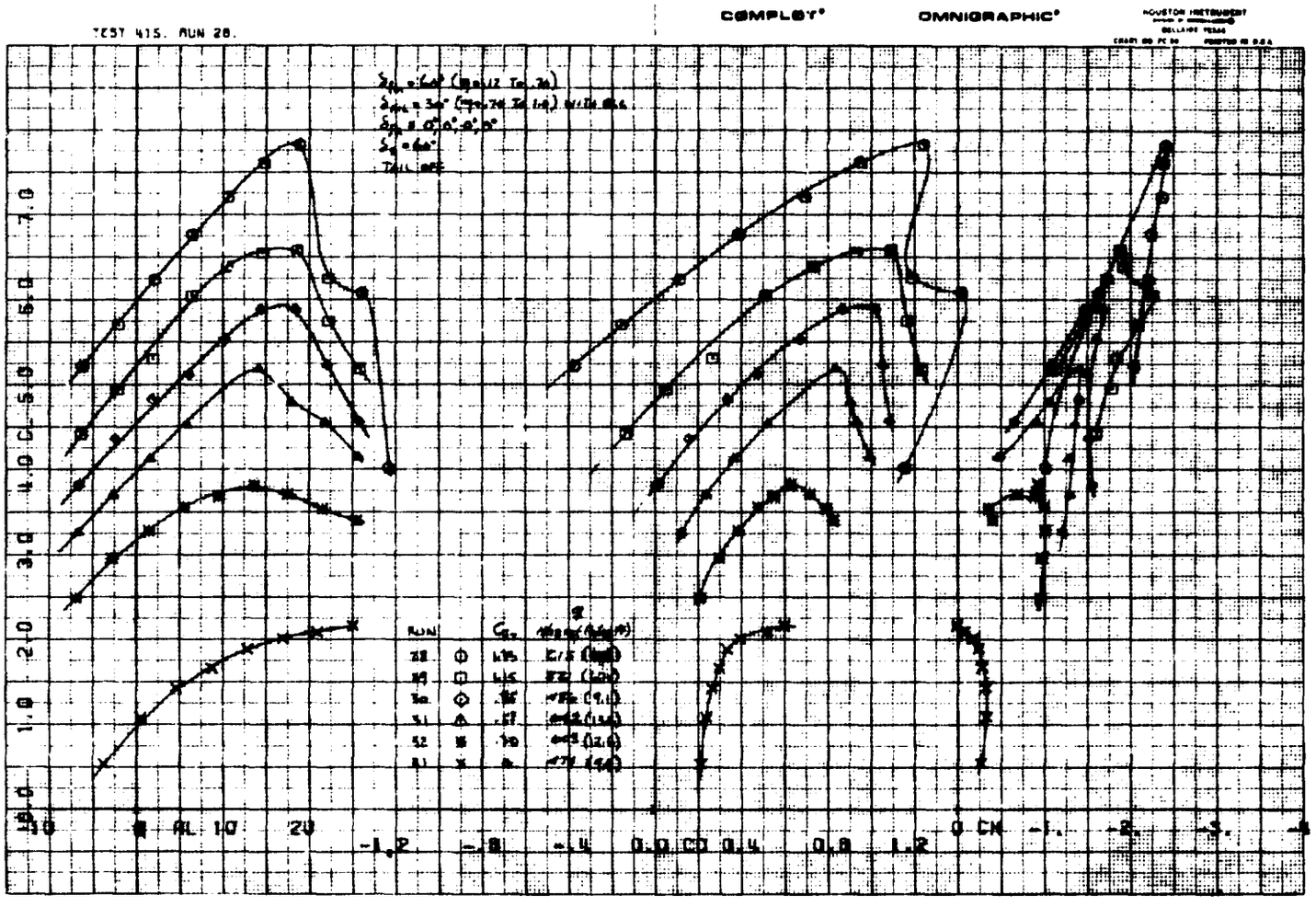


(a) $\delta_c = 0°$, $\delta_{s_1} = 60°$.

Figure 8. — The effect of $C_{J_I}$ on the longitudinal characteristics of the model; part-span flap, $\delta_f = 60°$, $\delta_a = 30°$, horizontal tail off.

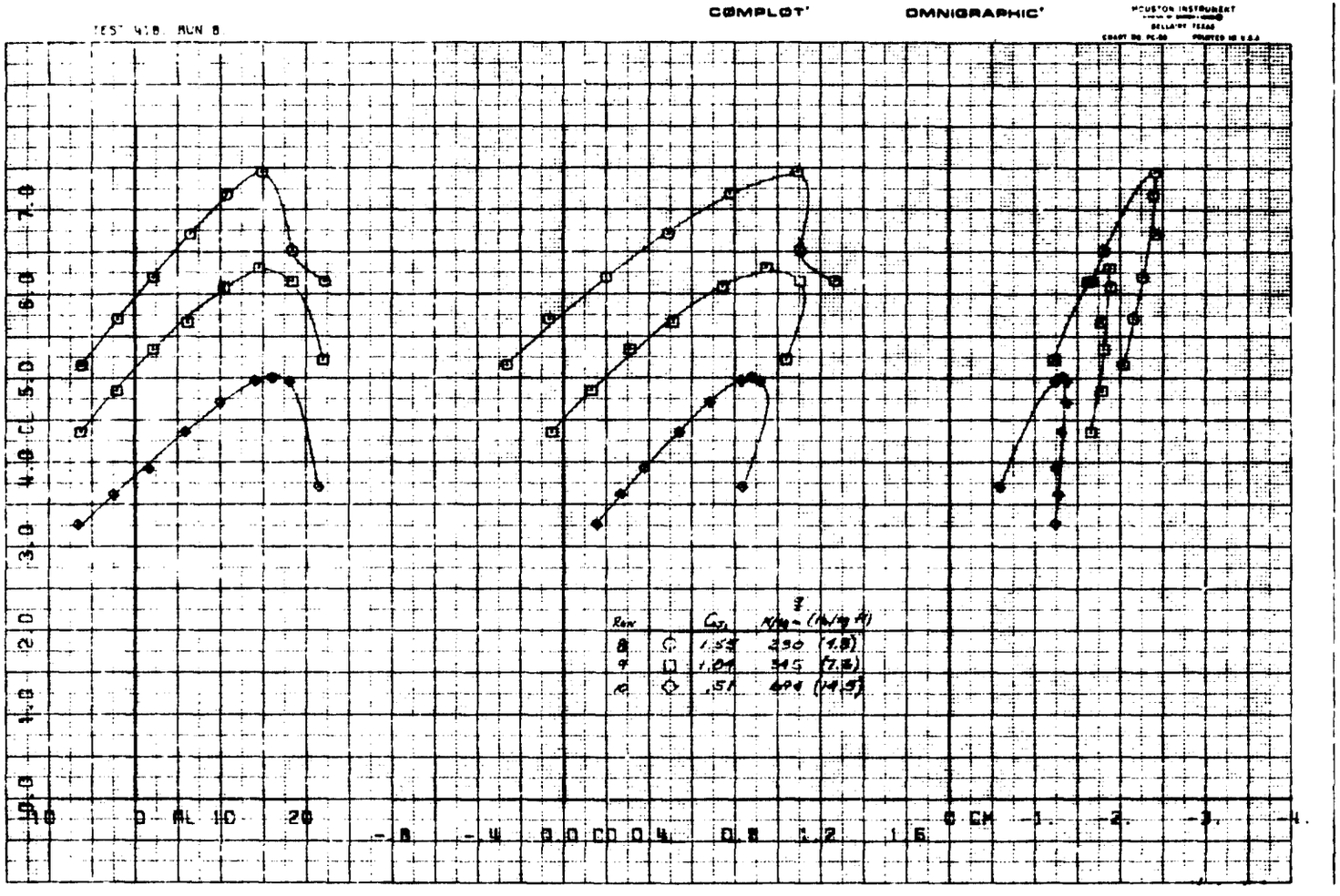


(b) $\delta_c = 0°$, $\delta_{s_2} = 60°$.

Figure 8. — Continued.

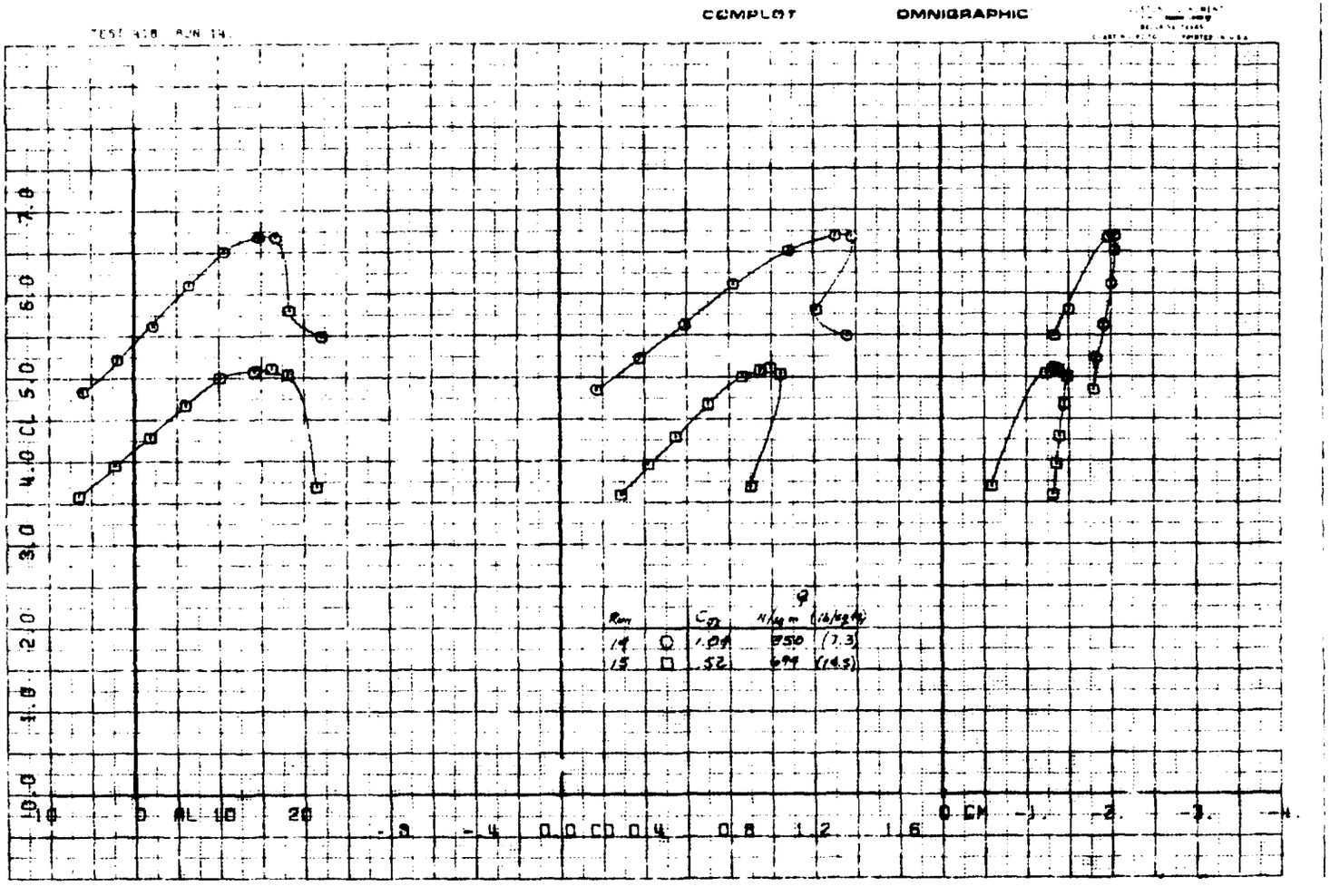


(c) $\delta_c = 10°$, $\delta_{s_2} = 60°$.

Figure 8. — Continued.

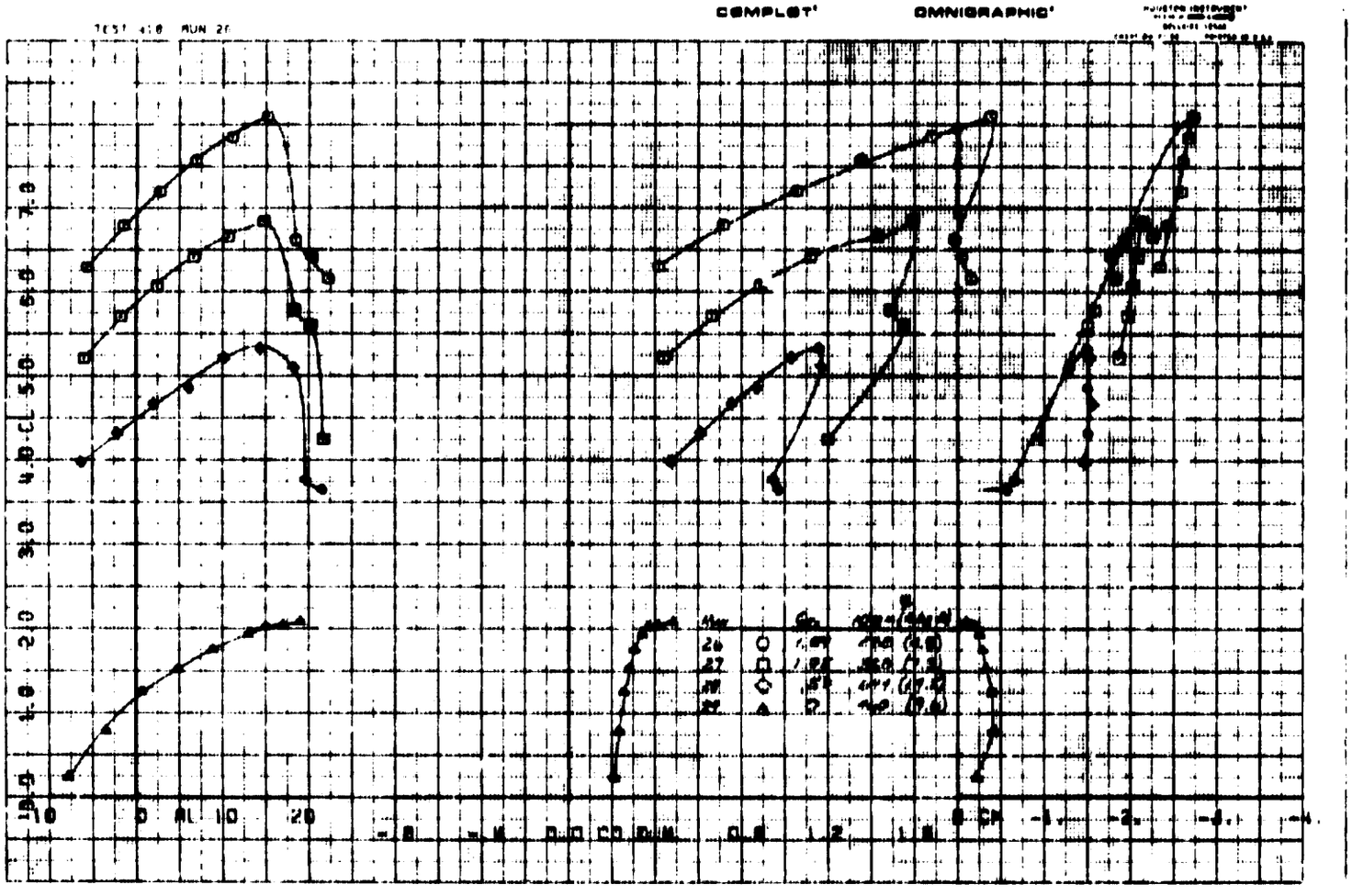


(d) $\delta_c = 20°$, $\delta_{s_2} = 60°$.

Figure 8. — Continued.

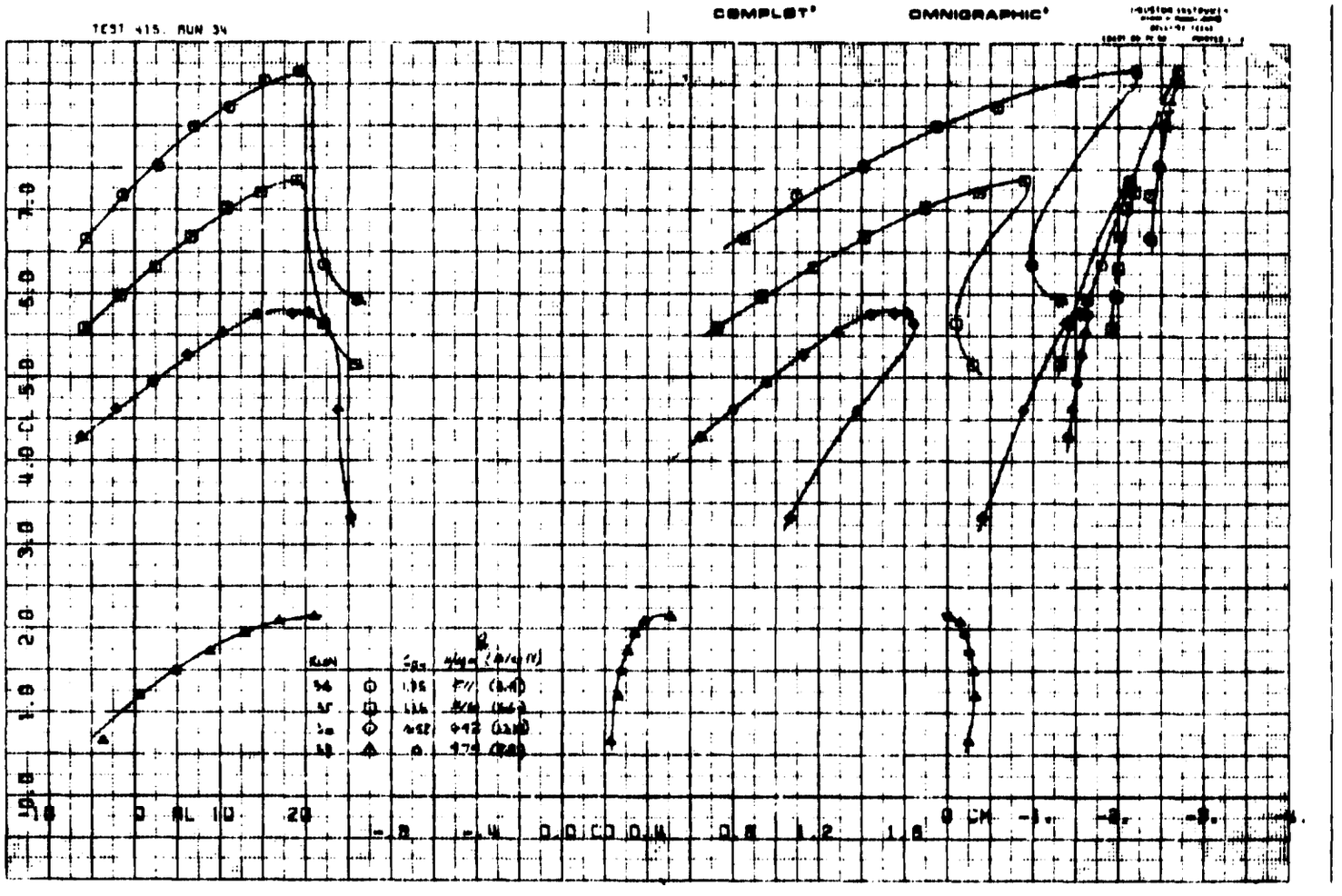


(e) $\delta_c = 30°$, $\delta_{s_1} = 60°$.

Figure 8. — Continued.

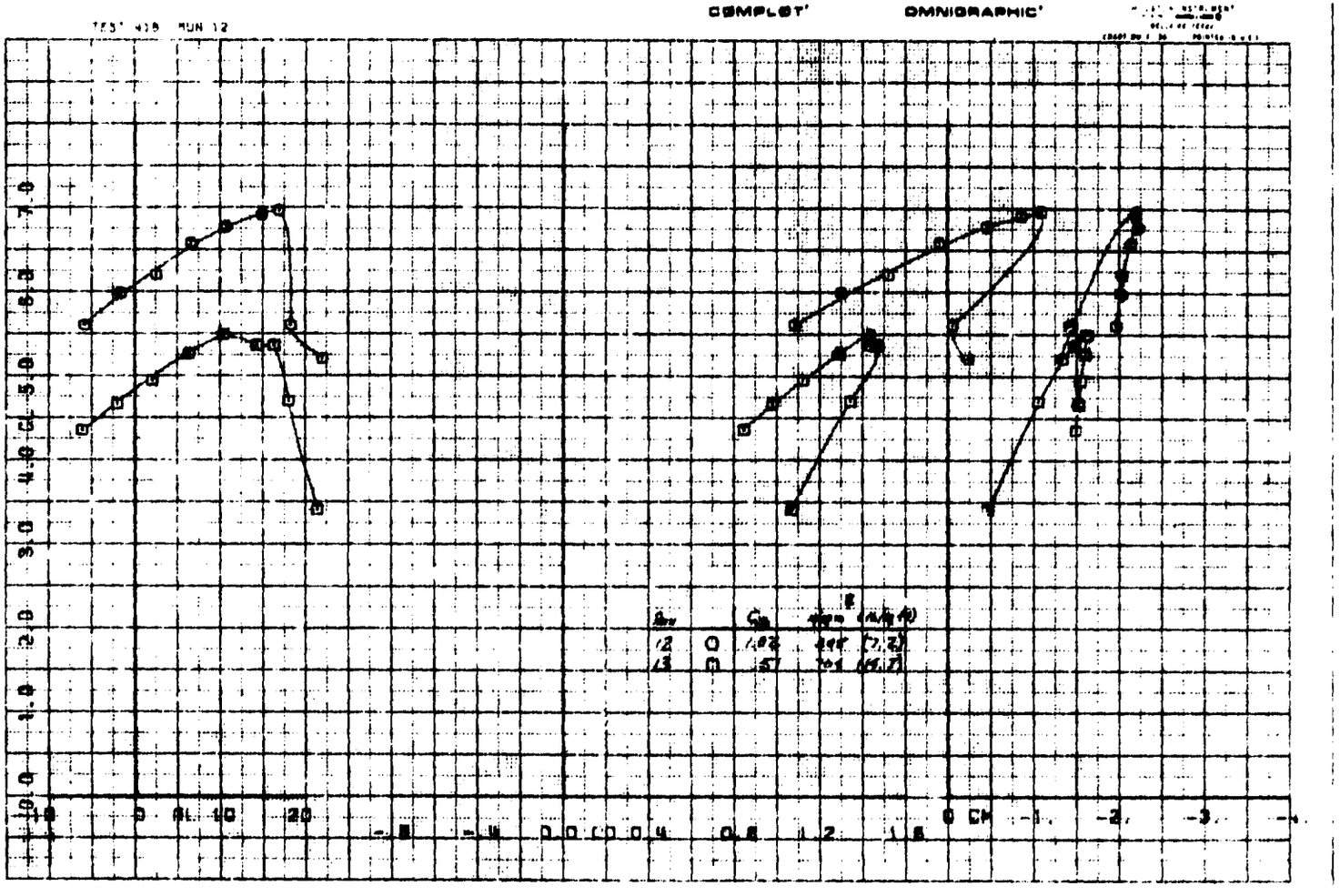


(f) $\delta_c = 40°$, $\delta_{s_2} = 60°$.

Figure 8. – Continued.

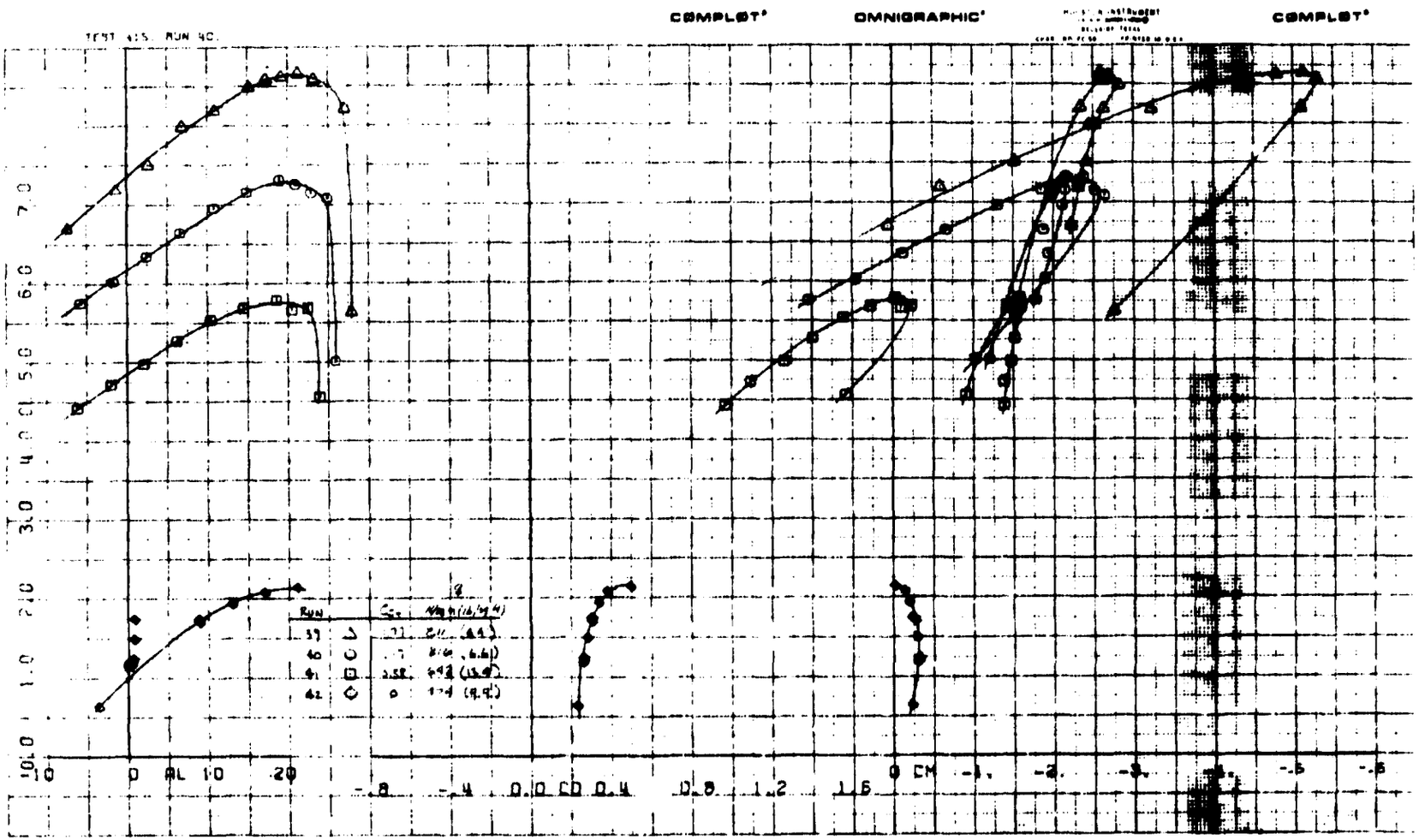


(g) $\delta_c = 50°$, $\delta_{s_1} = 60°$.

Figure 8. — Concluded.

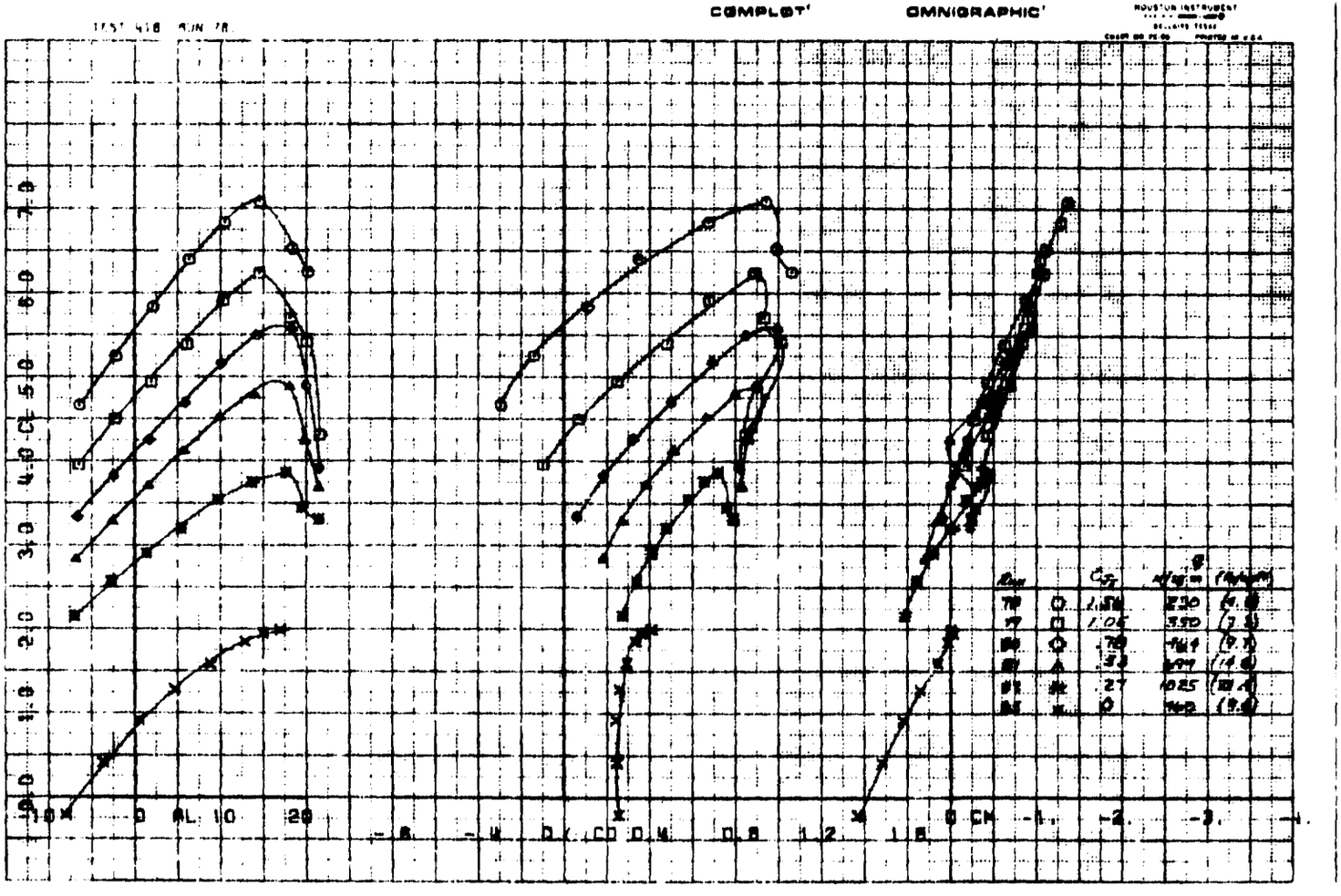


(a) $\delta_c = 0°$.

Figure 9. — The effect of $C_{J_I}$ on the longitudinal characteristics of the model; part-span flap, $\delta_f = 60°$, $\delta_a = 30°$, $\delta_{s_2} = 60°$, $i_t = -10°$.

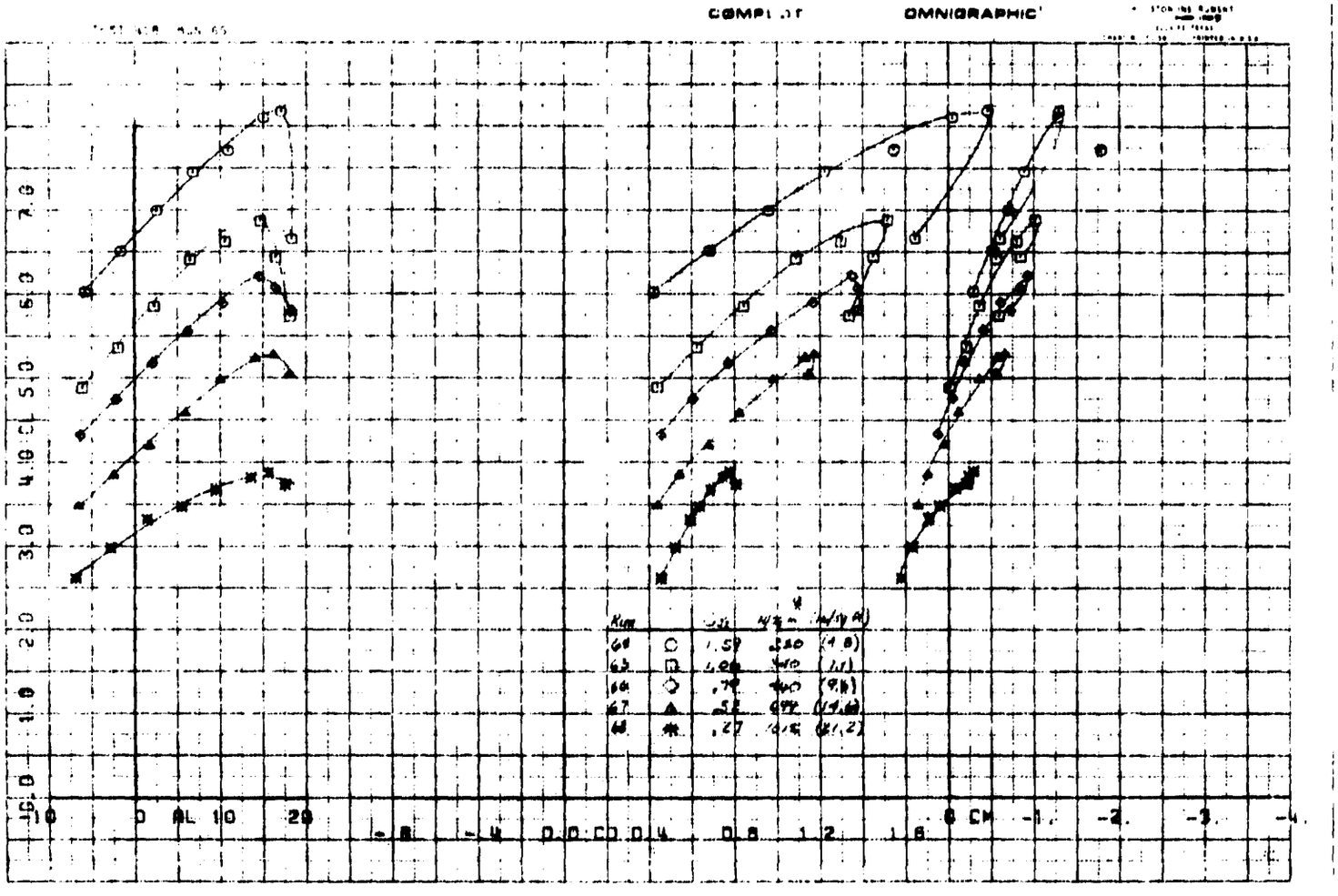


(b) $\delta_c = 20°$.

Figure 9. — Continued.

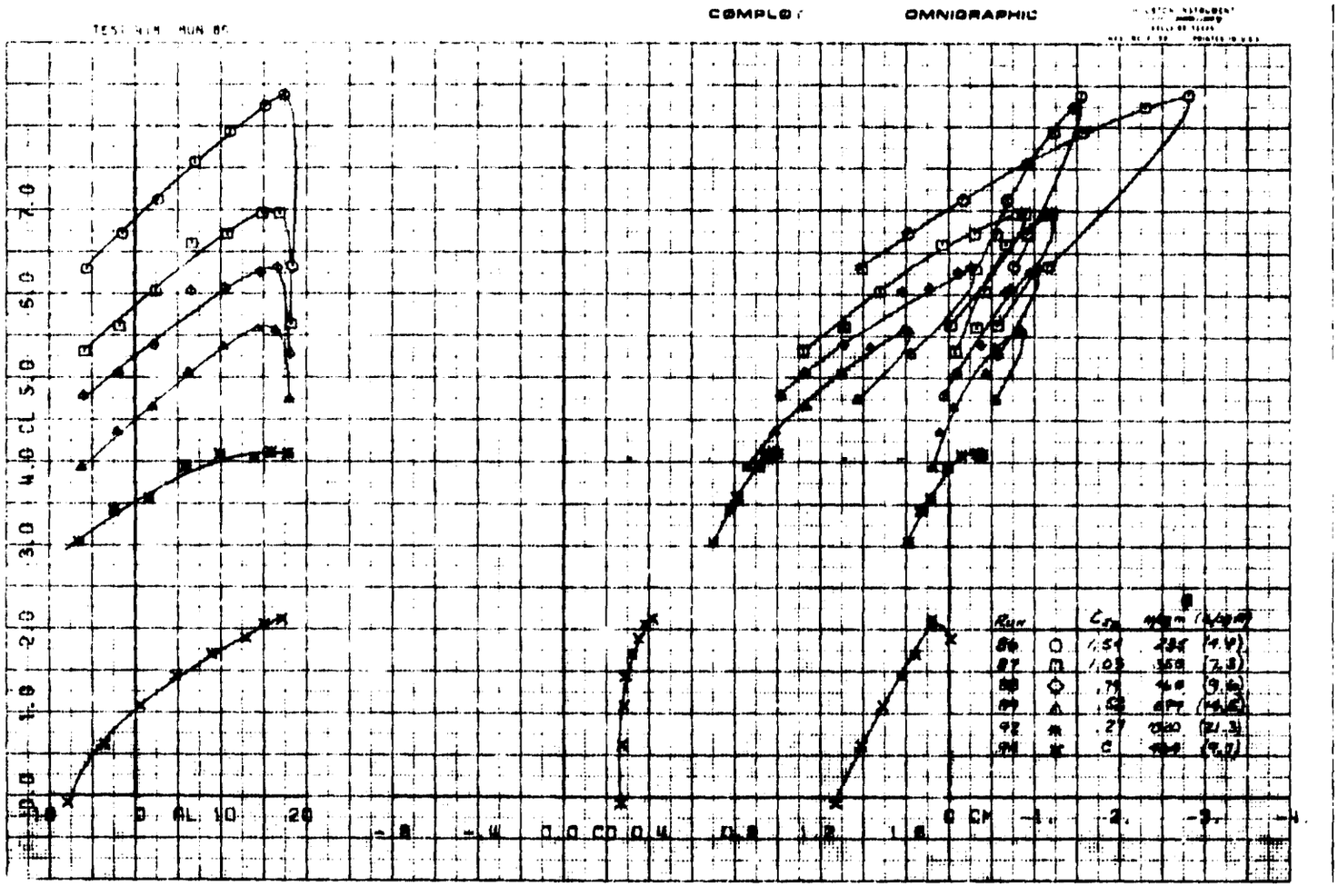


(c) $\delta_c = 40°$.

Figure 9. — Concluded.

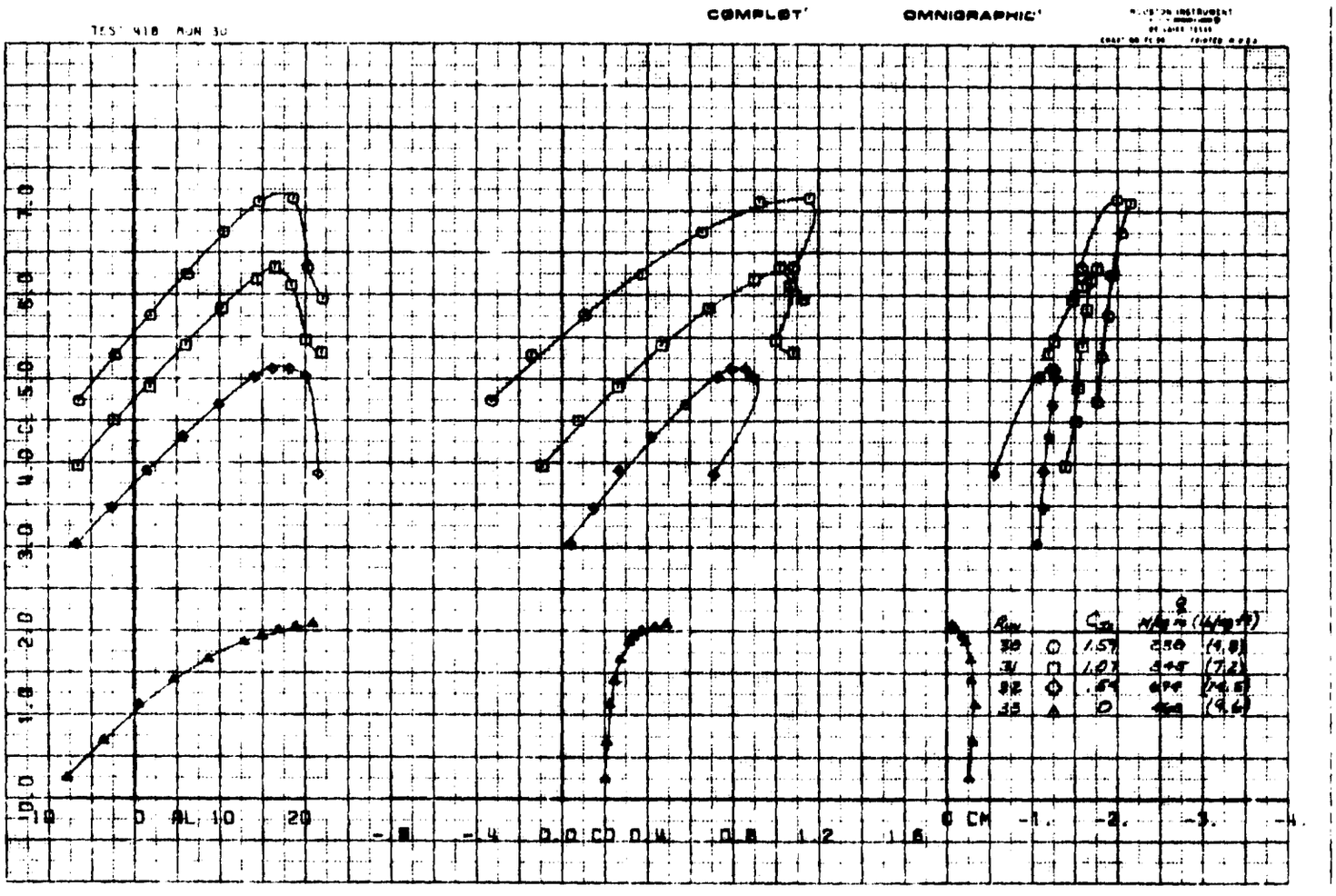


Figure 10. — The effect of $C_{J_I}$ on the longitudinal characteristics of the model; part-span flap, $\delta_f = 60°$, $\delta_a = 10°$, $\delta_{s_2} = 60°$, horizontal tail off.

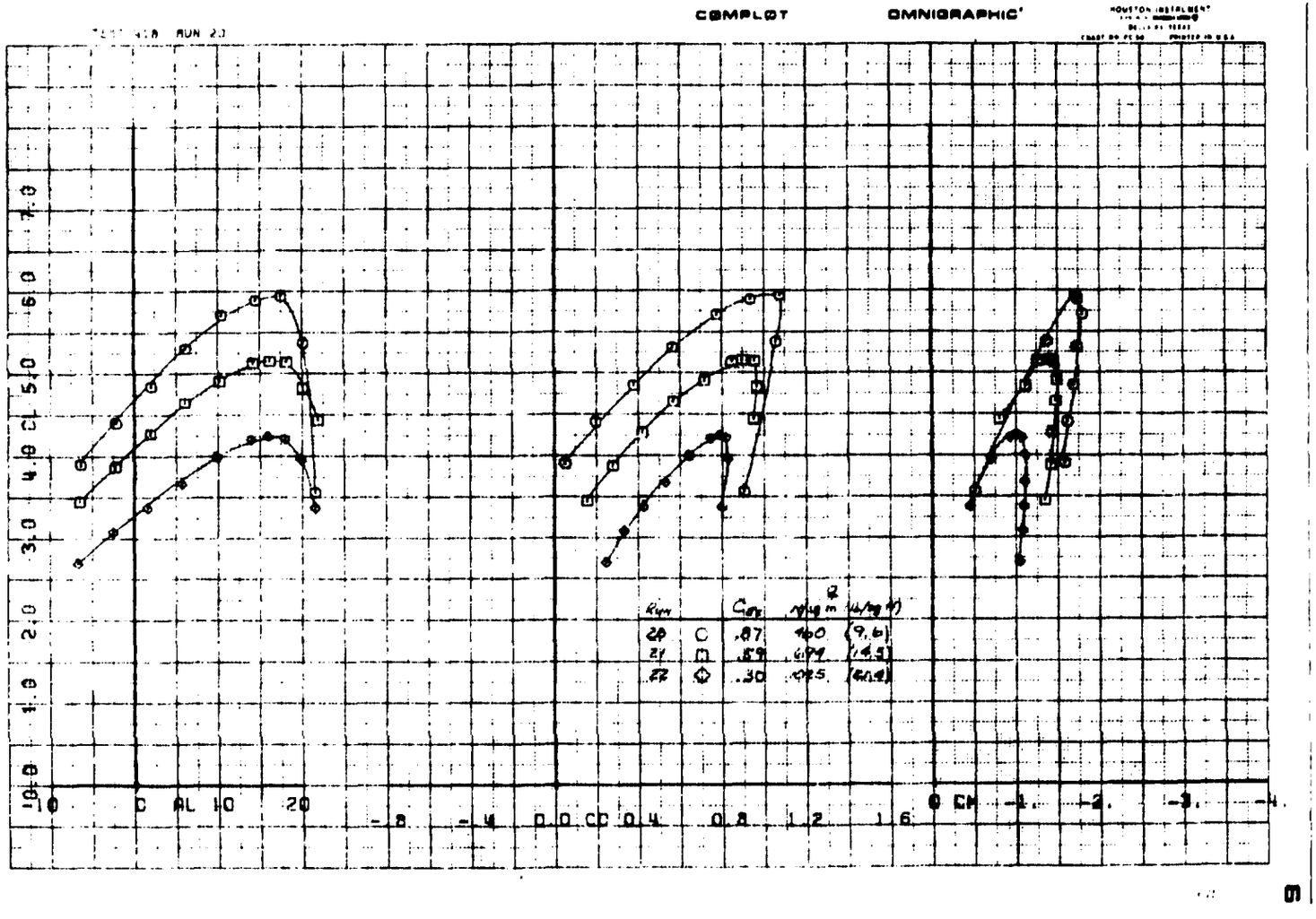


Figure 11. — The effect of $C_{J_I}$ on the longitudinal characteristics of the model with twice normal $C_{\mu_{BLC}}$; part-span flap, $\delta_f = 60°$, $\delta_a = 30°$, $\delta_{s_2} = 60°$, horizontal tail off.

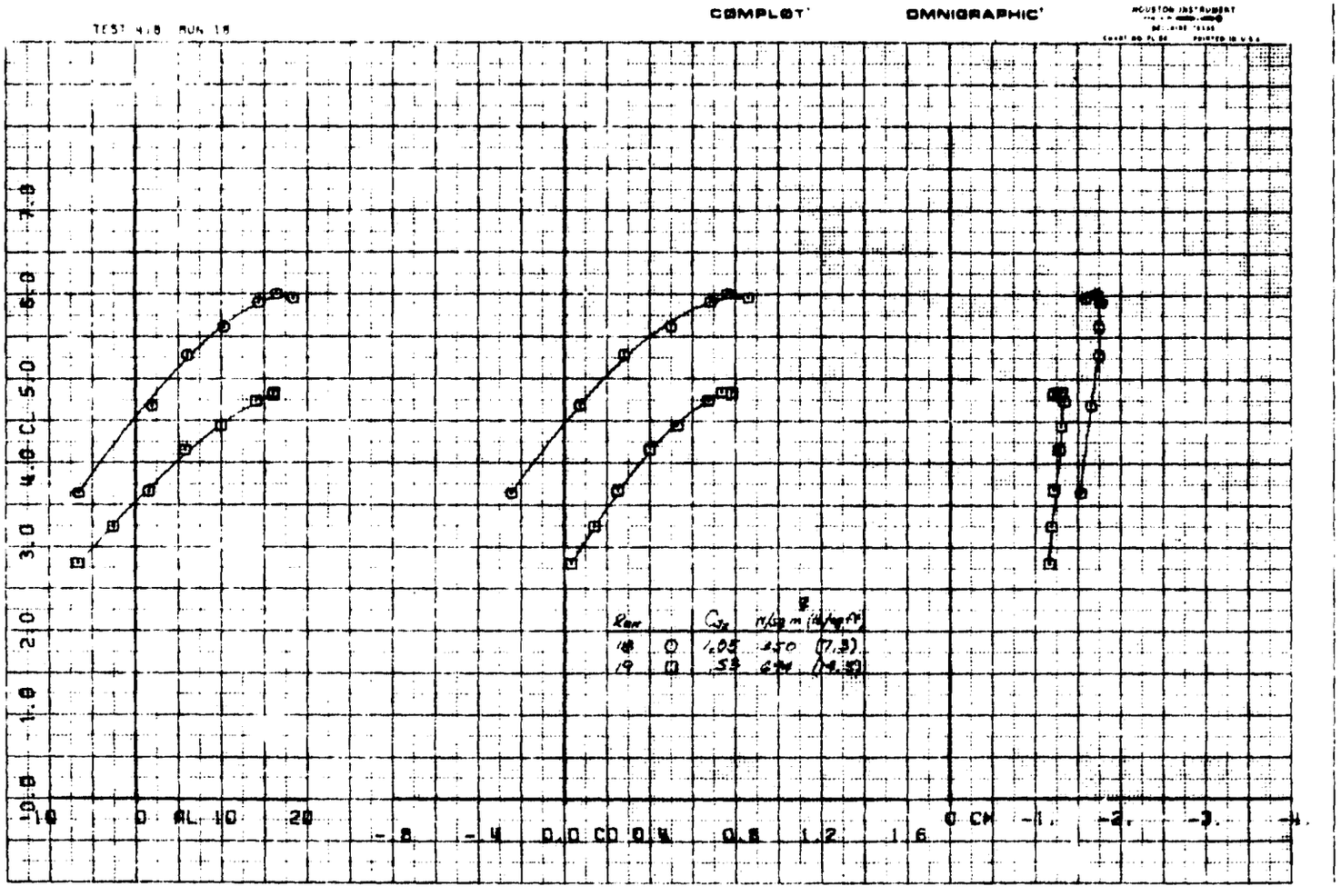


(a) $\delta_c = 0°/-20°$.

Fggure 12. — The effect of $C_{J_I}$ on the longitudinal characteristics of the model; part-span flap, $\delta_f = 60°$, $\delta_a = 30°$, $\delta_{s_2} = 60°$, horizontal tail off.

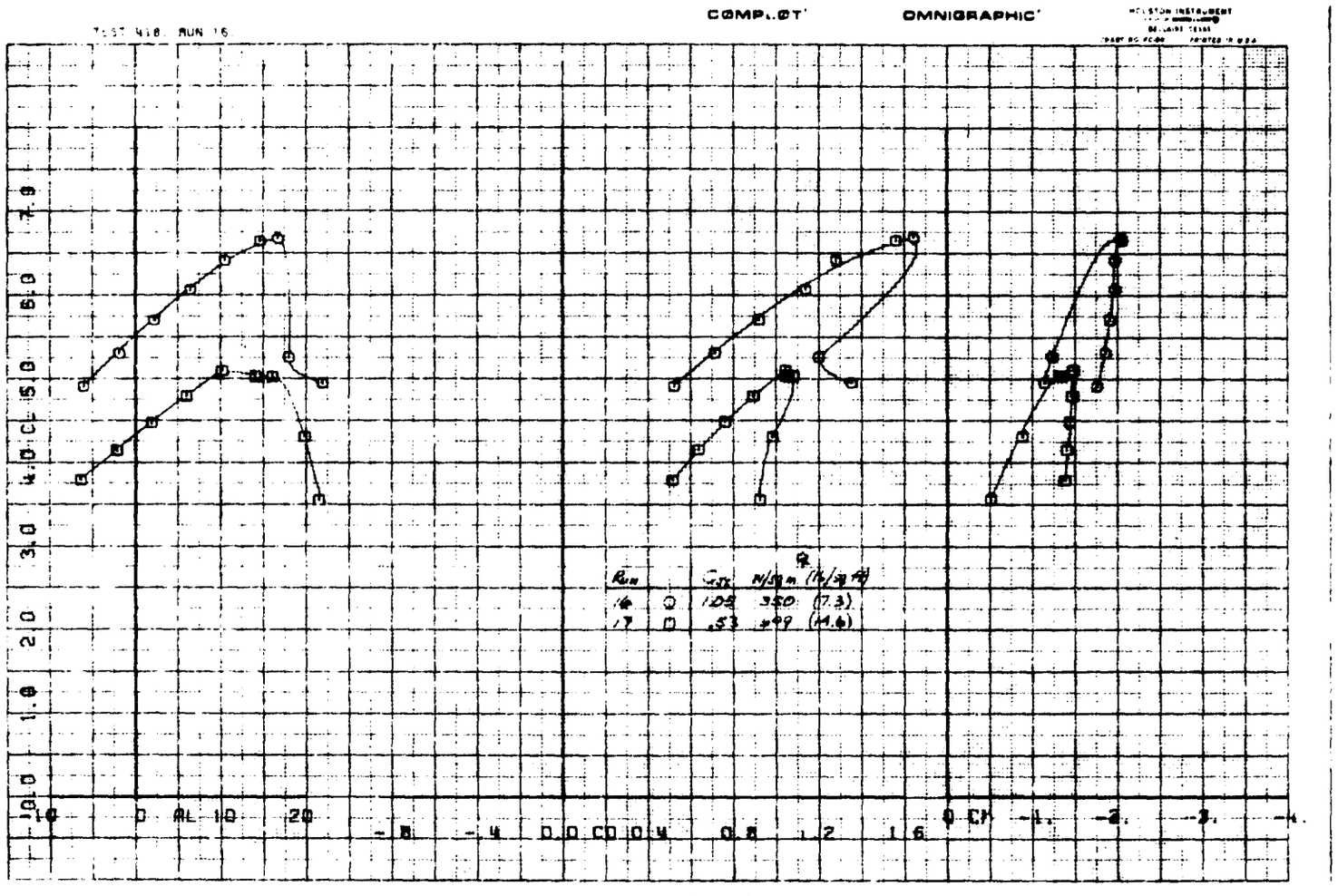


(b) $\delta_c = 0°/40°$.

Figure 12. — Concluded.

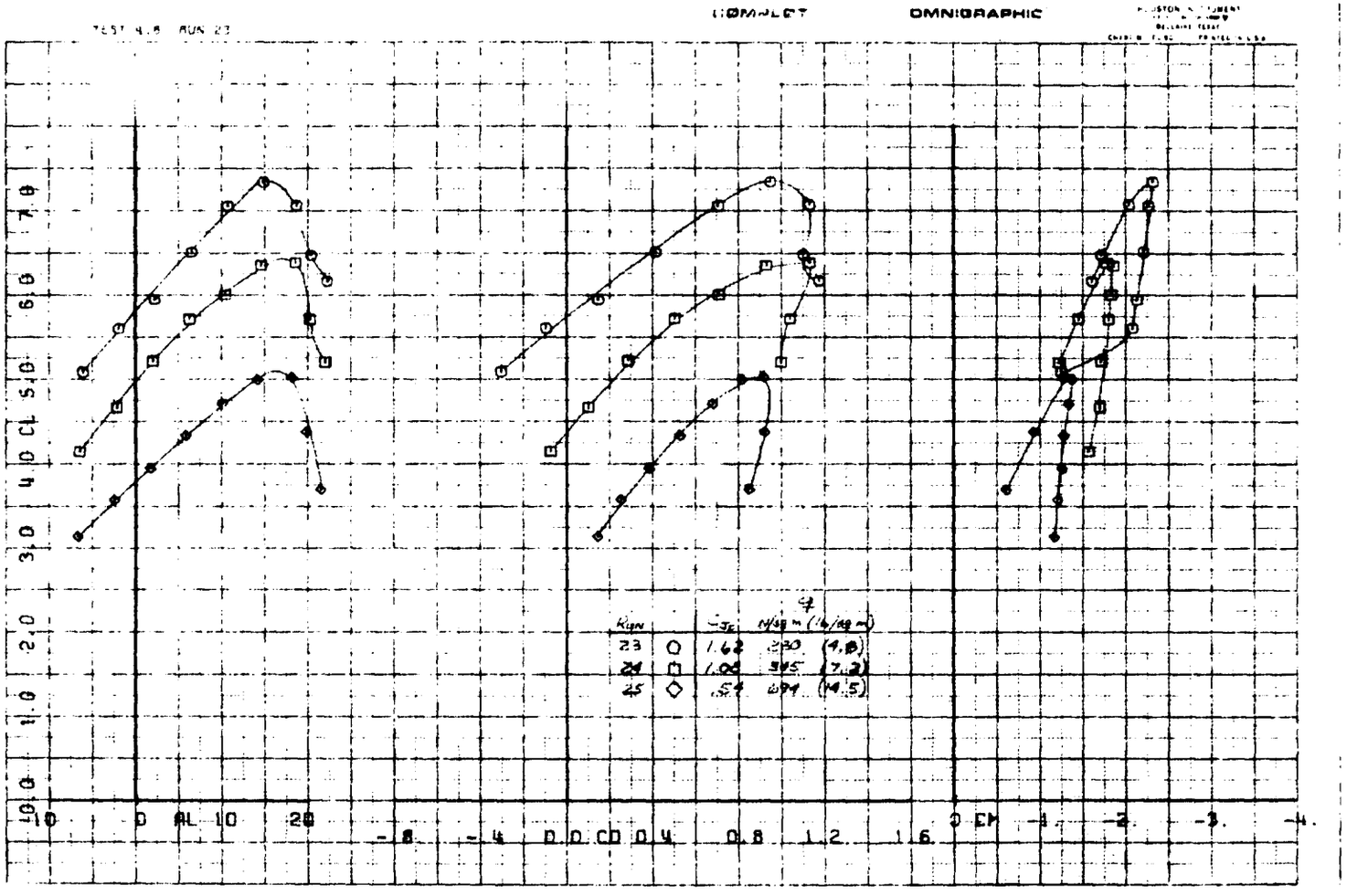


Figure 13. – The effect of $C_{J_I}$ on the longitudinal characteristics of the model; part-span flap, $\delta_f = 60°$, $\delta_a = 30°/10°$, $\delta_c = 0°$, $\delta_{s_2} = 60°$, horizontal tail off.

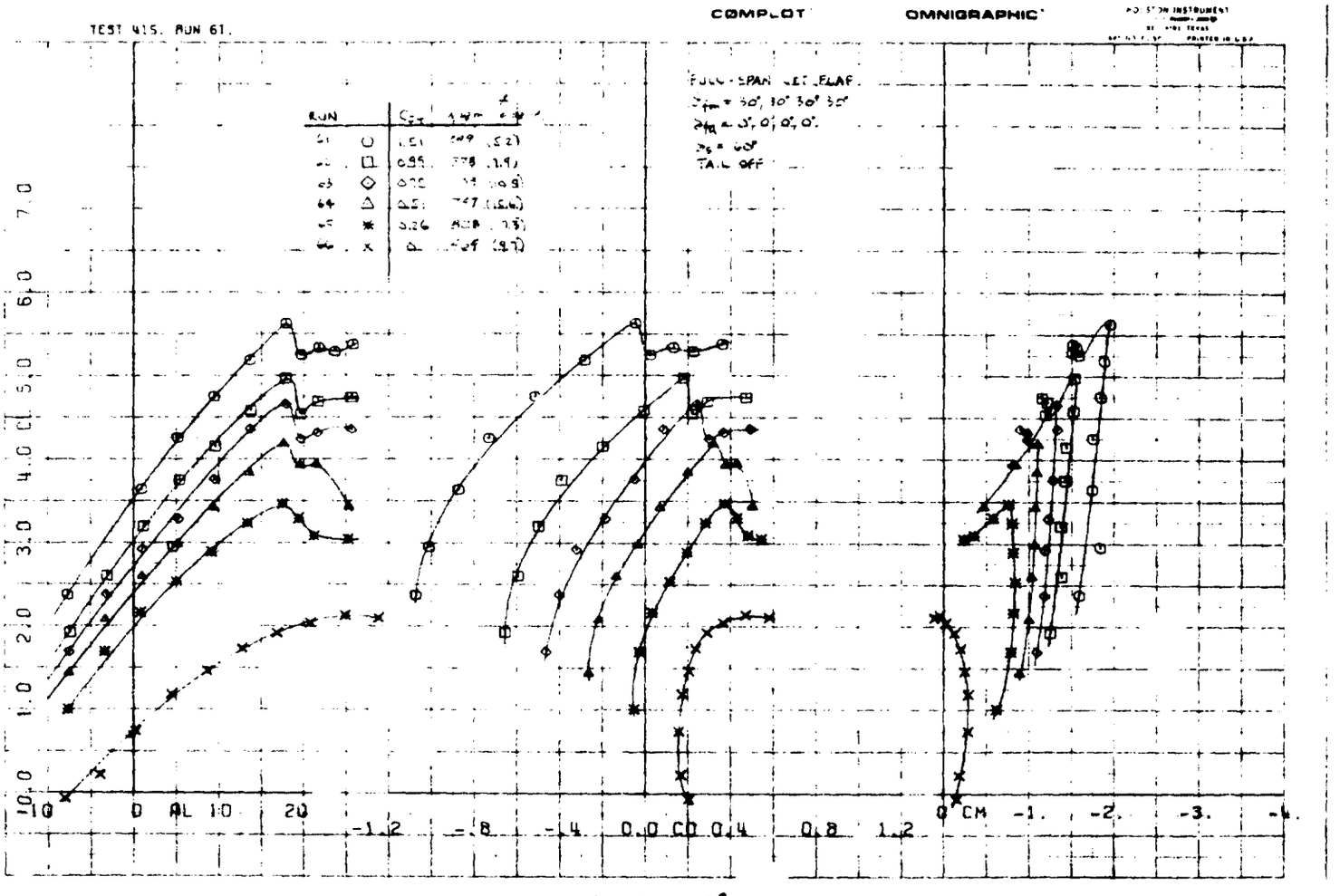


(a) $\delta_c = 0°$.

Figure 14. — The effect of $C_{J_I}$ on the longitudinal characteristics of the model; full-span flap, $\delta_f = 30°/30°$, $\delta_{s_1} = 60°$, horizontal tail off.

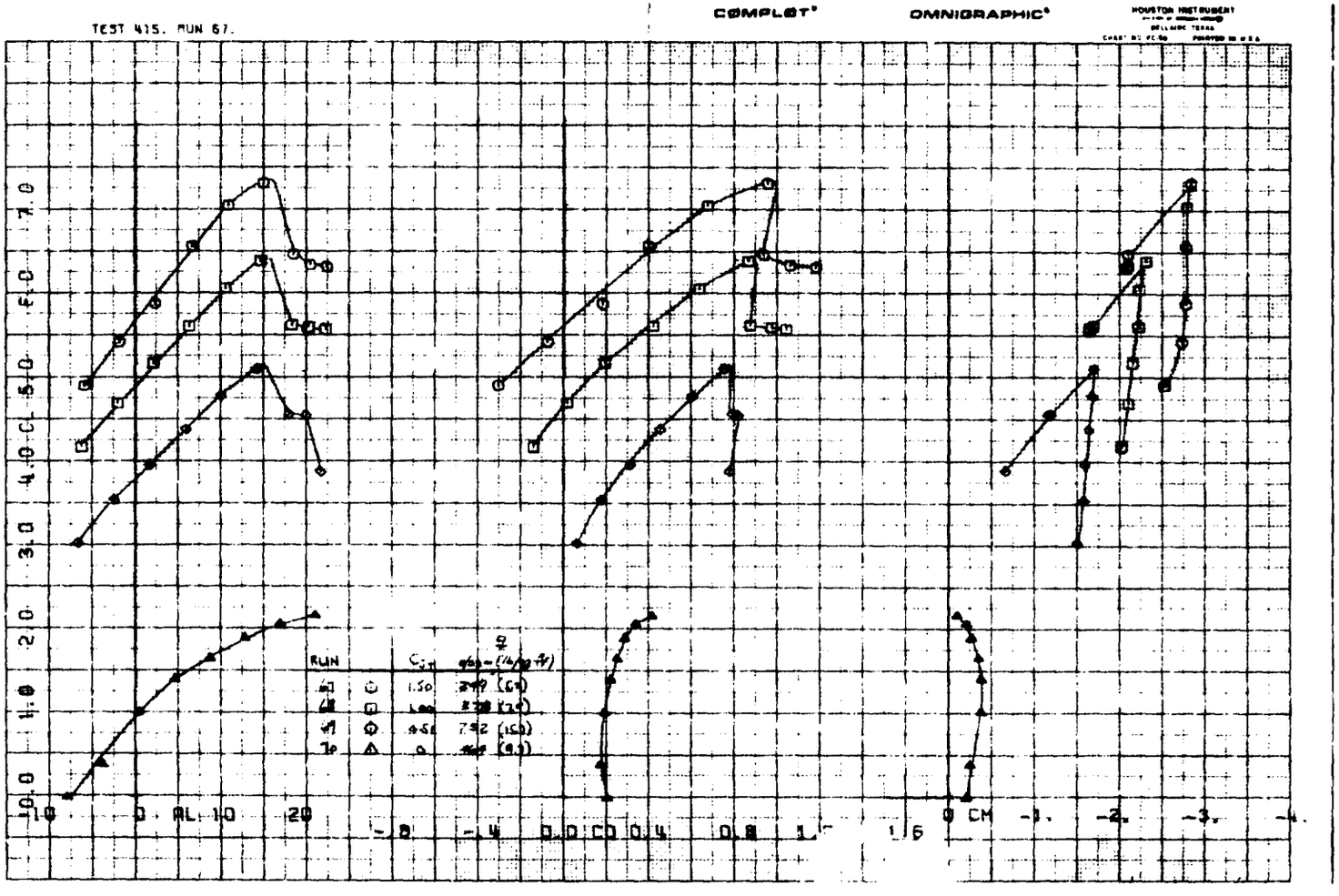


(b) $\delta_c = 30°$.

Figure 14. — Concluded.

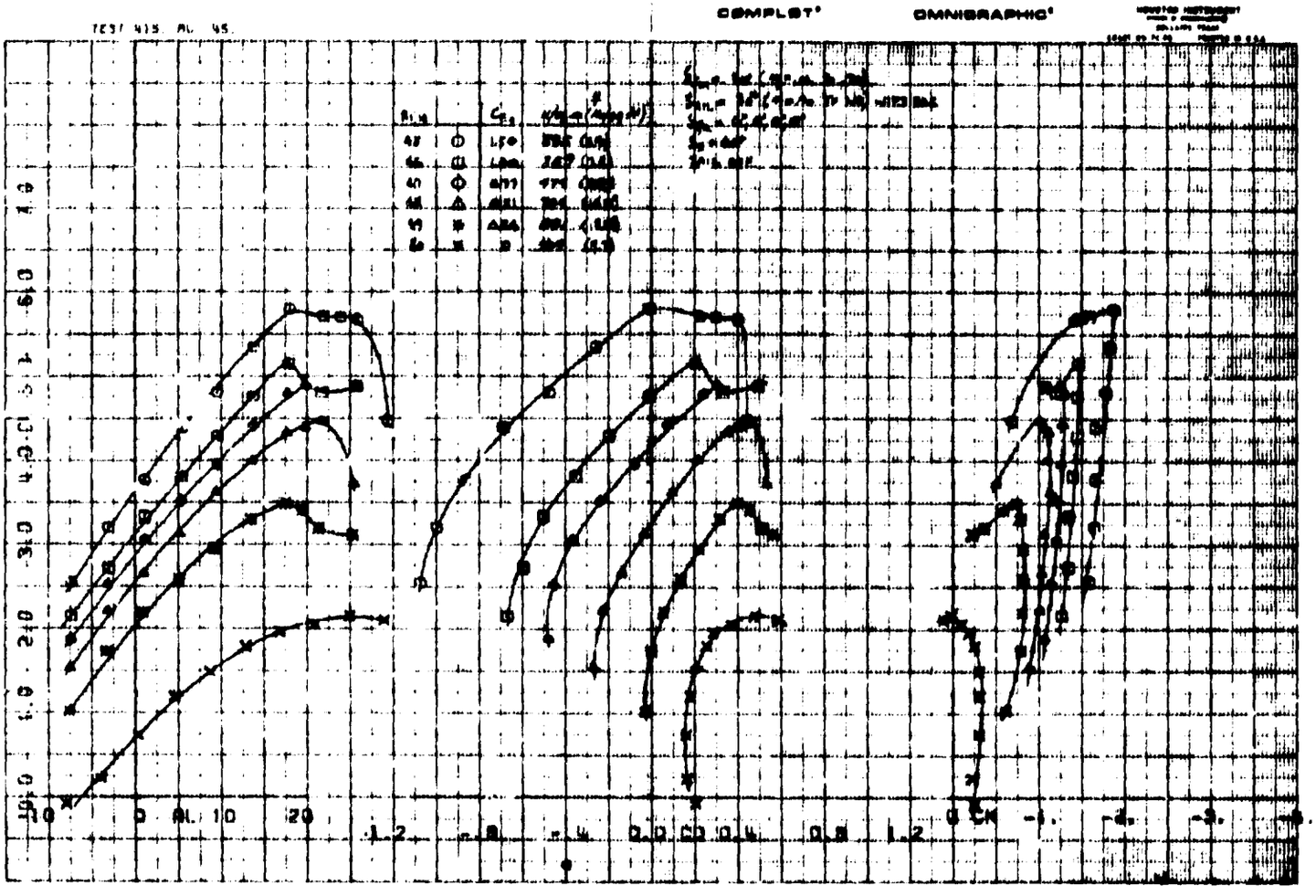

(a) $\delta_c = 0°$, $\delta_{s_1} = 60°$.

Figure 15. -- The effect of $C_{J_I}$ on the longitudinal characteristics of the model; part-span flap, $\delta_f = 30°$, $\delta_a = 30°$, horizontal tail off.

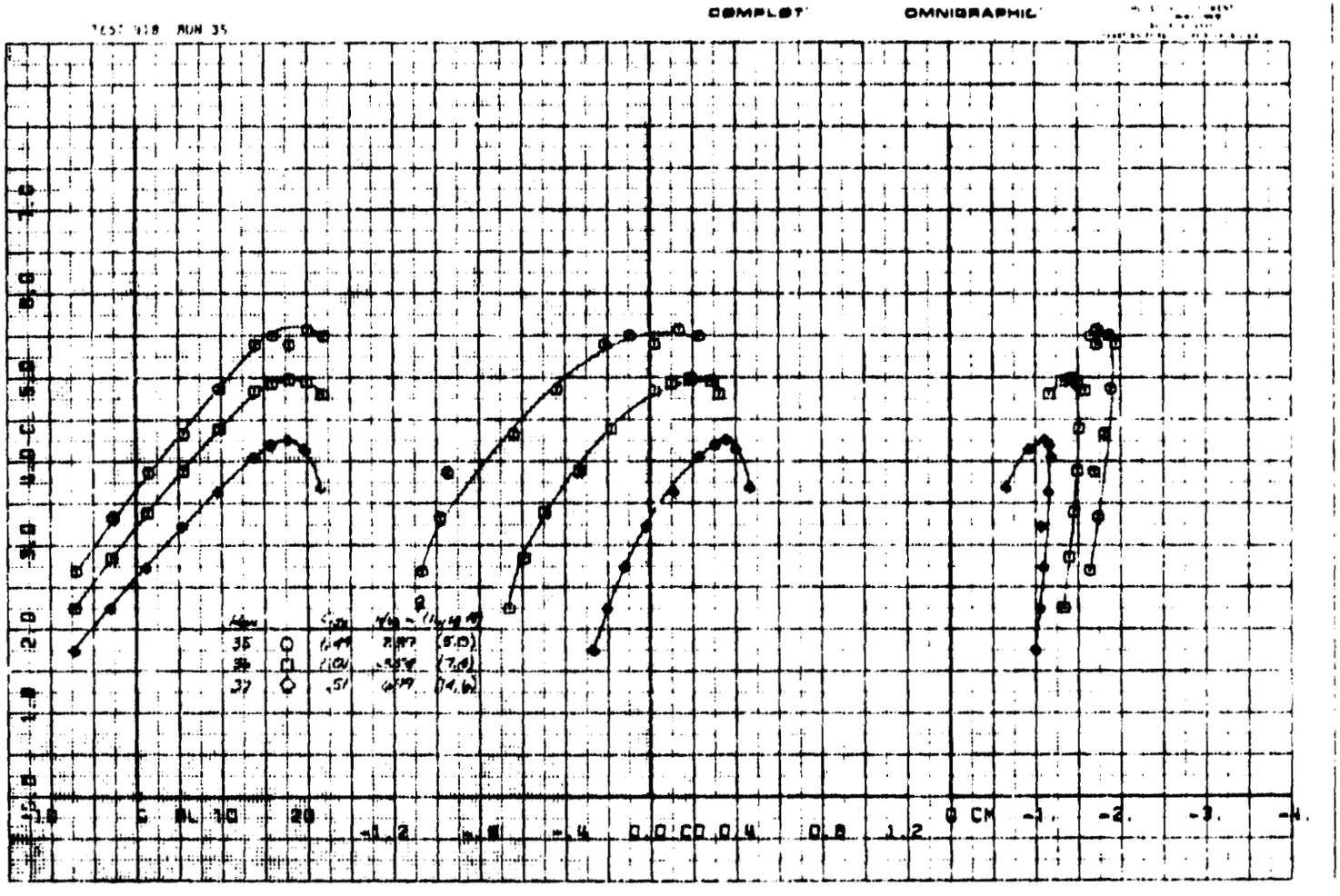


(b) $\delta_c = 0$, $\delta_{s_2} = 60°$.

Figure 15. — Continued.

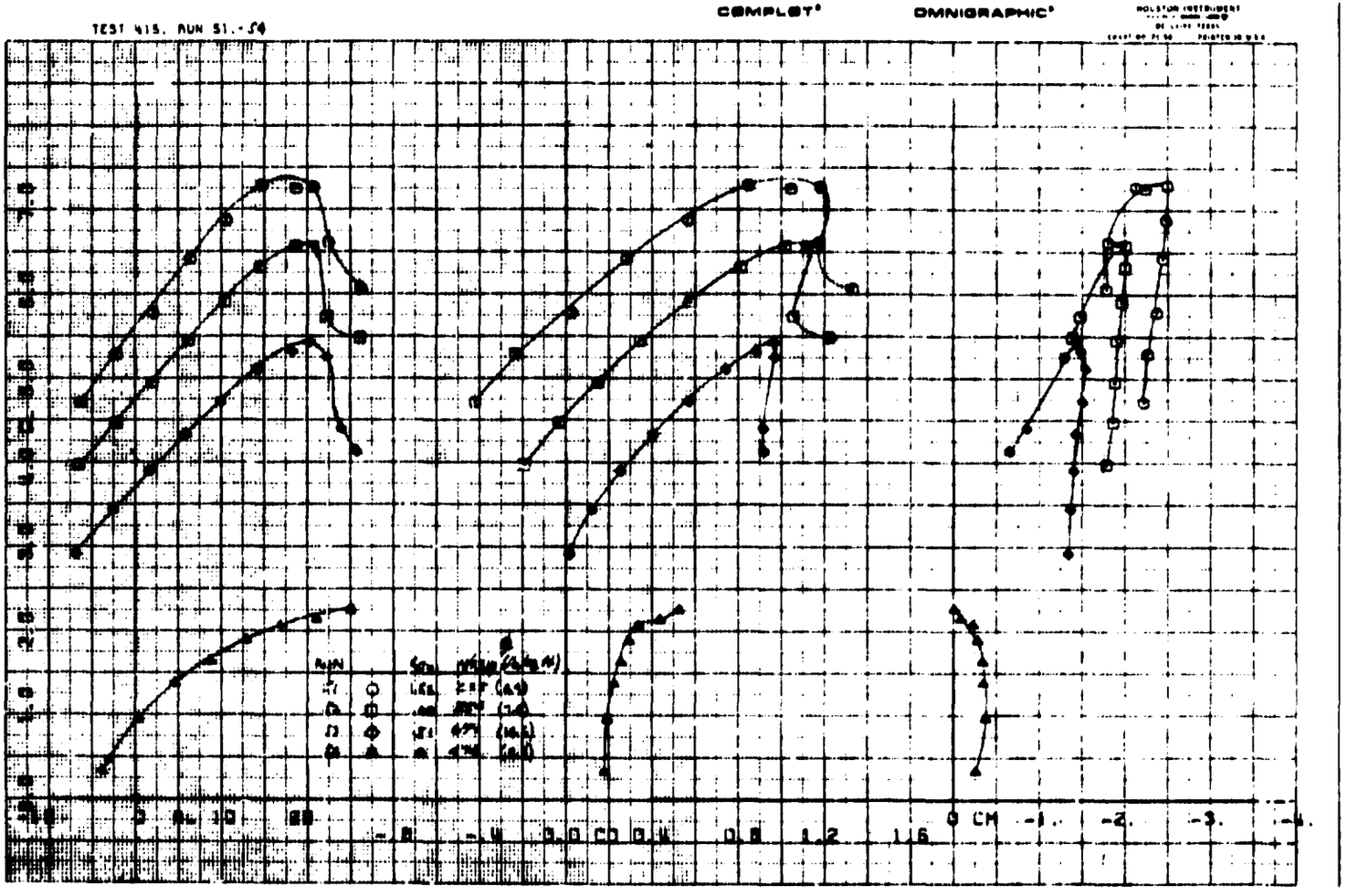


(c) $\delta_c$ - 30°, $\delta_{s_1}$ = 60°.

Figure 15. — Continued.

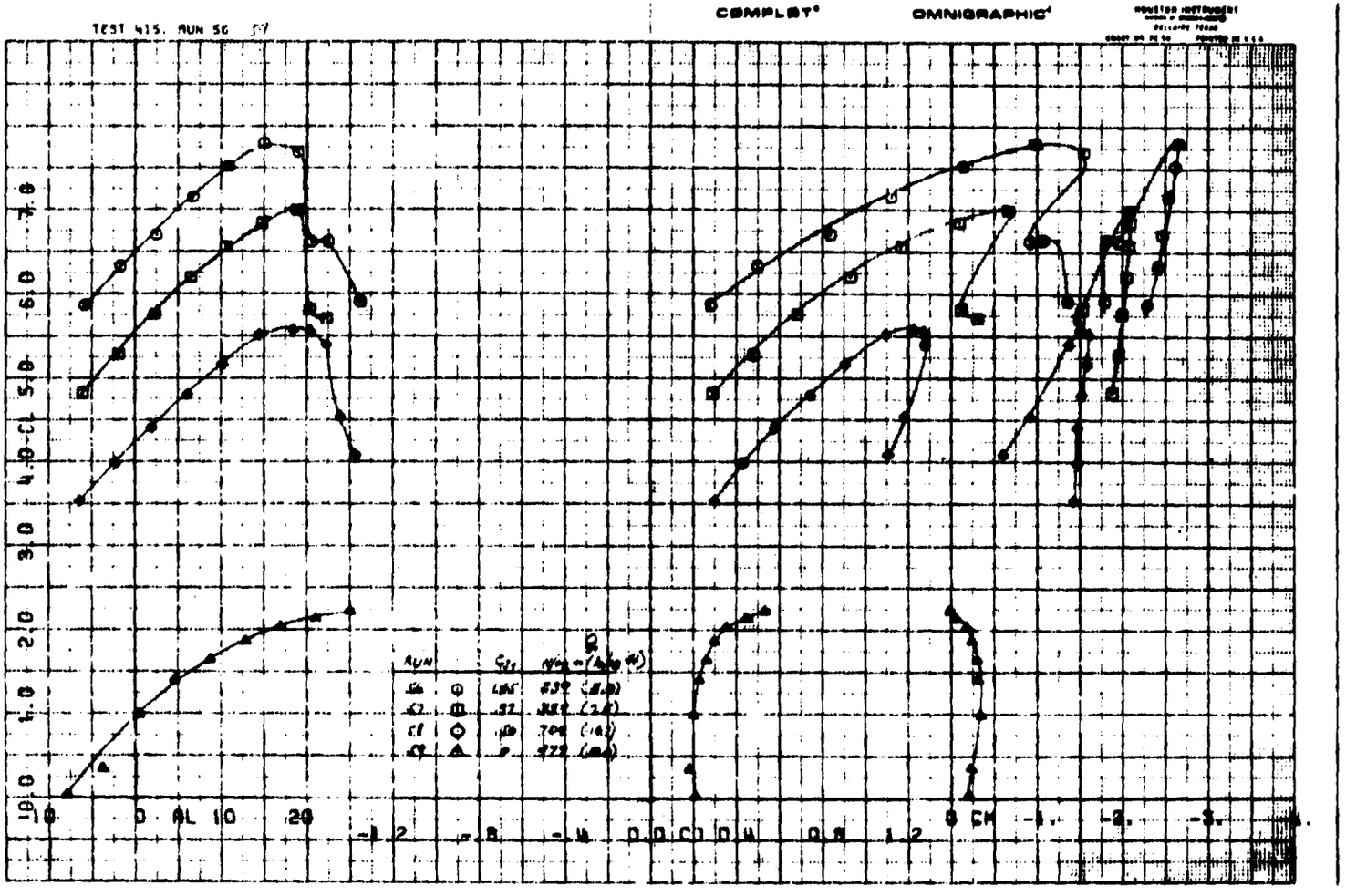


(d) $\delta_c = 50°$, $\delta_{s_1} = 60°$.

Figure 15. — Concluded.

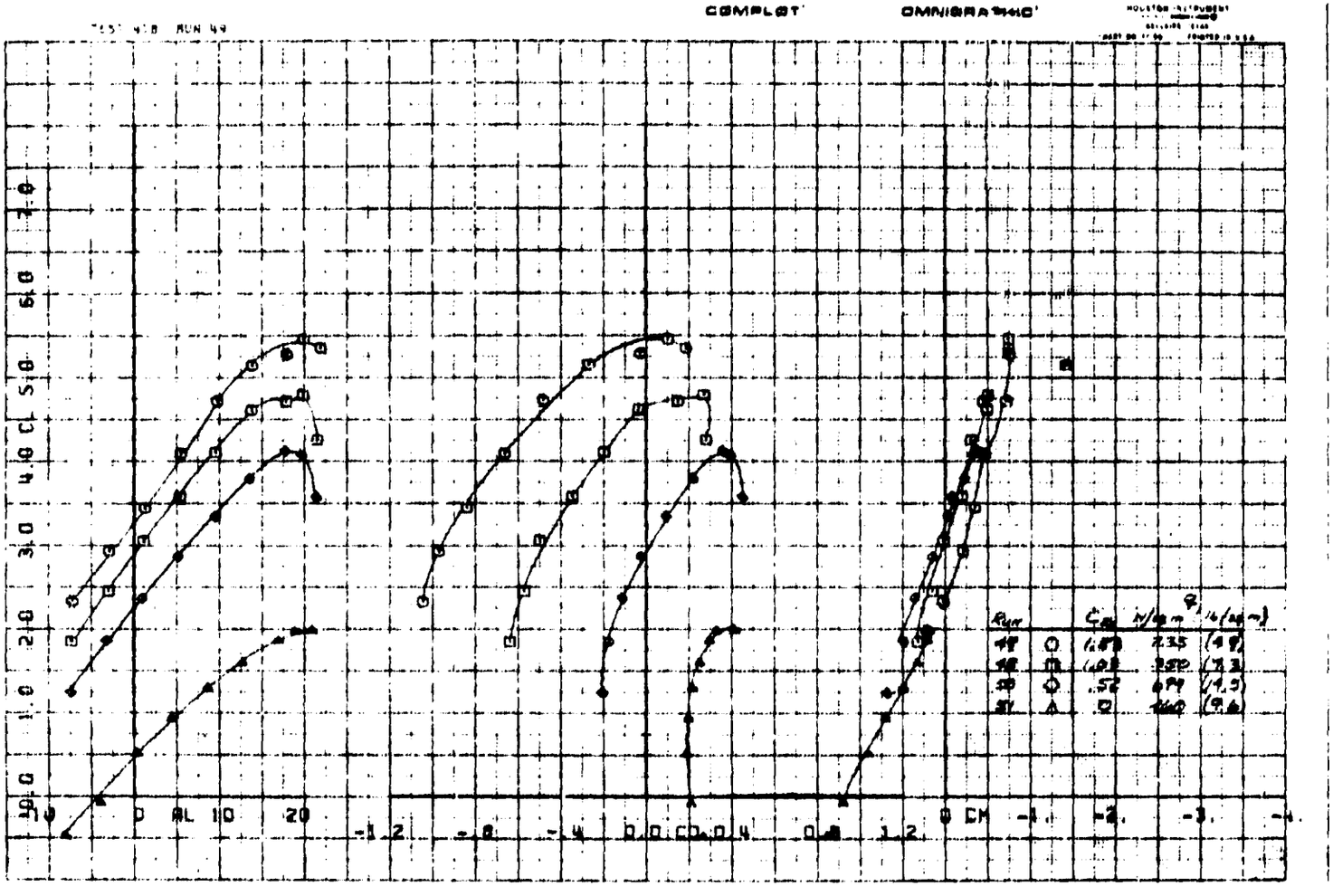


(a) Effect of $C_{J_I}$; $i_t = -15$ .

Figure 16. — Longitudinal characteristics of the model with the horizontal tail installed; part-span flap, $\delta_f = 30°$, $\delta_a = 30°$, $\delta_c = 0°$, $\delta_{s_2} = 60°$.

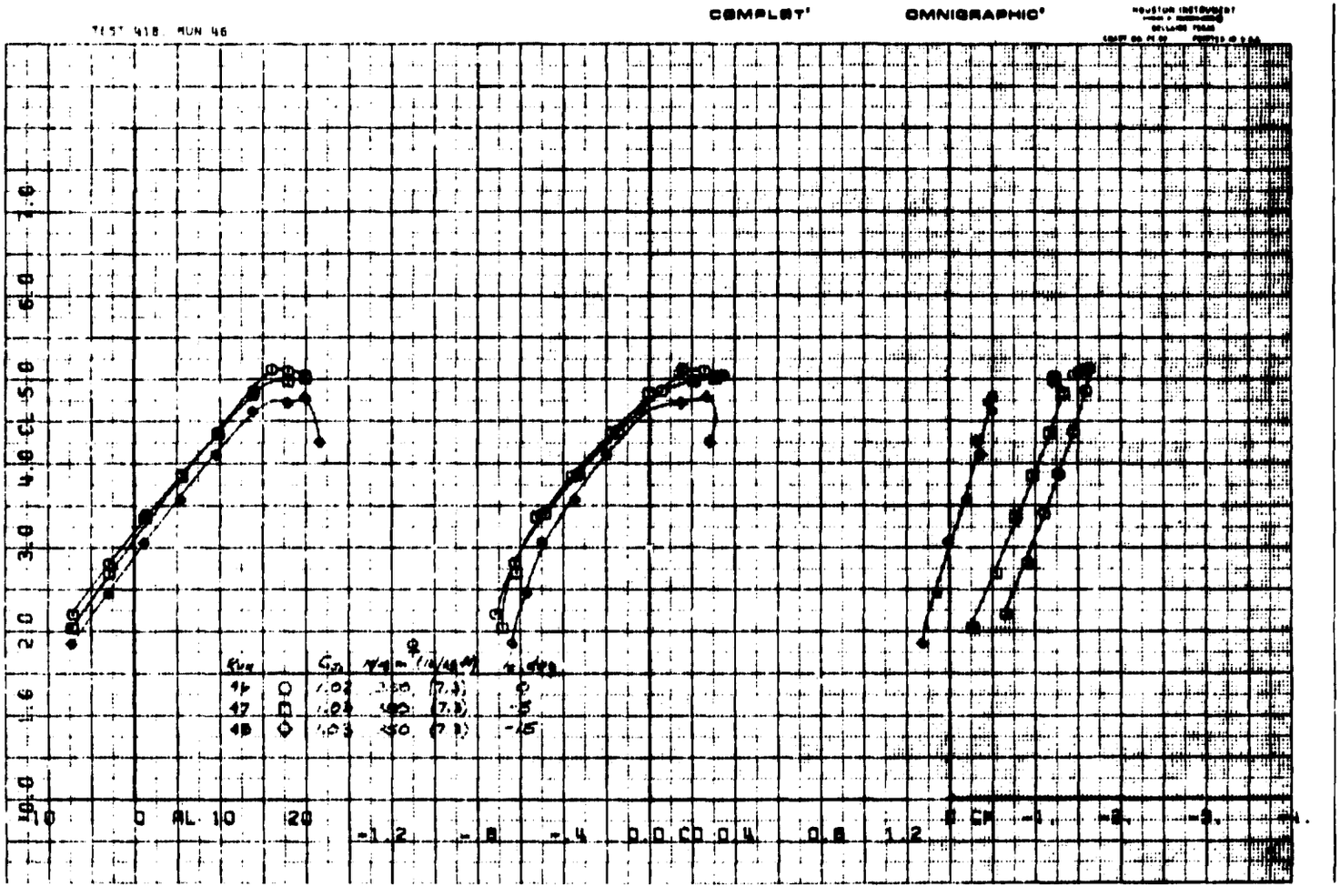


(b) Effect of $i_t$.

Figure 16. — Concluded.

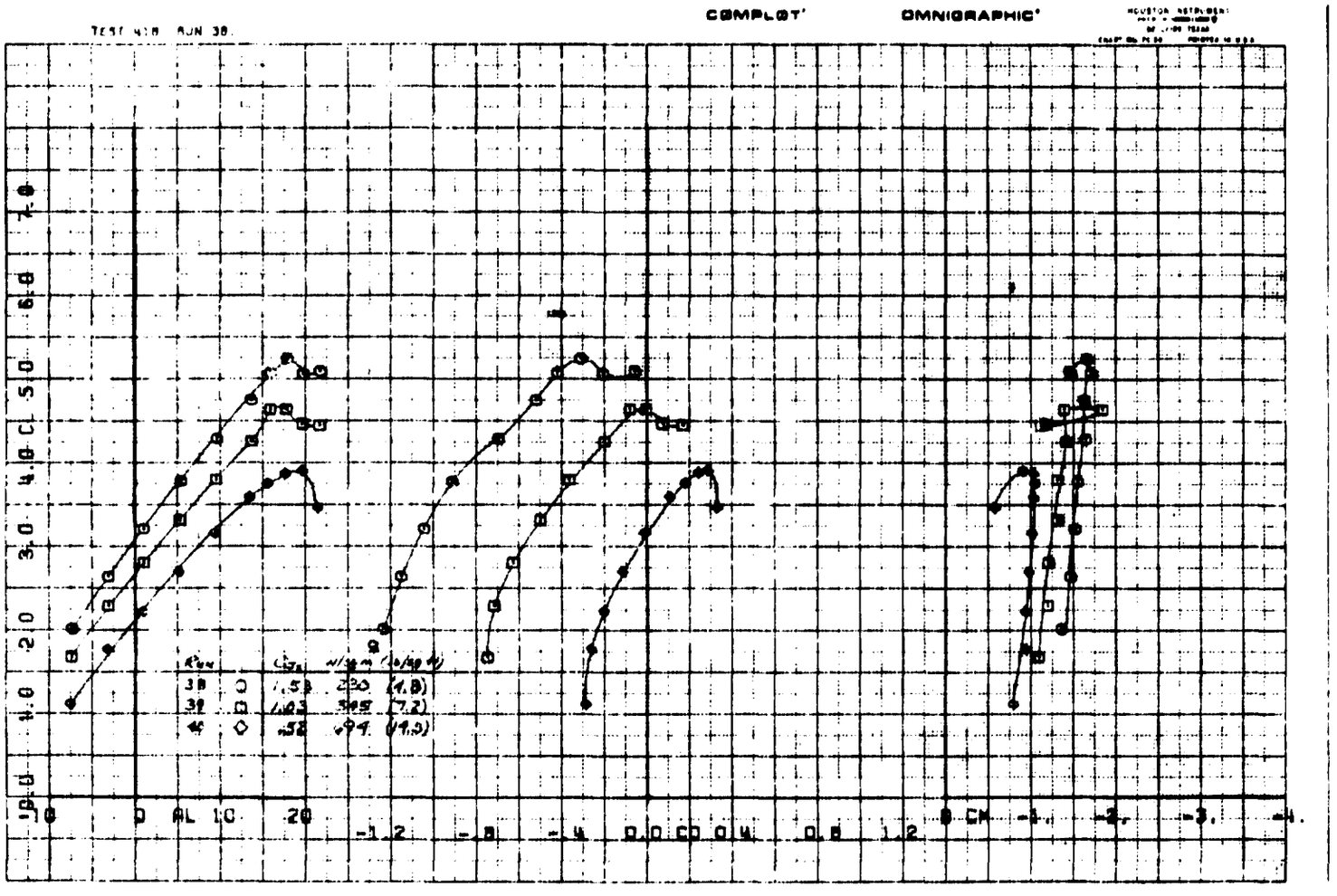


(a) $\delta_c = 0°/-20°$.

Figure 17. — The effect of $C_{J_I}$ on the longitudinal characteristics of the model; part-span flap, $\delta_f = 30°$, $\delta_a = 30°$, $\delta_{s_2} = 60°$, horizontal tail off.

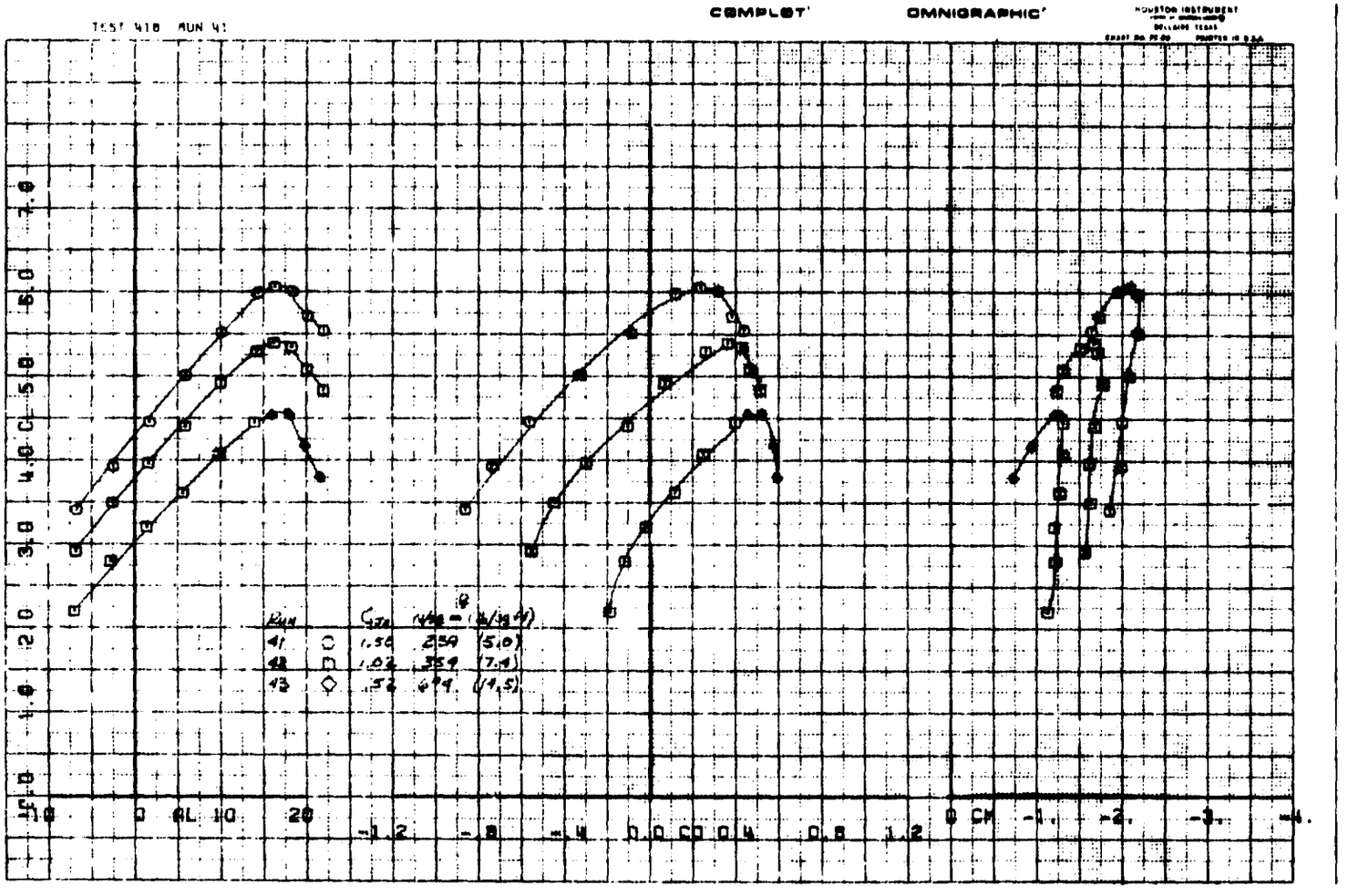


(b) $\delta_c = 0°/20°$.

Figure 17. — Continued.

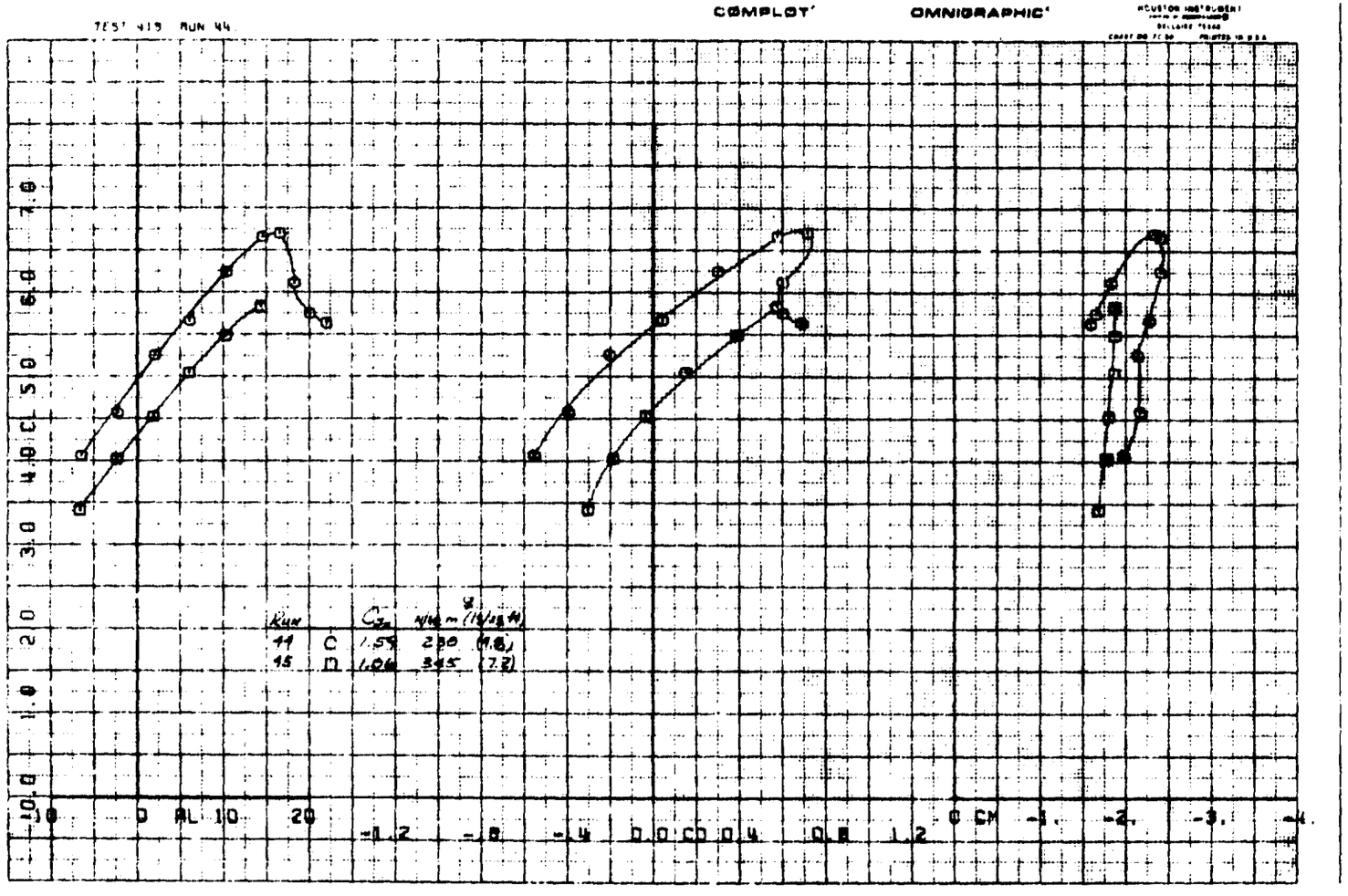


(c) $\delta_c = 0°/40°$.

Figure 17. — Concluded.

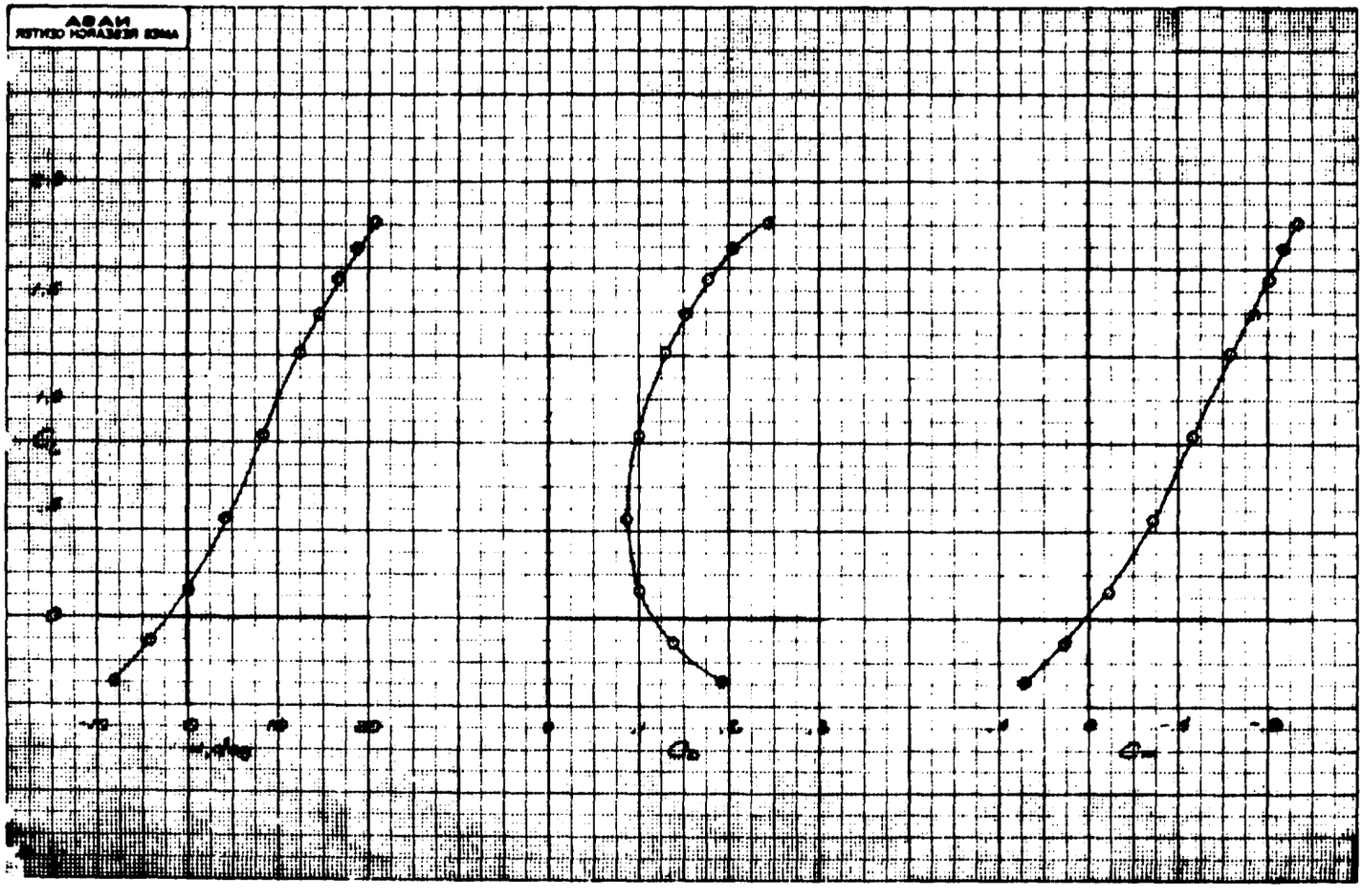

Figure 18. – Longitudinal characteristics of the model with the nose fairing and horizontal tail installed; $\delta_f = 0°$, $\delta_c = 0°$, $\delta_{s_2} = 60°$, $i_t = 0°$, tail slot off, $C_{J_I} = 0$.

REPRODUCIBILITY OF THE ORIGINAL PAGE IS POOR.

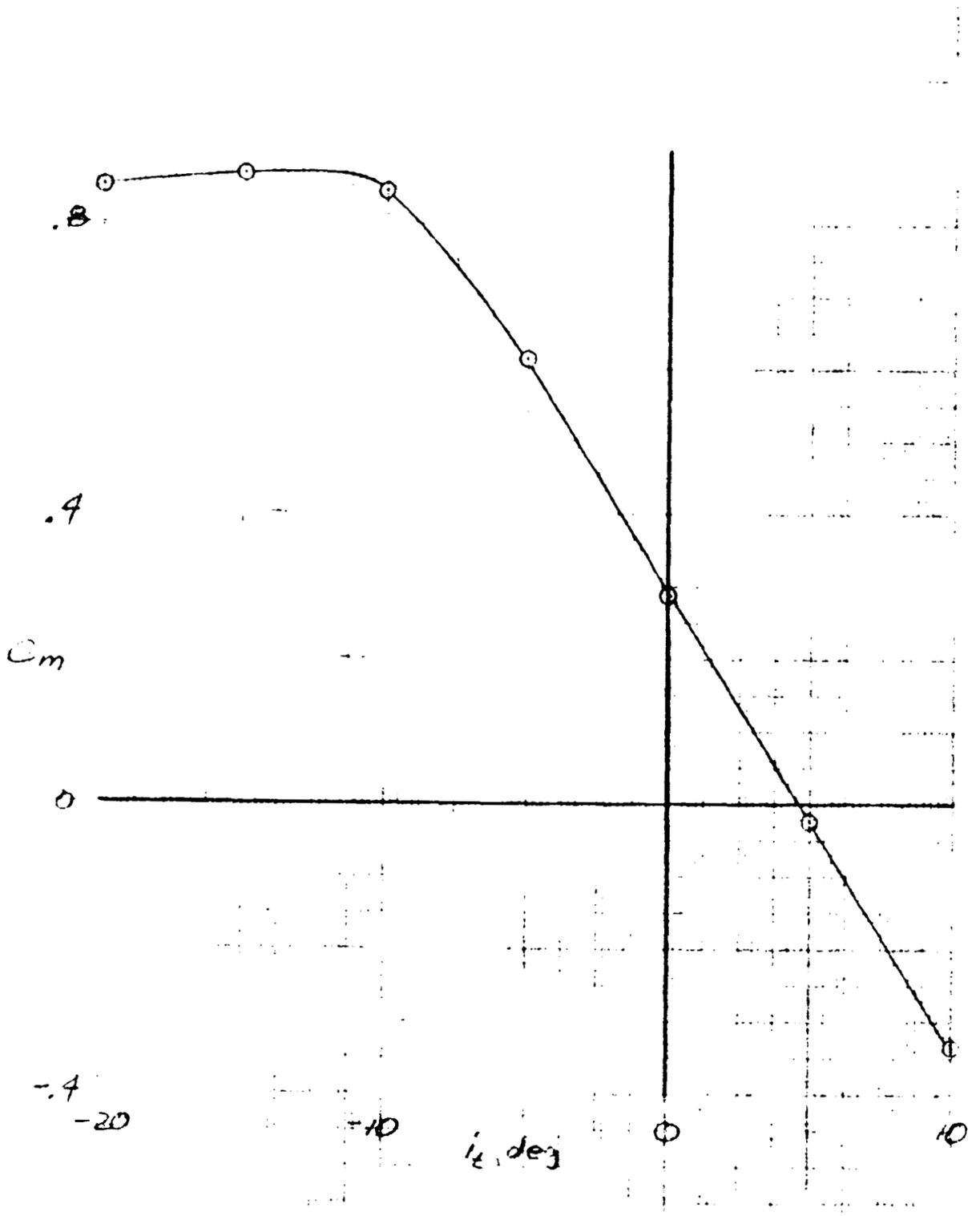


Figure 19. – The effect of tail incidence, $i_t$, on the model pitching moment, nose fairing and horizontal tail installed; $\delta_f = 0°$, $\delta_c = 0°$, $\delta_{s_2} = 60°$, tail slot off.

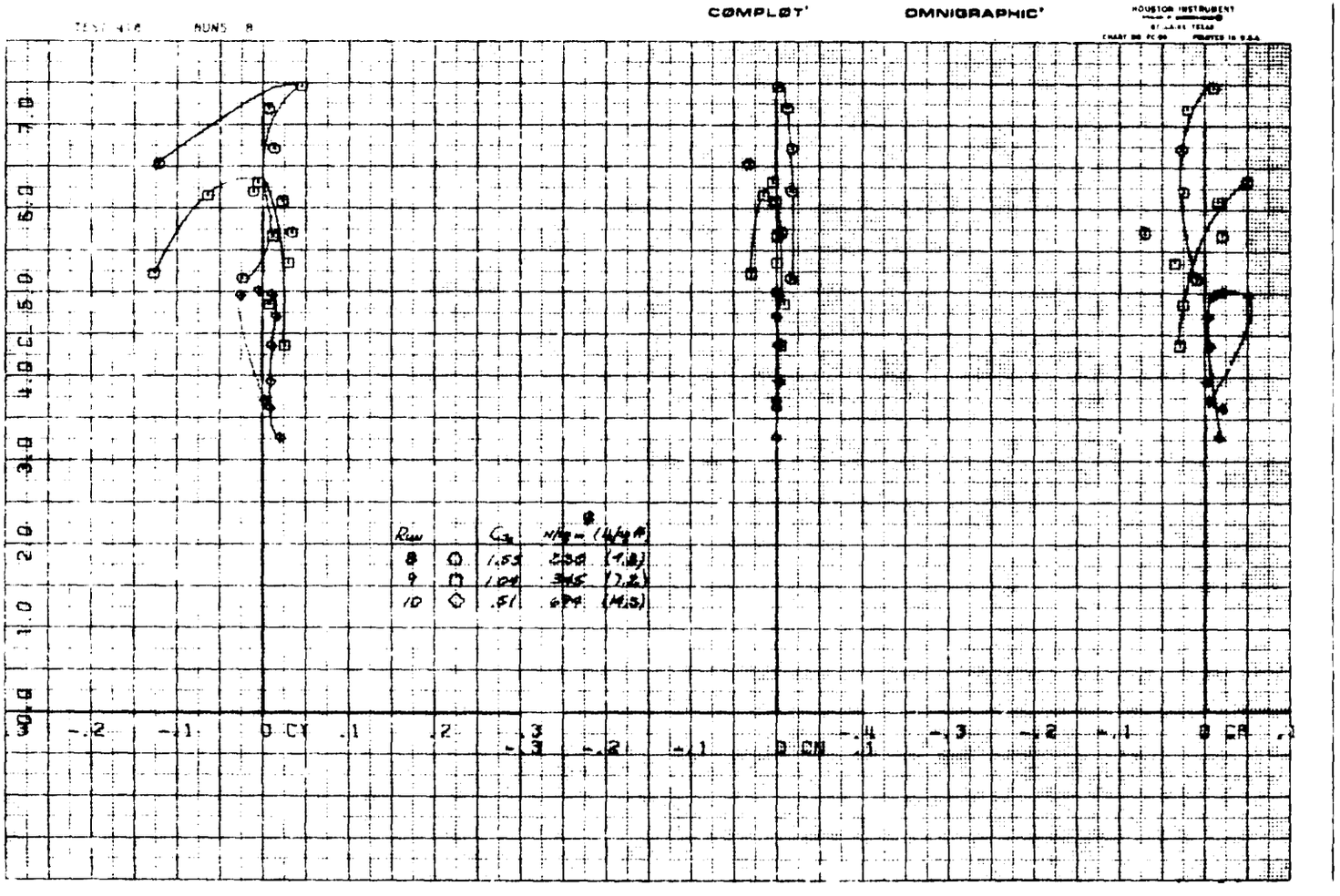


(a) $\delta_c = 0°$.

Figure 20. — The effect of $C_{J_I}$ on the lateral-directional characteristics of the model; part-span flap, $\delta_f = 60°$, $\delta_a = 30°$, $\delta_{s_2} = 60°$, horizontal tail off, $C_{J_I} = 0$.

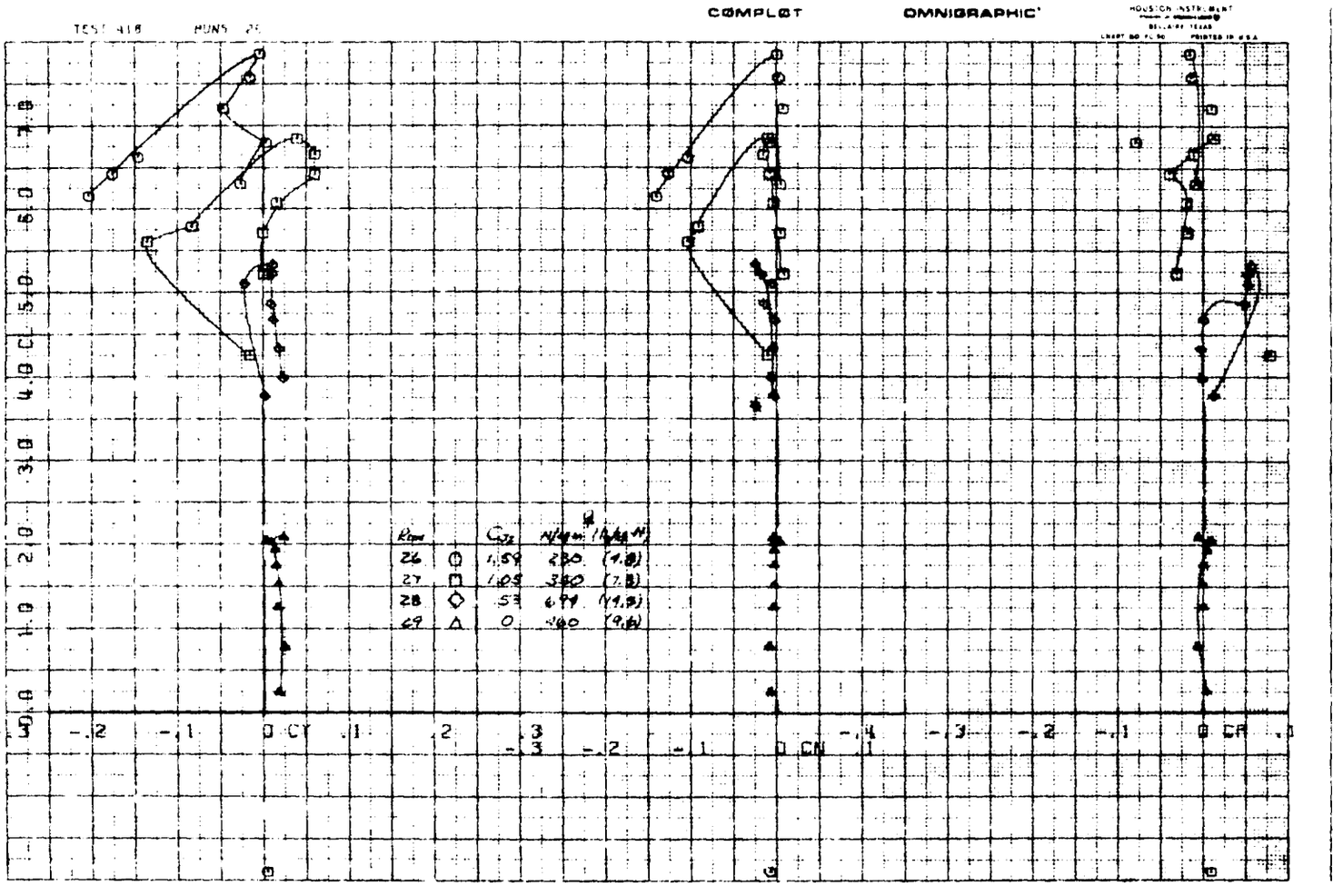


(b) $\delta_c = 20°$.

Figure 20. — Continued.

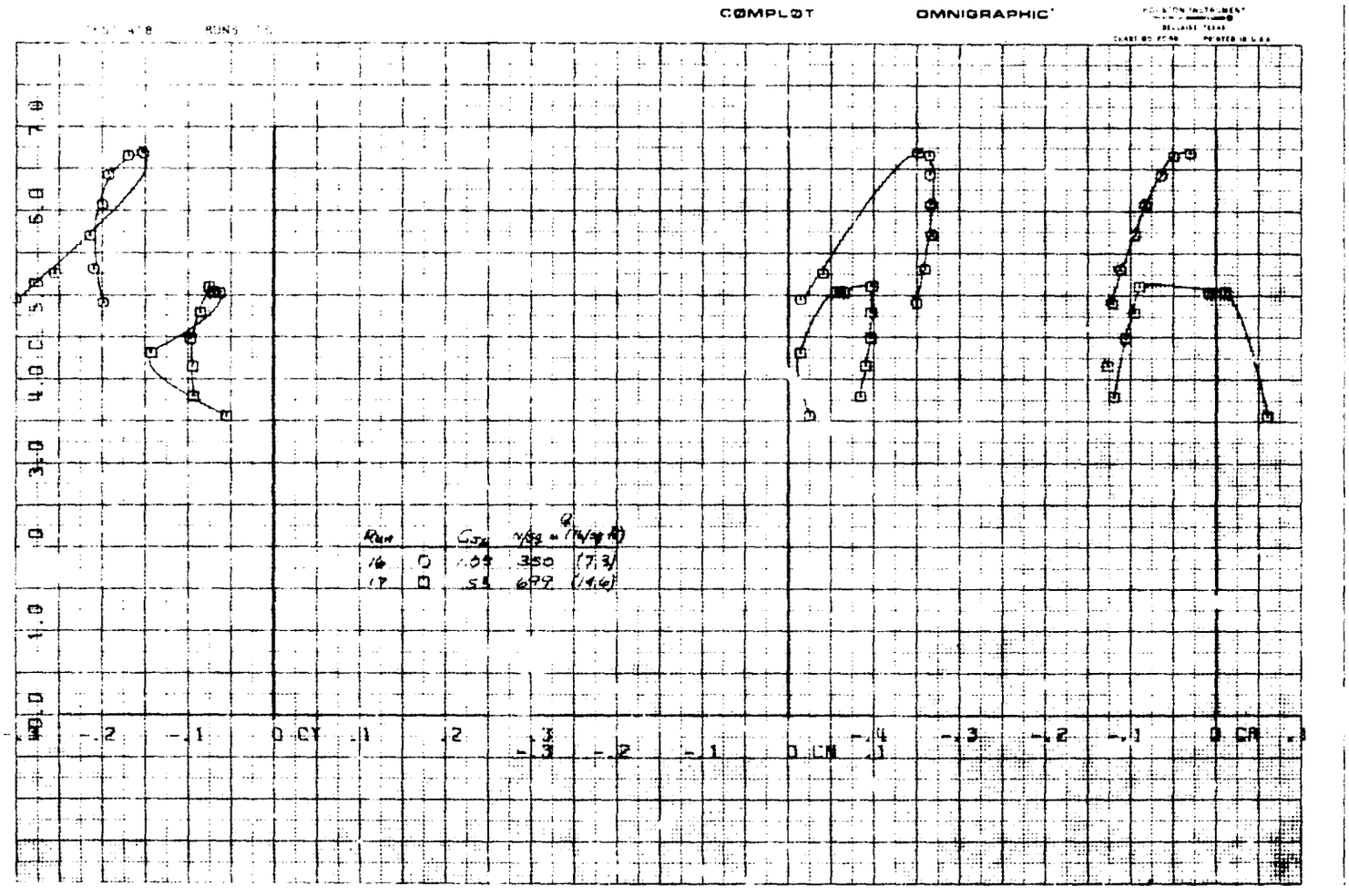


(d) $\delta_c = 0°/40°$.

Figure 20. — Concluded.

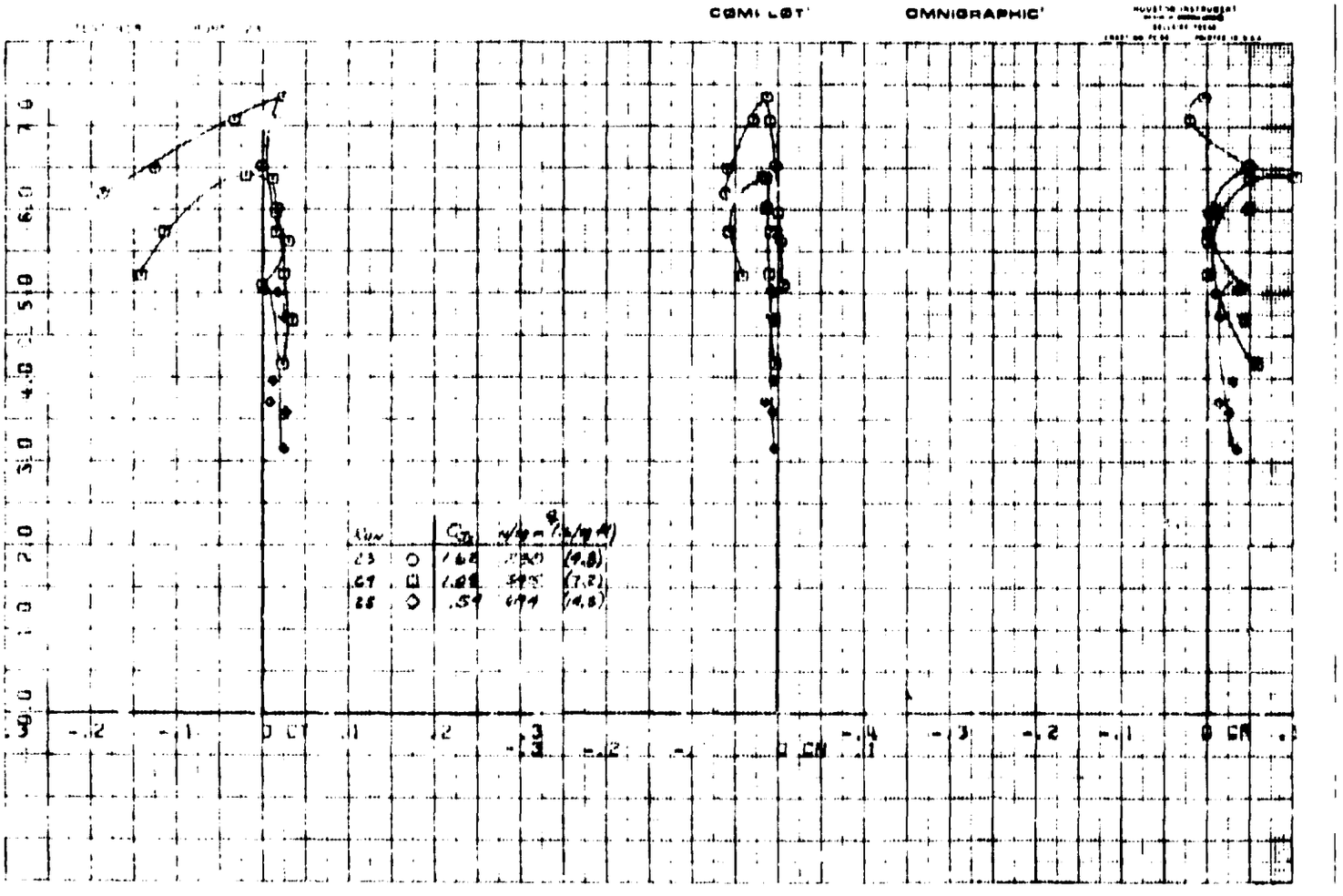

Figure 21. — The effect of $C_{J_I}$ on the lateral-directional characteristics of the model; part-span flap, $\delta_f = 60°$, $\delta_a = 30°/10°$, $\delta_c = 0°$, $\delta_{s_2} = 60°$, horizontal tail off.

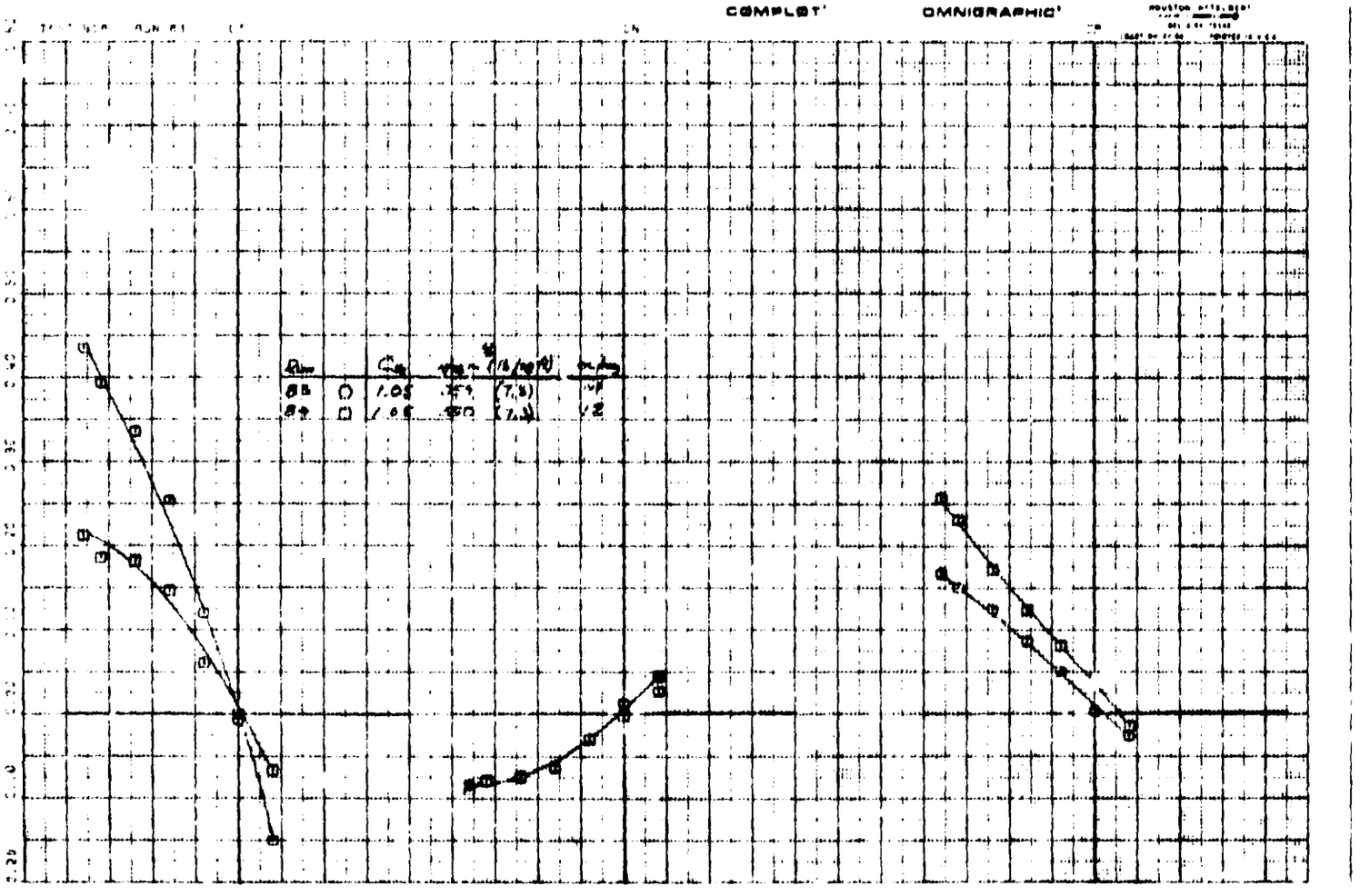


(a) Effect of $\alpha$, $\delta_c = 0°$.

Figure 22. — Lateral-directional characteristics of the model in sideslip; part-span flap, $\delta_f = 60°$, $\delta_a = 30°$, $\delta_{s_2} = 60°$, $i_t = 10°$.

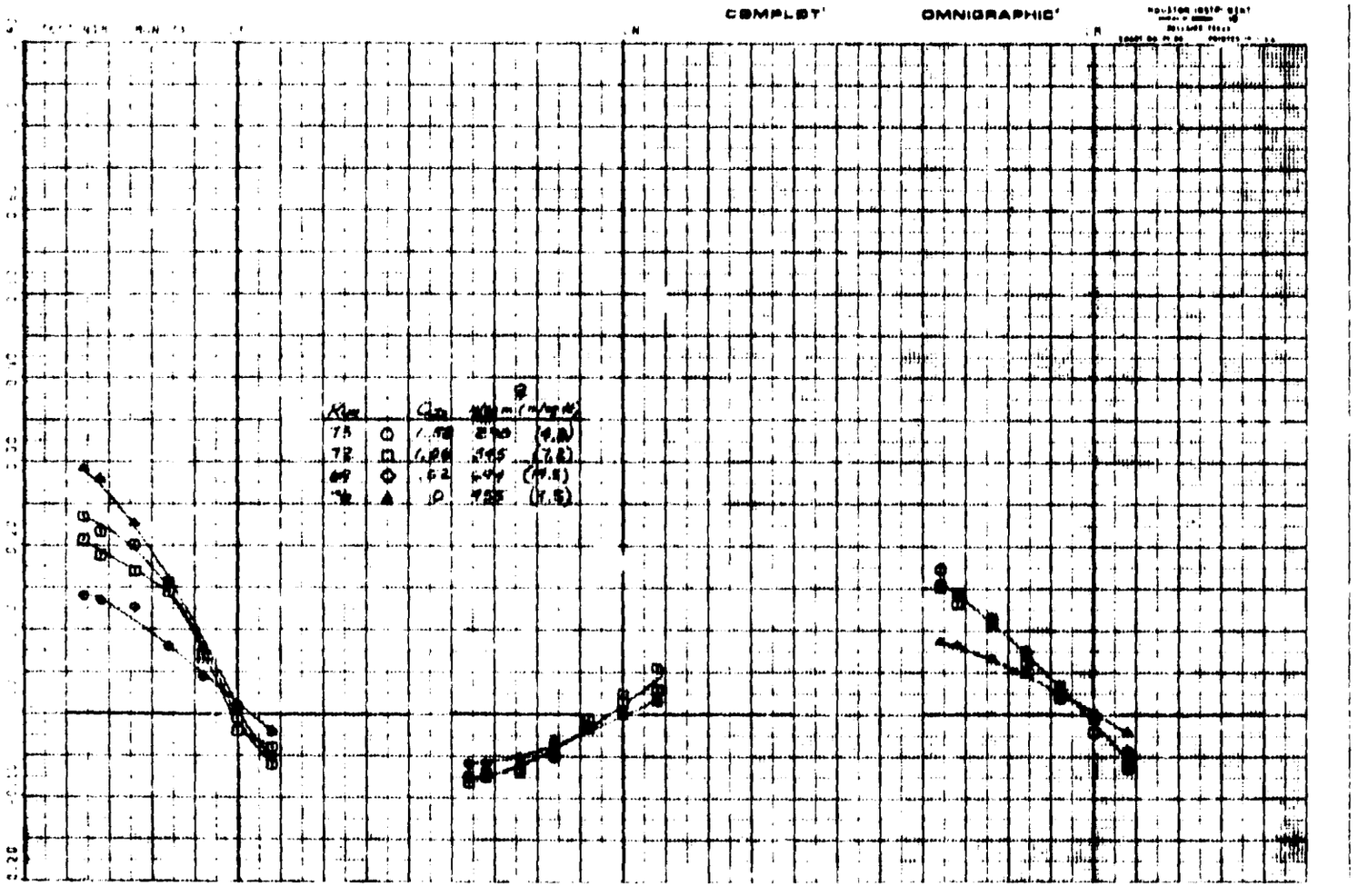


(b) Effect of $C_{J_I}$, $\alpha = 4°$, $\delta_c = 20°$.

Figure 22. — Continued.

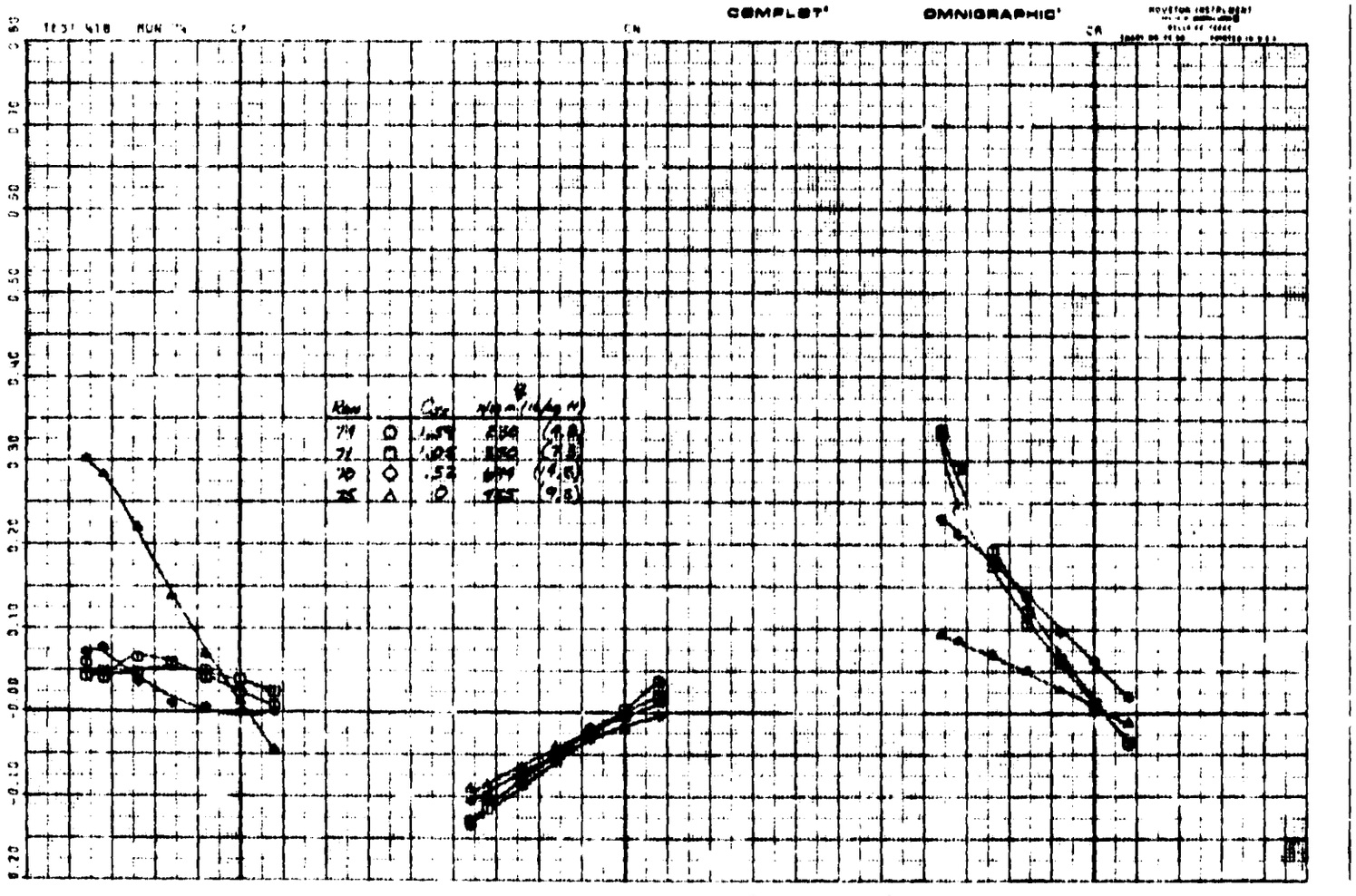


(c) Effect of $C_{J_I}$, $\alpha = 12°$, $\delta_c = 20°$.

Figure 22. – Continued.

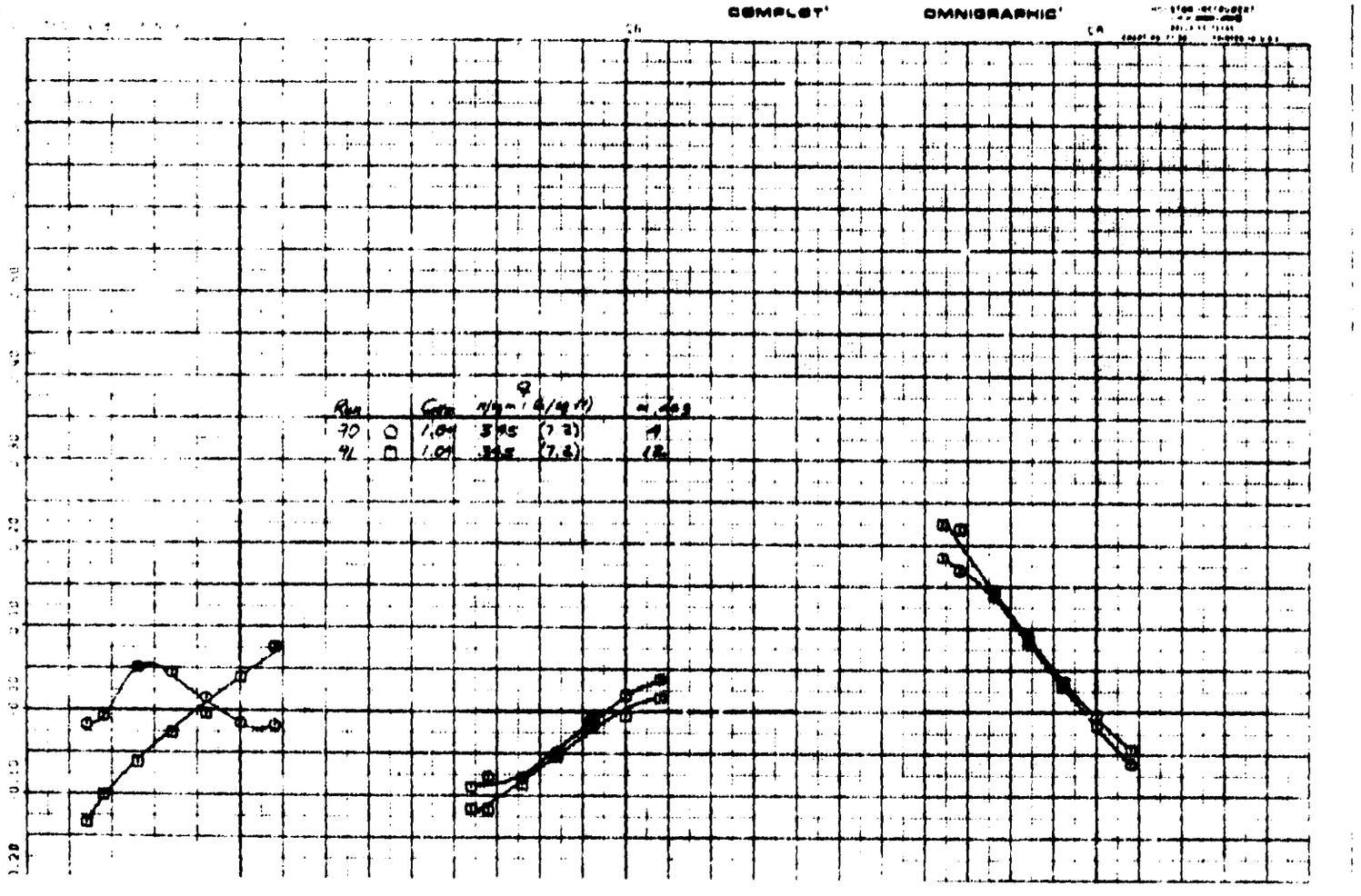


(d) Effect of $\alpha$, $\delta_c = 40°$.

Figure 22. — Concluded.

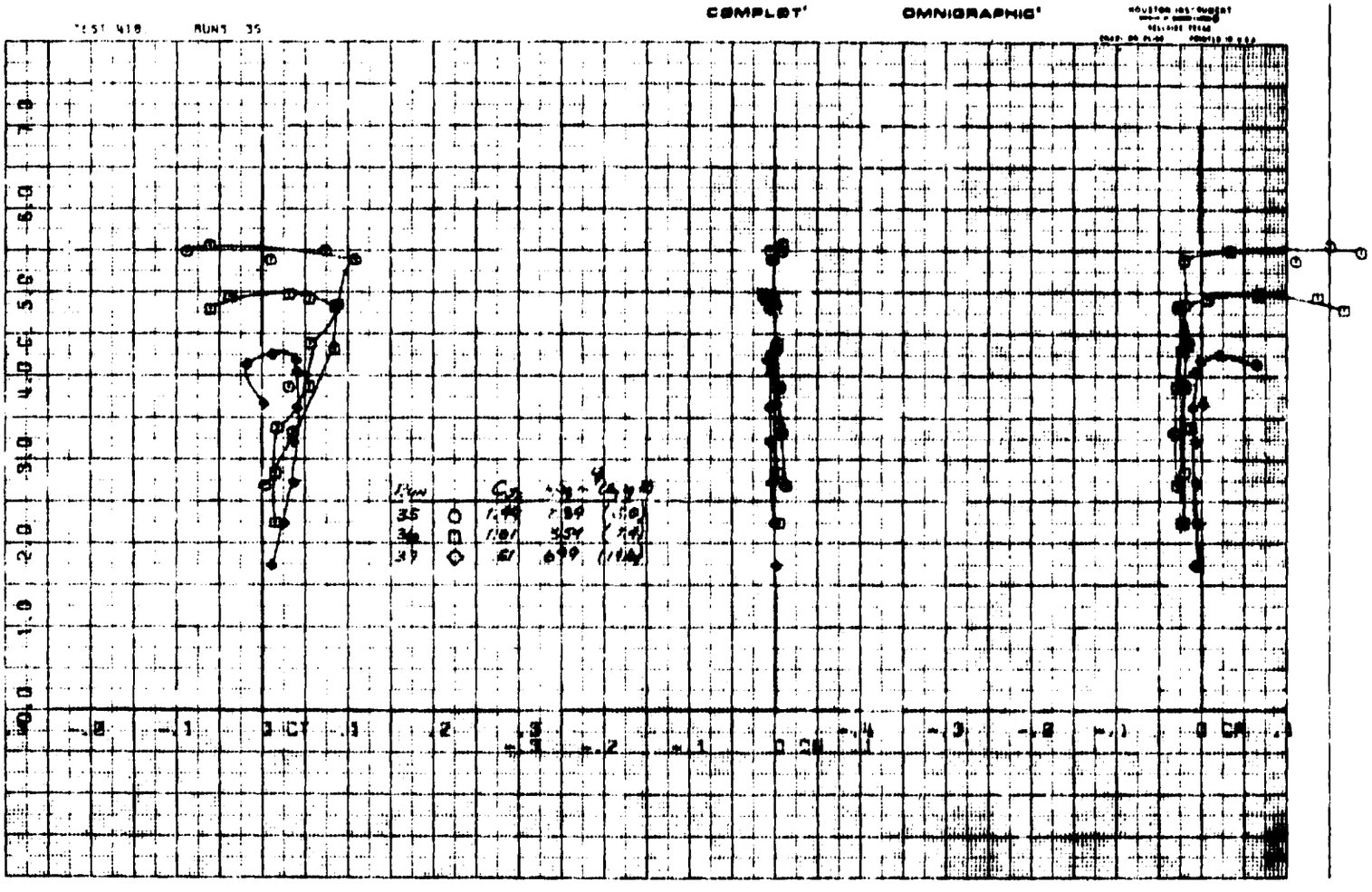

(a) $\delta_c = 0°$.

Figure 23. — The effect of $C_{J_I}$ on the lateral-direction characteristics of the model, part-span flap, $\delta_f = 30°$, $\delta_a = 30°$, $\delta_{s_2} = 60°$, horizontal tail off.

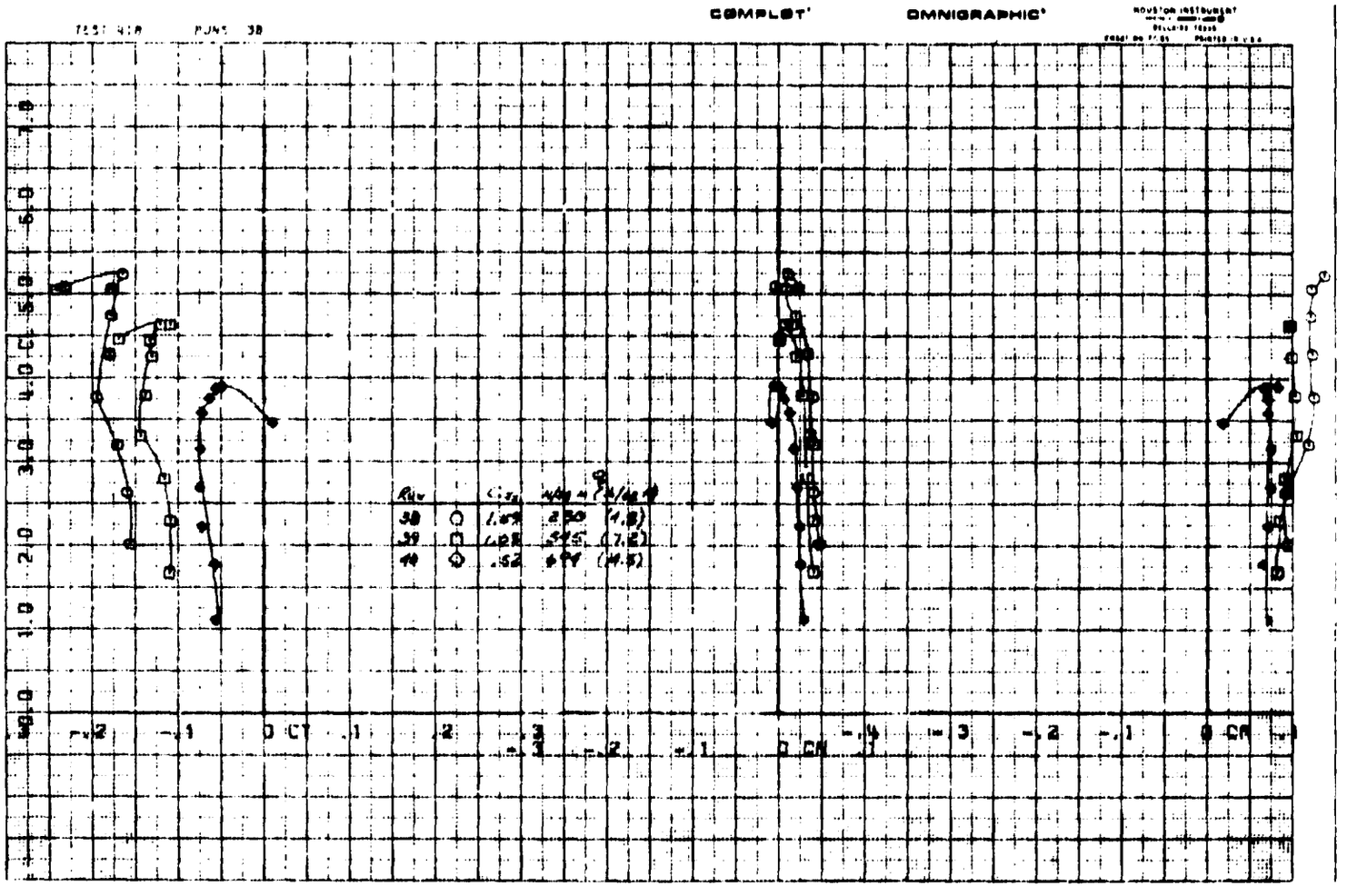


(b) $\delta_c = 0°/-20°$.

Figure 23. — Continued.

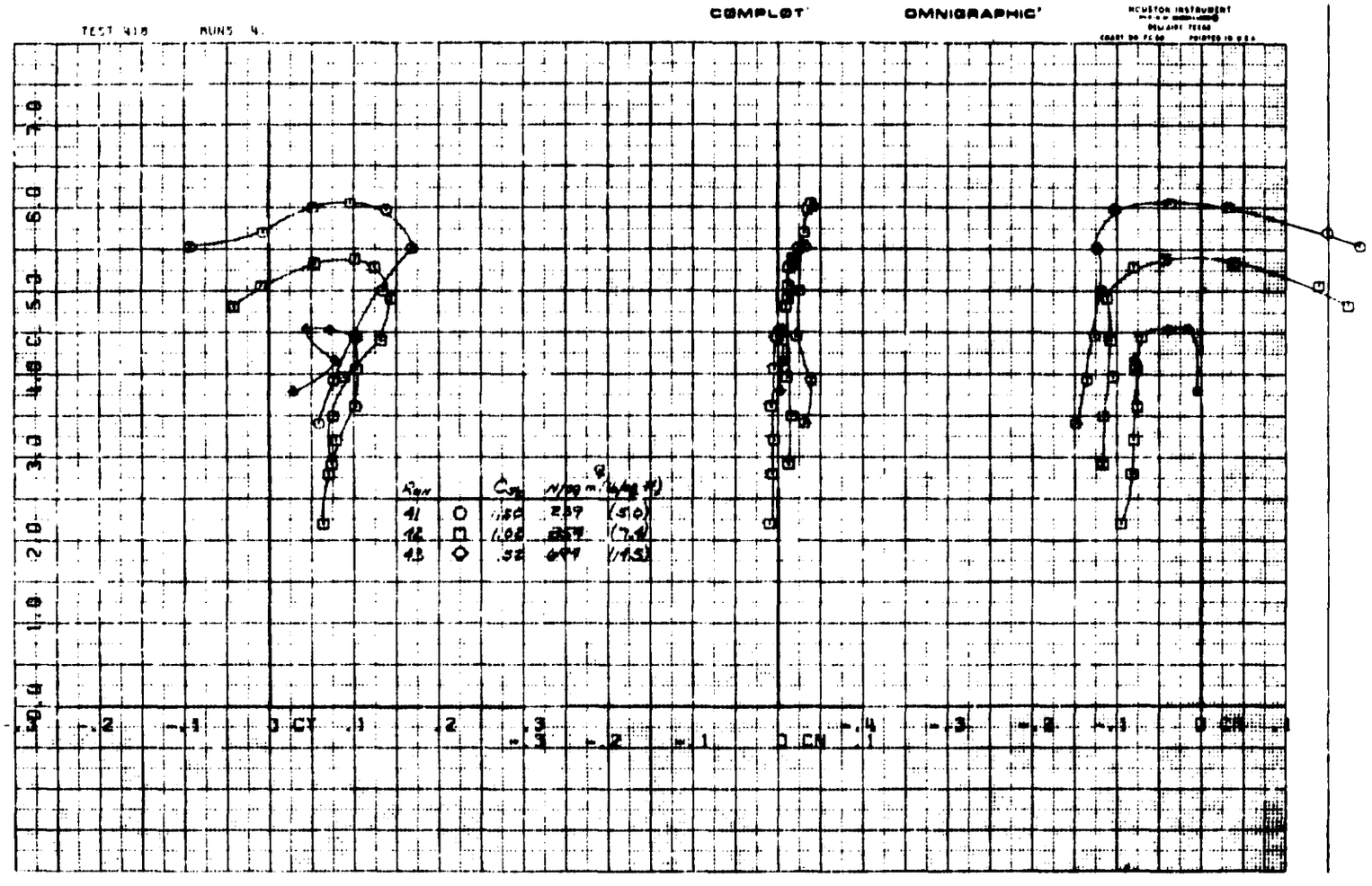


(c) $\delta_c = 0°/20°$.

Figure 23. — Continued.

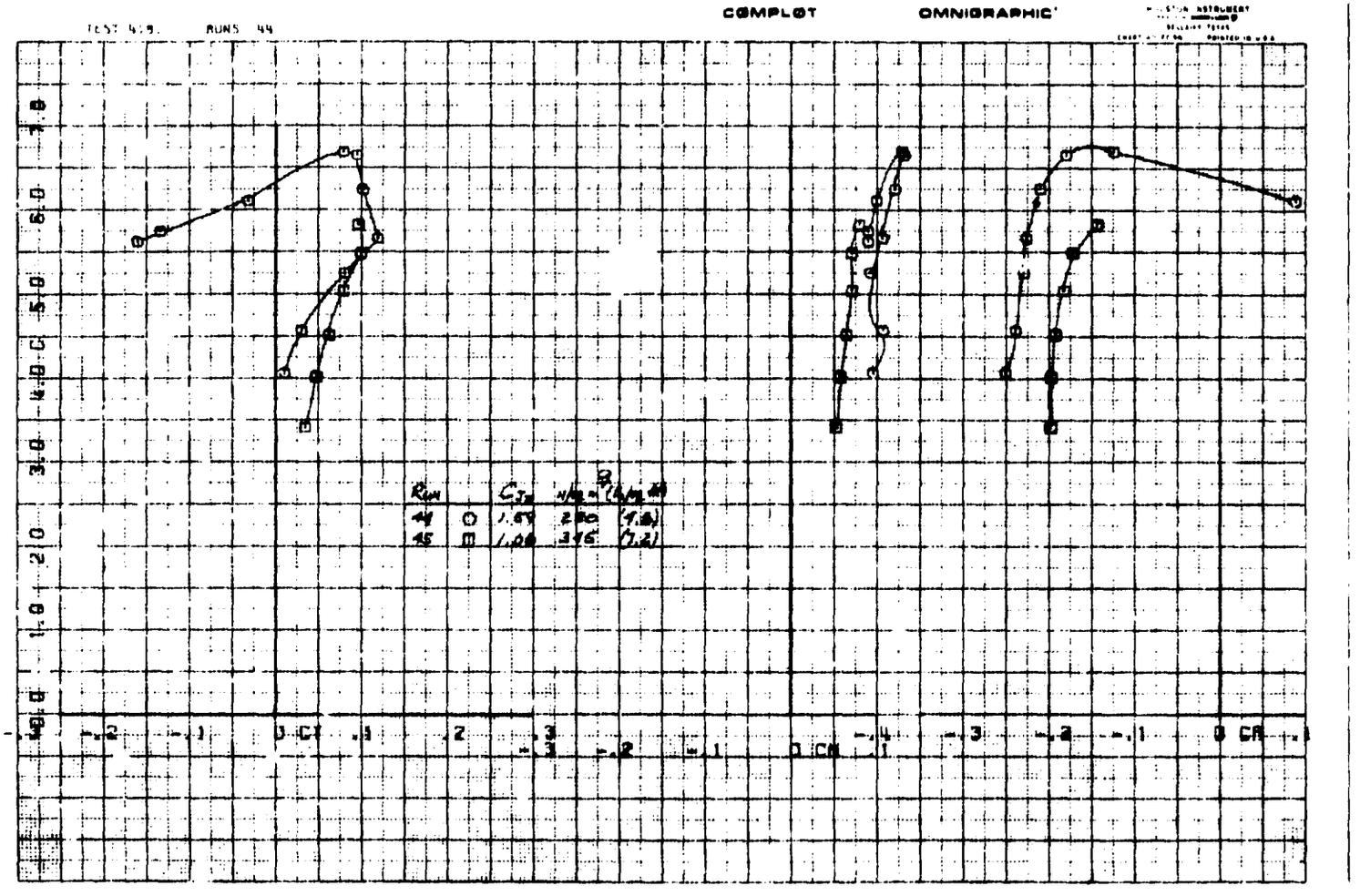


(d) $\delta_c = 0°/40°$.

Figure 23. — Concluded.

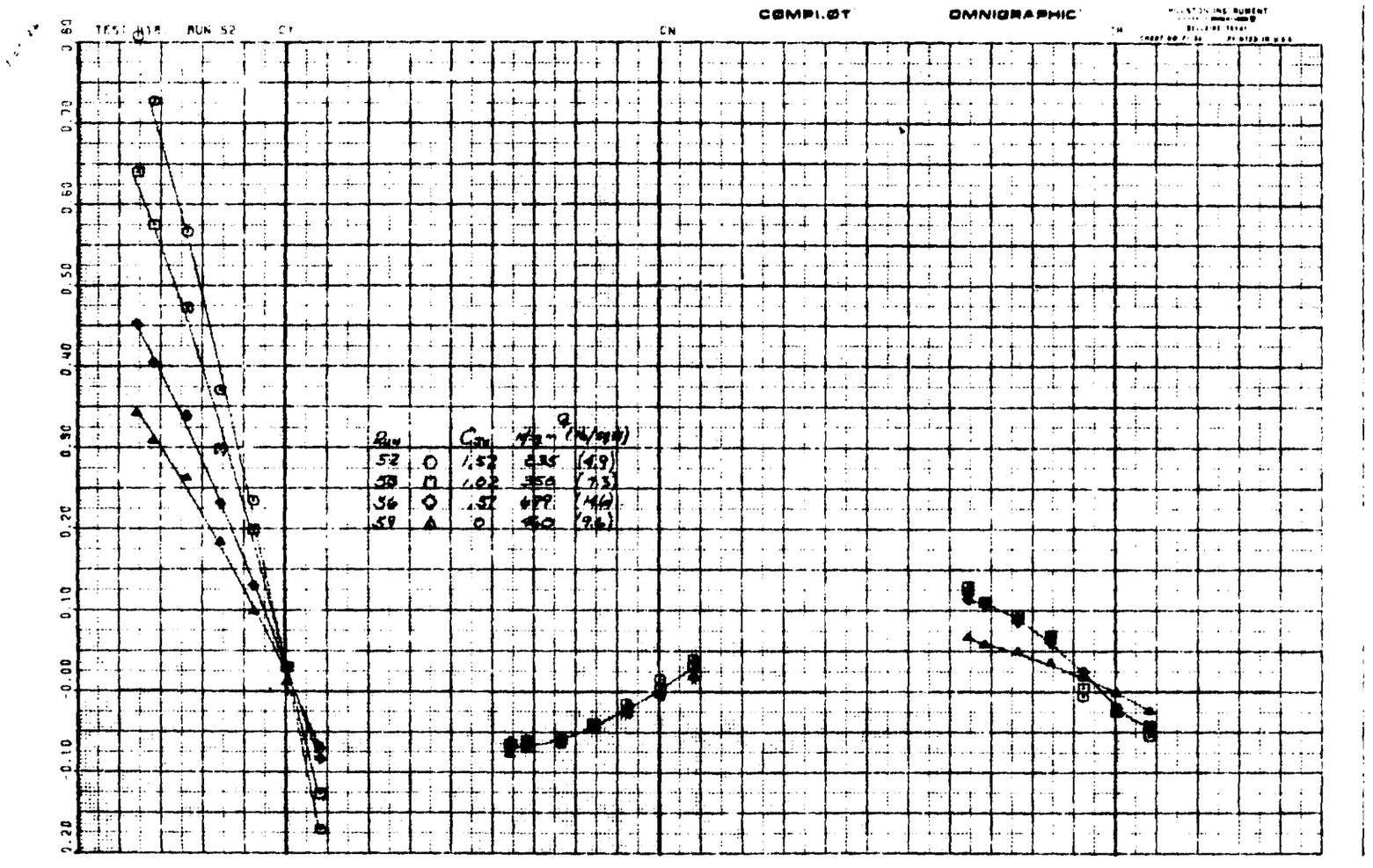


(a) $\alpha = 4°$.

Figure 24. — The effect of $C_{J_I}$ on the lateral-directional characteristics of the model in sideslip; part-span flap, $\delta_f = 30°$, $\delta_a = 30°$, $\delta_c = 0°$, $\delta_{s_2} = 60°$, $i_t = -15°$.

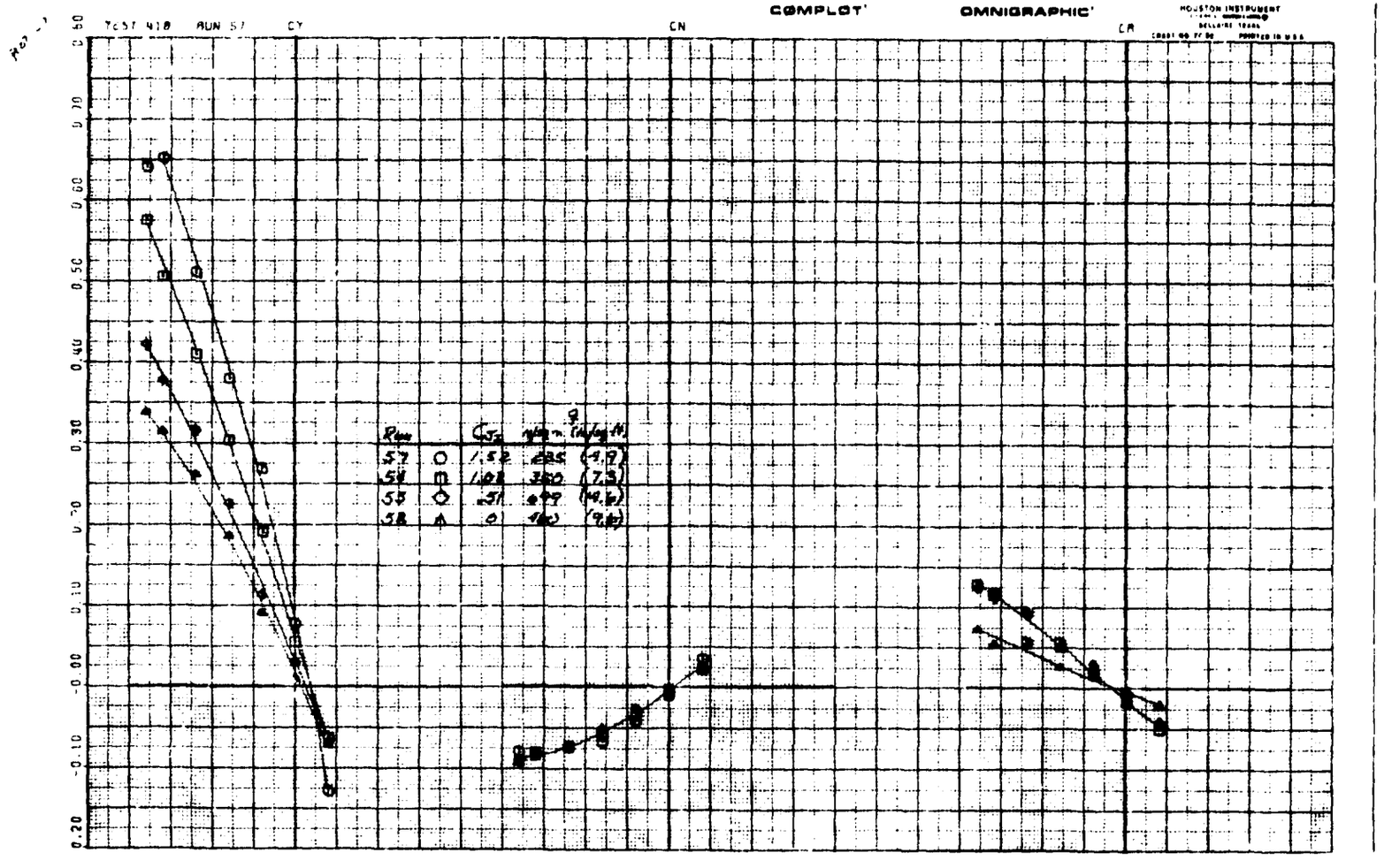


(b) $\alpha = 12°$.

Figure 24. – Concluded.

☆ GPO 791-610